2015-04-29

Extending the Window of Use for Human Mesenchymal Stem Cell Seeded Biological Sutures

Spencer Coffin
Worcester Polytechnic Institute

Extending the Window of Use for Human Mesenchymal Stem Cell Seeded Biological Sutures

Spencer Thomas Coffin

A thesis to be submitted to the faculty of Worcester Polytechnic Institute in partial fulfillment of the requirements for the Degree of Master of Science

Submitted by:
Spencer T Coffin
Department of Biomedical Engineering

_____

Approved by:

Glenn R Gaudette, PhD Associate Professor Department of Biomedical Engineering	Raymond L Page, PhD Professor of Practice Department of Biomedical Engineering	George D Pins, PhD Associate Professor Department of Biomedical Engineering
_____	_____	_____

April 30, 2015

Acknowledgements

I would like to thank my advisors: Glenn Gaudette, Ray Page, and George Pins for their constant feedback, support, and guidance throughout the course of this project and my education at WPI.

I would like express my gratitude to the following people who have assisted me in the completion of this project, whether it be learning lab techniques, troubleshooting, assisting with experiments, editing, or general support:

- John Favreau PhD
- Katrina Hansen
- Emily Abbate
- Josh Gershlak
- Robert Orr
- John Fitzpatrick
- The Pins Lab
- The Page Lab
- The Rolle Lab
- The Jain Lab
- The WPI Swimming and Diving and Worcester Area Master communities
- Paul Bennett
- My family
- My friends

Abstract

Cell therapy, including human mesenchymal stem cell (hMSC) therapy, has the potential to treat different pathologies, including myocardial infarctions (heart attacks). Biological sutures composed of fibrin have been shown to effectively deliver hMSCs to infarcted hearts. However, hMSCs rapidly degrade fibrin making cell seeding and delivery time sensitive. To delay the degradation process, we propose using aprotinin, a proteolytic enzyme inhibitor that has been shown to slow fibrinolysis. This project investigated the effects of aprotinin on hMSCs and suture integrity. Viability of hMSCs incubated with aprotinin, examined using a LIVE/DEAD stain, was similar to controls. No differences in proliferation, as determined by Ki-67 presence, and were observed. hMSCs incubated in aprotinin differentiated into adipocytes, osteocytes, and chondrocytes, confirming multipotency. CyQuant assays were used to determine the number of cells adhered to fibrin sutures. The number of adhered cells was increased through aprotinin supplementation at Days 2, 3, and 5 time points. To examine the effect of aprotinin on suture integrity, sutures were loaded to failure to determine ultimate tensile strength (UTS) and modulus (E). Sutures exposed to aprotinin had higher UTS and E when compared to sutures exposed to standard growth media. Degradation of fibrin was quantified using an ELISA to quantify fibrin degradation products (FDP) and by measuring suture diameter. Fibrin sutures incubated in aprotinin had larger diameters and less FDP compared to the controls, confirming decreased fibrinolysis. These data suggest that aprotinin can reduce degradation of biological sutures, providing a novel method for extending the implantation window and increasing the number of cells delivered for hMSC seeded biological sutures.

Contents

Table of Figures

Table of Tables

Chapter 1: Introduction/Background

This project investigates the use of aprotinin as a novel method of extending the culture time of human mesenchymal stem cell (hMSC) seeded fibrin sutures for use in delivery to infarcted myocardium. Previous work in the Gaudette lab indicates that fibrin sutures have the capacity to serve as a scaffold for hMSCs and are capable of cell delivery to infarcted myocardium [1]. This section will serve as a review of cardiac anatomy, the effects of infarction on healthy cardiac tissue, and a summary of current technologies aimed at the treatment of myocardial infarctions (MI).

1.1 Myocardial Function and Infarcted Myocardium

In the body, the heart acts as a pump circulating oxygen and nutrient rich blood to all parts of the body. The mammalian heart consists of four chambers: the right atrium, the right ventricle, the left atrium, and the left ventricle, all of which are comprised of cardiac muscle or myocardium. The inner surface of the cardiac muscle is the endocardium while the exterior is known as the epicardium [2]. Deoxygenated blood from the body is received into the right atrium, which contracts and pumps blood to the right ventricle. The right ventricle pumps deoxygenated blood to the lungs where the blood becomes oxygenated and then travels to the left atrium before being pushed into the left ventricle. From the left ventricle, oxygenated blood is forced into the aorta and circulated throughout the whole body [3]. Because the left ventricle pumps blood to the whole body, it typically consists of the thickest muscle and exhibits the highest pressure. Gap junctions allow the propagation of an action potential across the myocardium and create controlled contractions to effectively pump blood [4, 5].

Coronary circulation provides nutrient and oxygen rich blood to the myocardium. When a portion of coronary circulation is blocked, cardiomyocytes (muscle cells of the heart) become starved of oxygen and nutrients. If this occurs there are several metabolic and physiological changes that occur [6, 7]. Without a continuous flow of oxygen and glucose to the myocardium, adenosine triphosphate (ATP) production switches from an aerobic pathway to an anaerobic pathway, which is much less efficient. With less ATP available, contractions become weaker. As creatine phosphate reserves become depleted, ATP production continues to slow. If myocardial ischemia continues, an anaerobic respiration byproduct, hydrogen ions, accumulate and the intracellular pH decreases [6]. This leads to osmotic flooding of the myocytes and edema causing

permanent myocardium damage. In the following weeks fibroblasts infiltrate the damaged area and begin depositing fibrous collagen. Additionally, monocytes, neutrophils, and macrophages migrate to the infarction site as part of the inflammatory responses. Neutrophils release matrix metalloproteinases (MMPs), causing further infarct expansion and myocyte collagen degradation [8].

Cardiovascular disease is currently the leading cause of death in the United States [9]. Annually, approximately 920,000 people in the United States suffer from myocardial infarction, with coronary heart disease costing over $320 billion a year [10, 11]. MI can affect up to a billion heart cells, which decreases the workload of the heart [12]. Following a MI, in 2010 alone over one million patients were diagnosed with heart failure, meaning their heart is unable to sufficiently pump blood to the body's organs. Heart failure alters a patient's ability to perform tasks requiring physical exertion or often even basic daily activities [13]. The number of deaths attributed to heart failure has remained relatively constant (approximately 287,000) between 1995 and 2011 [11].

1.2 Clinical Treatments

The heart has an extremely limited regenerative capacity and cannot repair itself following an MI, requiring medical intervention. If an infarction is left untreated, remodeling can occur, changing the dimensions of the left ventricle and causing ventricular wall thinning [14]. The ejection fraction, or the fraction of blood contained within the left ventricle that is actually ejected with each heartbeat, declines with an increase in infarct size [14]. In an effort to maintain normal stroke volume and cardiac output, the contractile pattern and length of the uninfarcted zone changes, often called compensatory responses, and increases the risk of ventricular aneurysm and rupture [14].

Currently the treatment for MI is aimed at treating the effects of the infarction, not heal the underlying problem, the infarct zone. Current treatments include cardiac bypass and ventricular remodeling. Coronary bypass is a revascularization method used to restore essential blood flow to the myocardium [15]. Coronary artery bypass grafting (CABG) uses a blood vessel to divert blood around the infarction site and restore blood flow to the ischemic area, however this will not regenerate myocardial cells or restore function in the stiff collagenous region [15]. Reshaping the heart involves using one of two procedures: direct linear closure or endocardial patch plasty [16].

Direct linear closing removes the infarct and sutures the heart back together. While this removes the infarct there may not be enough healthy myocardial tissue, depending on the size of the infarct, to effectively reconstruct the heart to proper dimensions [17]. If an infarct is too large to be safely removed, an endocentricular patch plasty is performed. The patch can be synthetic or autologous tissue and is anchored to the ventricular wall. This method surgically places a patch over the infarcted site and sutures the patch into place (infarct can also be removed and the patch is placed over the hole left by the removed infarct) [17].

Ventricular remodeling surgery is used to reshape the heart following a MI and the removal of the infarct. A balloon is inflated within the left ventricle, showing the surgeon the initial shape and volume of the original heart. While the infarct is removed this balloon aids the surgeon by providing a guide in restoring the heart to the original, more efficient shape. The infarct is then removed. A suture is placed around the incision site and tightened bringing the ventricle to the shape of the balloon. A synthetic patch is used to close any remaining gaps in the ventricular wall; this patch is made of either polyethylene terephthalate (PET, or commercially called Dacron) or polytetrafluoroethylene (PTFE). The patch restores the volume of the ventricle and prevents shrinking of the heart [17, 18]. This surgical procedure restores the original dimensions of the heart and maintains pressure, but contractile tissue regeneration occurs. PET and PTFE are inert and have mechanical properties much stronger than native cardiac tissue [19]. This leads to regions of fibrosis caused by the large difference in mechanical properties between the tissues and implant, similar to stress shielding; scar tissue formation still occurs and can still grow [19].

1.3 Cellular Therapies in Cardiac Regeneration

Cellular therapies in cardiac regeneration are aimed at restoring the original function of cardiac tissue as opposed to removing the infarct. Several cell types have been used in cellular therapies for restoring cardiac tissue, including bone marrow stem cells, skeletal myoblasts, embryonic stem cells, cardiac stem cells, and fetal cardiomyocytes [20-23]. Skeletal myoblasts will not electrically couple with myocardium tissue and have been known to cause fibrillation, embryonic stem cells have potential tumor formation, cardiac stem cells have controversial existence, and fetal cardiomyocytes cannot be obtained in sufficient numbers to be an effective

treatment [20-23]. This leaves bone marrow stem cells, specifically hMSCs a promising cell type for cardiac repair [24-26].

1.3.1 Mesenchymal Stem Cells in Cardiac Repair

Isolated from adult bone marrow, hMSCs are an adherent, multipotent cell type having the ability to differentiate into bone, cartilage, and fat. hMSCs consist of between 0.001 to 0.01% of the nucleated cells within bone marrow [27, 28]. They have several characteristics which make them appealing in regenerative medicine. These include relative ease of isolation, high expansion potential in-vitro, and genetic stability [27-29]. Specifically in cardiac regeneration, hMSCs can induce angiogenesis, be used allogenically without an immune response, and differentiate into cardiac myocyte-like phenotype [24, 28, 30]. hMSCs have been delivered to the heart and found to have improved cardiac function in terms of reduced infarction size and an increase in ventricular pressure [31-36].

Table 1: MSCs in cellular therapies.

Species	Delivery Method	Cell Population (and Quantity)	Results	Reference
Rat	IM	Autologous MSCs (10^6): freshly isolated, 5-aza treated, untreated	• Cellular engraftment at 5 weeks • Increase in cardiac capillary density • LVSP and LVDP increase (5-aza) • Decrease: scar area and LV chamber size	[37]
Rat	IM	Autologous MSCs and CMEC (10^8)	• Increase in cardiac capillary quantity and density • Increased myocardial perfusion • LVEF increase (45±2.2)	[38]
Rat	IM	Autologous MSCs (10^7)	• Increase in capillary density • Increase in LVEF and perfusion to scarred region	[39]
Rat	IM	Autologous MSCs and peripheral blood	• Increase in capillary density • LVD and LVEDV restored	[40]

		mononucleated cells ($5*10^6$)	to baseline (MSC) • Increase in FS • Decrease in collagen deposition (MSC)	
Rat	IM	Allogenic MSC (10^7)	• Increase in capillary density • Increase in LVSP and wall thickness • Decrease in LVEDP and infarct size	[41]
Rat	IM	Allogenic MSC, ASC, or AD-CMG (10^6)	• Low engraftment at ASC and MSC at 1 week (none at 4 weeks) • Increase in capillary density • Increase in LVEF at 4 weeks (ASC only) • Decrease in infarct size	[42]
Mouse	IM	Xenogenic MSC - human ($5*10^5$ or $1*10^6$)	• Majority of delivered cells in: spleen, liver, and lungs • Transplanted MSCs morphologically similar to native myocardium and express demsin, β-myosin heavy chain, α-actinin, cardiac troponin T, and phospholamban • Low engraftment (0.44% after 4 days)	[30]
Mouse	IM	Allogenic MSC ($5*10^4 – 5*10^5$)	• Increase in LVDP • Decrease in LVEDP and infarct area	[43]
Mouse	IM	Allogenic MSC ($5*10^4 – 5*10^5$)	• Engraftment at 2 weeks (not quantified) • New cardiomyocytes in infarcted area • Decrease in infarct size and fibrosis	[44]
Mouse	IM	Allogenic MSC ($5*10^4$)	• Engraftment at 10 days (not quantified) • Increase in capillary density and number for arterioles • Decrease in LVEDP and infarct size	[45]
Mouse	IM	Allogenic MSC	• Engraftment at 2 days	[46]

		($6*10^4$)	(25% of donor cells detected in border zone) • Gap junctions between donor cells and host cells • Restore contraction • Increase in LVDP and wall thickness • Decrease in LVEDP, scar formation, and chamber volume	
Pig	IM	Autologous MSC ($6*10^7$)	• "Significant" engraftment (not quantified) • Preservation of wall thickness	[47]
Pig	IM	Allogenic MSC ($2*10^8$)	• >50% MSC engraftment in 8 weeks • Decrease in infarct size • Increase in cardiac function • By 4 weeks myocardial efficacy returned to normal • Engrafted cells: express VEGF and VanWillebrand factor	[48]
Pig	IC	Autologous ASC or MSC ($2*10^6$)	• Engraftment at 30 days (not quantified) • Increase in capillary density • Increase in LVEF and wall thickness (both groups)	[49]
Dog	IM	Allogenic MSC (10^8)	• Increase in vascular density and LVEF • Decrease in collagen fibrosis	[50]

5-aza: 5-azacytidine, IM: intramyocardial, IC: intracoronary, LV: Left Ventricle, LVEDP: Left Ventricular End Diastolic Pressure, LVEDV: Left Ventricular End Diastolic Volume, LVEF: Left Ventricular Ejection Fraction, LVDP: Left Ventricular Developed Pressure, LVSP: Left Ventricular Systolic Pressure, LVD: Left Ventricular Dysfunction,

1.3.2 Myocardial Cellular Therapy Limitations

As seen in Table 1, IM injections have been widely examined as a method for improvement in cardiac function following a MI. There are several limitations associated with IM injections, including low cellular engraftment and retention, poor localization, low survival rates, and no matrix for cell adhesion, which often leads to cell death [12, 24-26, 51].

In order for cellular therapies to provide any benefits, cells must be effectively delivered to the desired area. Studies have investigated engraftment of hMSC following IM injections. In a study performed by Hou et al, peripheral blood mononuclear cells were radiolabeled and delivered using the intramyocardial (IM), intracoronary (IC), or interstitial retrograde coronary venous (IRV) into a swine model. Myocardial ischemia was induced using balloon occlusion for forty-five minutes. 10^7 111 indium-oxine–labeled human PBMNCs were delivered using IC, IM, or IRV injection after 6 days. After cell delivery, animals were euthanized and organs were harvested for cell distribution assessment using γ-emission counting. Upon investigation of the heart, a majority of the delivered cells were not retained by the heart (IM injection (11±3%), IC (2.6±0.3%), and IRV (3.2±1%) [52]. Many of these cells that were intended for delivery to the heart were in fact entrapped in other organs including the lungs, spleen, and liver [52].

Another study performed by Guyette et al, used IM injections to delivery 100,000 hMSCs to infarcted rat hearts. Following one hour after injection, hearts were fixed and sectioned to quantify the amount of engrafted hMSCs via quantum dots. Rats that underwent IM injections had engraftment rates of 11.8 ± 6.2% [53].

Injecting a liquid cellular suspension into contracting heart muscle resulted in a high percentage of cells leaking out of the heart, partially due to the heart's contraction and the puncture hole created by the needle [12, 51]. A liquid suspension (Phosphate Buffered Solution (PBS) or media) is required to deliver cells via IM injection. A liquid does not provide a matrix for cell attachment, which plays a role in cell death [25, 26, 54].

1.4 Fibrin Microthread Biological Sutures

1.4.1 Fibrin Scaffolds and Tissue Engineering

Fibrin is a naturally occurring biopolymer and has been used as a biomaterial for tissue regeneration. A series of coagulation reactions are triggered by platelet adhesion which occurs following an injury. Platelet adhesion initiates the production of thrombin, a protease which cleaves fibrinogen. Fibrinogen is a protein found in blood and when cleaved by thrombin fibrin forms. Fibrin is an insoluble protein that stops bleeding at a wound site and promotes healing [55]. In the body, fibrin forms a provisional matrix that aids in the healing process by creating a scaffold for cell adhesion, migration, and infiltration [55]. Fibrin contains the protein sequence: arginine-glycine-aspartic acid (RGD), this ligand binding motif promotes cell adhesion. In addition to promoting cell adhesion, fibrin can be produced from autologous fibrinogen and thrombin, contains natural growth factors, is angiogenic, and is Food and Drug Administration (FDA) approved for clinical glues and sealants [56-58].

Fibrin is a versatile biopolymer with a variety of uses in tissue engineering. Fibrin hydrogels have been used in: adipose, cardiovascular, ocular, muscle, liver, skin, cartilage, neural, and bone applications [59]. These fibrin hydrogels can be composited with different plastics (polyurethanes, polycaprolactone-based polyurethanes, polycaprolactones, b-tricalciumphosphates, b-tricalciumphosphates/ploycaprolactones, and polyethylene glycols), to create customizable properties (mechanicals, surface properties, or degradation) [59]. Fibrin glue is used as a sealant or a tissue adhesive, used in surgical procedures to reduce blood loss, accelerate healing, and protect against infection [60]. Fibrin glues can be sued as a delivery mechanism for cells or a scaffolding matrix [61-63]. Fibrin glues have been used in maxillofacial bone, periodontal bone, bone, ear cartilage, cartilage, cornea, heart, blood vessel, tendon, and ligament regeneration, in addition to wound healing following severe burns and chronic wounds [59]. Fibrin scaffolds can be coated with extracellular matrix proteins, such as fibronectin, vitronectin, laminin, and collagen, to incorporate biological activity and cellular adhesion [64].

1.4.2 Fibrin Microthreads

A fibrin extrusion process has been developed at WPI [65]. Fibrinogen and thrombin are coextruded to form discrete fibrin threads. These threads are bunched and intertwined together forming bundles which are then made into sutures. These sutures have been shown to an effective scaffold, allowing hMSC seeding on the sutures surface. hMSCs delivered using fibrin microthread sutures exhibited an engraftment rate of 63.6 ± 10.6%, a significant increases when compared to the 11.8 ± 6.2% seen in the IM injection group [53]. In addition to the improved engraftment rate, fibrin sutures evoked a different delivery mechanism when compared to IM injections. IM injections, involve a liquid being injected into the contracting heart muscle, which often has poor engraftment rate and a low percentage of hMSCs that remain in the heart [53]. The delivery of hMSC seeded sutures to the infarcted heart involves stitching the seeded fibrin directly into the infarcted region. This delivers the hMSCs very specifically and to a more localized when compared to IM injections.

Despite having an improved engraftment and more localized delivery, there is a low initial seeded. 100,000 cells are seeded on the fibrin sutures, however after twenty four hours of seeding, less than 10,000 hMSCs adhere to sutures [66]. There are two methods to increase the number of cells that are adhered to cells (excluding coating sutures with adhesion proteins): increasing the seeding density, and increasing the culture time. Increasing the seeding density with introduce more cells to the 24 hour seeding period. If the adhesion percentage remains the same, there are still a high number of cells that are being wasted, not adhering to the suture. The large number of cells that would be wasted makes this an unfavorable approach. Increasing the culture time would allow hMSCs to proliferate on the suture, leading to more hMSCs on the suture. The problem with this approach is that hMSCs secrete fibrinolytic enzymes [67]. The longer the hMSCs are cultured the more of the suture degrades, creating a weaker suture that will not have the mechanical strength to suture through the heart and deliver hMSCs.

1.4.2 Degradation of Fibrin

Fibrinolysis, or the breakdown of fibrin, is a heavily regulated by numerous receptors, cofactors, inhibitors, activators, and substrates [68]. The components of fibrinolysis of are listed in Table 2 and illustrated in Figure 1.

Table 2: Components of fibrinolysis

Zymogen	Plasminogen activators	Inhibitors	Attenuator	Major Receptors - Activating	Major Receptors - Clearance
Plasminogen (N-terminal glutamic acid and lysine variants)	Tissue plasminogen activator (tPA)	Plasmin inhibitors	Thrombin-activatable fibrinolysis inhibitor (TAFI)	Annexin 2	Low-density lipoprotein receptor-related protein (LRP)
		α2-plasmin inhibitor (α2-PI)			
		α2-macroglobulin (α2-MG)			
		Protease nexin		αMβ2 integrin	
	Urokinase (uPA)	Plasminogen activator inhibitors			Mannose receptor
		Plasminogen activator inhibitor-1 & -2 (PAI-1, PAI-2)			
		C1-esterase inhibitor		Urokinase receptor (uPAR)	
		Protease nexin			
		Plasmin inhibitors			

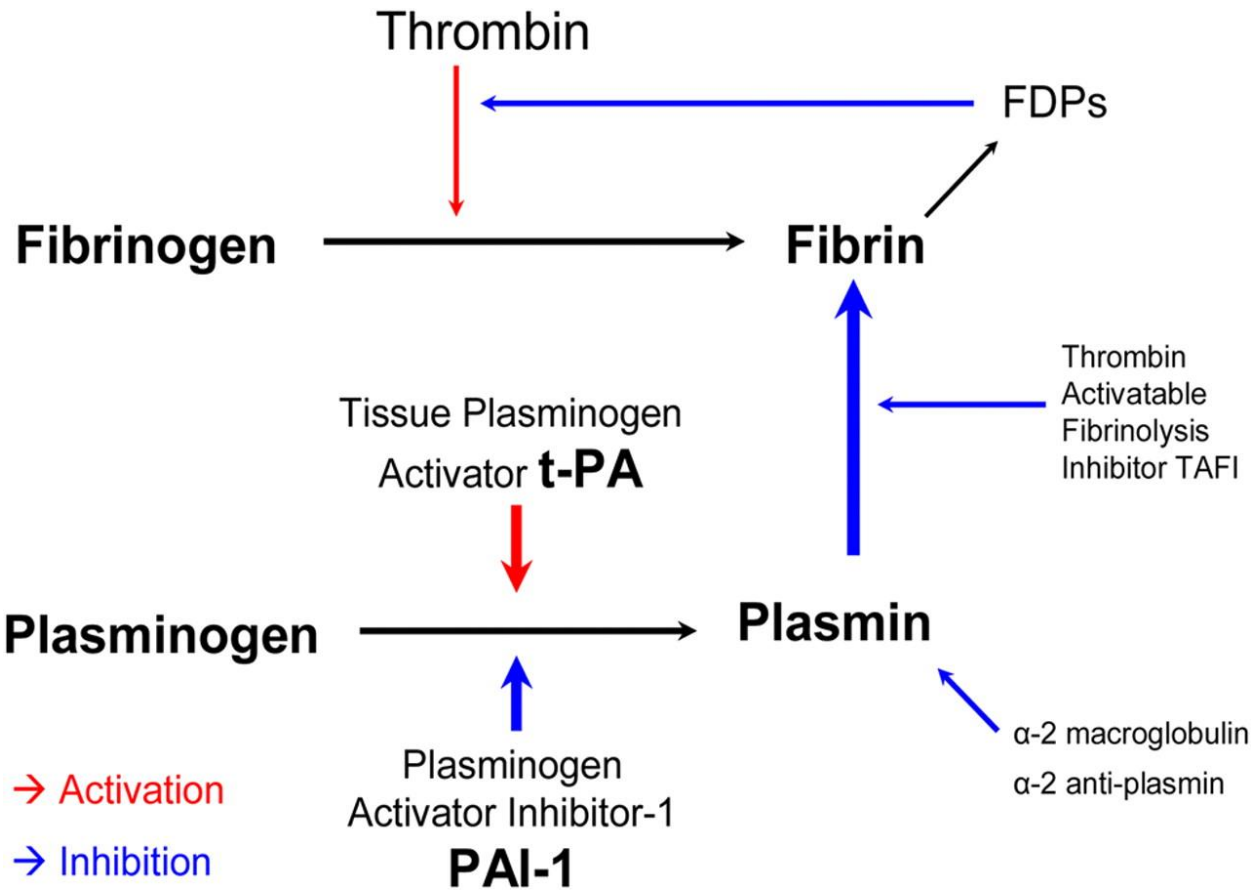

Figure 1: Fibrinolysis Pathway. Red arrows indicate activation. Blue arrows indicate inhibition. (Image adapted from cri.sagepub.com/content/15/5/188/F1.large.jpg)

Plasmin is one the primary fibrinolytic proteases *in vivo*. A zymogen found naturally circulating in blood; plasminogen (PLG) can be cleaved and converted to plasmin by tissue plasminogen activator (tPA) or urokinase plasminogen activator (uPA). Plasmin is also involved in a positive feedback mechanism, deactivating tPA and uPA. Fibrin regulates its degradation by actively binding to PLG and tPA, which localizes and enhances plasmin generation in close proximity to fibrin. When unbound to fibrin, tPA is a weak activator of PLG, but in the presence of fibrin, the binding affinity and activation are greatly enhanced [68].

Plasmin cleaves fibrin into soluble fibrin degradation products (FDP). During degradation, carboxy-terminal lysine residues are exposed, further enhancing binding to the lysine binding sites of tPA and PLG. The lysine binding sites can be blocked by thrombin-activatable fibrinolysis inhibitor (TAFI), which in turn decreases plasmin generation and slows fibrinolysis. Fibrinolysis is

also regulated by PLG activation inhibitors (PLG activator inhibitor-1 (PAI-1)) and plasma inhibitors (α2-plasmin inhibitor (α2-PI)). However, because fibrin bound plasmin has lysine binding sites are occupied; it is blocked from α2-PI [68]. Cells can also promote plasmin formation by surface receptors. Endothelial cells, monocytes, macrophages, neutrophils, and some tumorigenic cells have been shown to bind to PLG, tPA, or uPA [69].

hMSCs are important in the wound healing process and have been shown to express PLG, uPA, tPA, and PAI. This indicates that hMSCs can regulate and control fibrinolysis in both autocrine and paracrine mechanisms. A study by Neuss et al, investigated the fibrin degradation by hMSCs. They found that when hMSCs were seeded in fibrin clots, the hMSCs could degrade fibrin clots as indicated by amounts of the fibrin degradation product, D-dimer, found in solution. The entrapped hMSCs released fibrinolytic enzymes that triggered fibrin degradation. It was also observed that fibroblasts produced similar amounts of D-dimers as fibroblasts trapped in fibrin clots [67].

1.4.3 Aprotinin

Aprotinin ($C_{284}H_{432}N_{84}O_{79}S_7$), known as the drug Trasylol, is protease inhibitor isolated from bovine lung. Aprotinin is a monomeric globular polypeptide chain. With a molecular weight of 6512, aprotinin is 58 residues long, consisting of 16 different proteins, shown in Figure 2 [70]. Three disulfide bonds, a β-hairpin, and an alpha helix describe the tertiary structure of aprotinin [71]. The specific amino acid sequence for aprotinin is as follows: RPDFC LEPPY TGPCK ARIIR YFYNA KAGLC QTFVY GGCRA KRNNF KSAED CMRTC GGA [72]. Positive charged side chains (lysine-K and arginine-R) outnumber the negative side chains (aspartate-D and glutamates-E) 10 to 4, making aprotinin basic in solution. The three disulfide bonds between cysteine proteins (specifically at: Cys5-Cys55, Cys14-Cys38 and Cys30-Cys51) make aprotinin highly stable [72]. One of the basic side chains (the 15-lysine) binds to active sites and inhibits trypsin and similar proteases. At pHs above 10 and below 3.2, aprotinin is inactive as a result of aprotinin-protease complex dissociation. Reactivity of protease inhibitors are measured in units of Trypsin Inhibitor Units (TIU). 1TIU will decrease the activity of 2 trypsin units by 50%, where the 1 trypsin until will hydrolyze 1.0 µmole of N-α-benzoyl-DL-arginine p-nitroanilide (BAPNA) per minute at pH 7.8 and 25 °C. Another common unit of activity is the inhibition of kallikreins, the kallikrein inhibitor unit (KIU). Similar to TIU, one KIU will inhibit 2 kallikrein units by 50% at pH 7.8 and 25 °C. 1 TIU is equal to approximately 1,025 KIU [73].

Aprotinin inhibits trypsin, chymotrypsin, and plasmin at a concentration of 125,000 IU/mL and Kallikrein at 300,000 IU/mL.

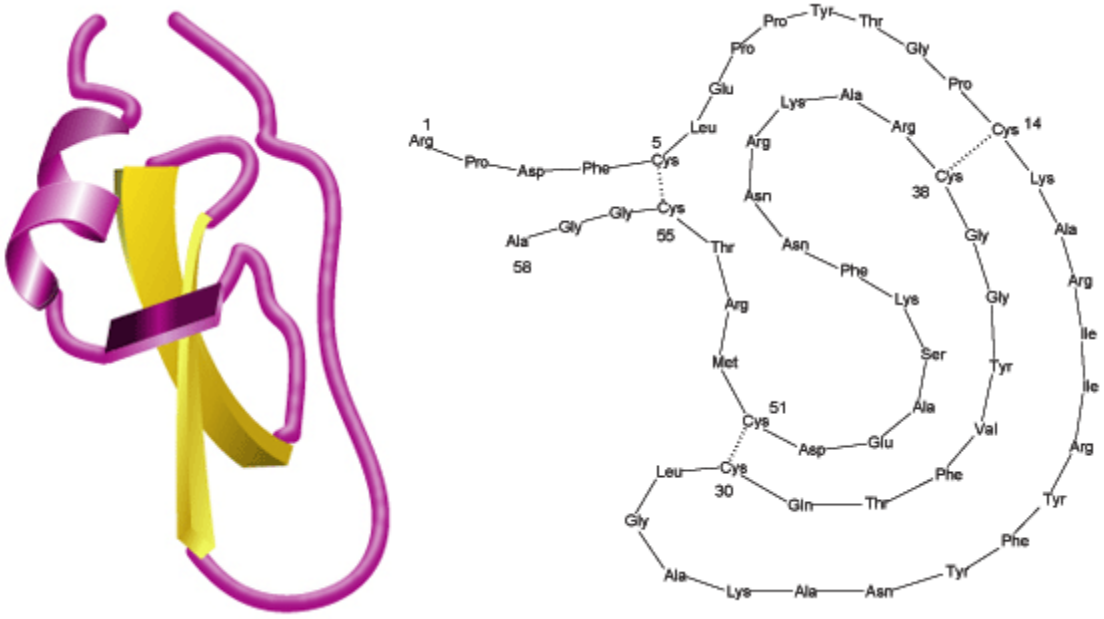

Figure 2: Aprotinin. 58 residues long with 3 disulfide bridges. (Image from Sigma-Aldrich information packet on Aprotinin)

Aprotinin, or Trasylol, was used in patients with an increased risk for blood loss, especially during CABG surgeries or any surgery with the need for blood transfusions. A study in 2006, studying the effects of aprotinin on cardiac surgery patients revealed that there was an increase in the risk of: acute renal failure, myocardial infarction, heart failure, stroke, and encephalopathy [74]. These results were exhibited again in 2007 [75]. Aprotinin was removed from clinical use in 2008, following the previously mentioned studies that suggested an increase in complications and death with aprotinin use [76]. However, in 2012 the European Medicines Agency scientific committee performed a full review of the "Blood conservation using antifibrinolytics" (BART) investigation of aprotinin. The committee found the BART study was skewed and the results were not indicative of the actual results. The investigation found that the benefits of the use of antifibrinolytic medicines, including aprotinin, outweigh the risks in a restricted range of indications and the suspension on aprotinin was lifted [77].

Chapter 2: Hypothesis and Specific Aims

We hypothesize that supplementing hMSC growth media with aprotinin will slow the degradation of hMSC seeded fibrin sutures. With a decrease in scaffold degradation, sutures will be able to be cultured for extended periods of time, without a loss of mechanical integrity.

Specific Aim 1: Examine the effect of aprotinin on cell-loaded sutures, in terms of suture degradation and suture mechanics

If aprotinin slows down the degradation of fibrin sutures, the amount of fibrin degradation products found in media will be decreased in sutures exposed to aprotinin. Using a range of concentrations of aprotinin: 0, 1, 5, 10, 50, and 100 μg per mL of standard mesenchymal stem cell growth media; the amount of fibrin degradation products will be quantified at Days 3, 6, and 9. An ELISA assay will be used to quantify the concentration of fibrin degradation products present in the media at each time point. The Elastic Modulus, Ultimate Tensile Strength, and Strain At Failure will be used to assess the mechanical properties after cells have been seeded for 24 hours and cultured for 3 days. Suture diameter will also be used to determine suture degradation.

Specific Aim 2: Determine the effect of aprotinin on hMSC viability, proliferation, and differentiation capacity

In order to aprotinin in an attempt to control suture degradation, it must not affect hMSC viability. To determine the effect of aprotinin on hMSC viability, hMSCs will be seeded and cultured on glass coverslips for one week before undergoing a LIVE/DEAD assay to determine the percentage of live cells. To examine cellular proliferation a stain for Ki-67 will be used to ensure aprotinin is not negatively effecting hMSC proliferation. hMSCs will be seeded on glass coverslips and cultured for three days, to ensure that confluence is not reached and proliferation decreases. hMSCs are

multipotent cells and aprotinin must not effect hMSC multipotency in order to be an effective method to reduce fibrin degradation. A differentiation assay will be used to determine the effect, if any, aprotinin has on hMSC differentiation. hMSCs will be differentiated into: adipocytes, chondrocytes, and osteocytes, after exposure to wither standard growth media or aprotinin supplemented growth media.

Specific Aim 3: Determine the effect of aprotinin on cell quantity on cell loaded sutures

For aprotinin to be useful, it must not negatively affect hMSCs loaded on fibrin based sutures. hMSCs will be seeded on fibrin sutures for twenty-four hours. The number of cells adhered to the sutures will be examined at Days 0 (immediately following the twenty-four hour seeding), 1, 2, 3, and 5. The number of cells remaining on the fibrin sutures will be determined via CyQuant Assays.

Chapter 3: Materials and Methods

3.1 Fibrin Microthread and Suture Production

Fibrin microthreads were coextruded using solutions of fibrinogen and thrombin, in a manner previously described [65]. In brief, thrombin isolated from bovine plasma (Sigma, St. Louis, MO T4648) at a concentration of 40 U/ml was frozen at -20°C as a stock solution; and diluted to a concentration of 6 U/ml in 40 mM $CaCl_2$ for extrusion. Fibrinogen (Sigma, St. Louis, MO F4753) was dissolved in HEPES buffered saline (HBS, 20 mM HEPES, 0.9% NaCl) at a concentration of 70 mg/mL and stored at -20°C. Fibrinogen and thrombin were warmed to 37°C and drawn up into two separate 1mL syringes. The fibrinogen and thrombin solutions were mixed in a blending applicator tip and coextruded through polyethylene tubing (0.38mm inner diameter, Beckton Dickinson, Franklin Lakes, NJ) at a crosshead speed of 4.25 mm/min. The polyethylene tubing extended into a bath of room temperature 10 mM HEPES at a pH of 7.4 (Figure 3). After fifteen minutes, the fibrin microthreads were removed from the bath and hung to air dry.

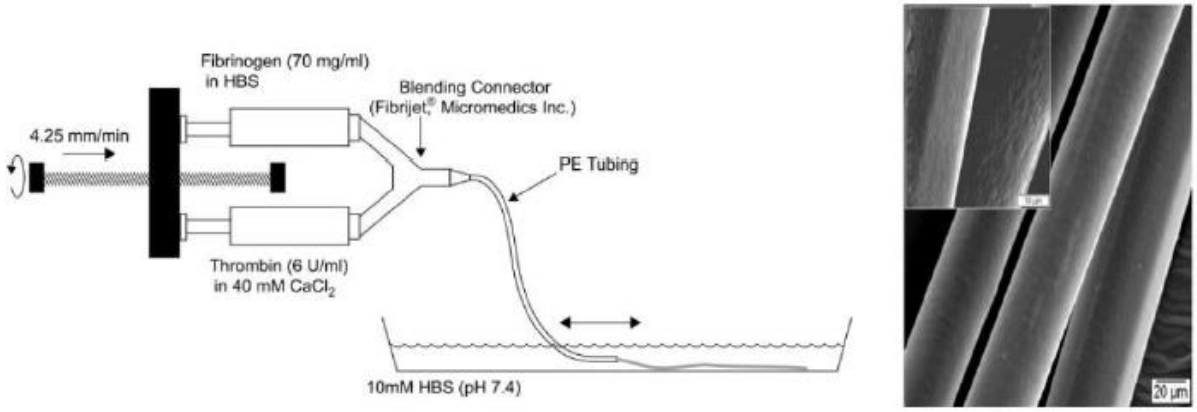

Figure 3: Fibrin microthread extrusion schematic and image of extruded threads [59].

To increase the mechanical properties of the fibrin microthreads and increase the area for cellular adhesion, several microthreads were bundled together to form a single large diameter microthread, as seen in Figure 4. Twelve microthreads were placed parallel to each other and grouped together by dragging a droplet of PBS along the threads. Once the twelve microthreads were grouped together the bundle was twisted to form an entwined bundle.

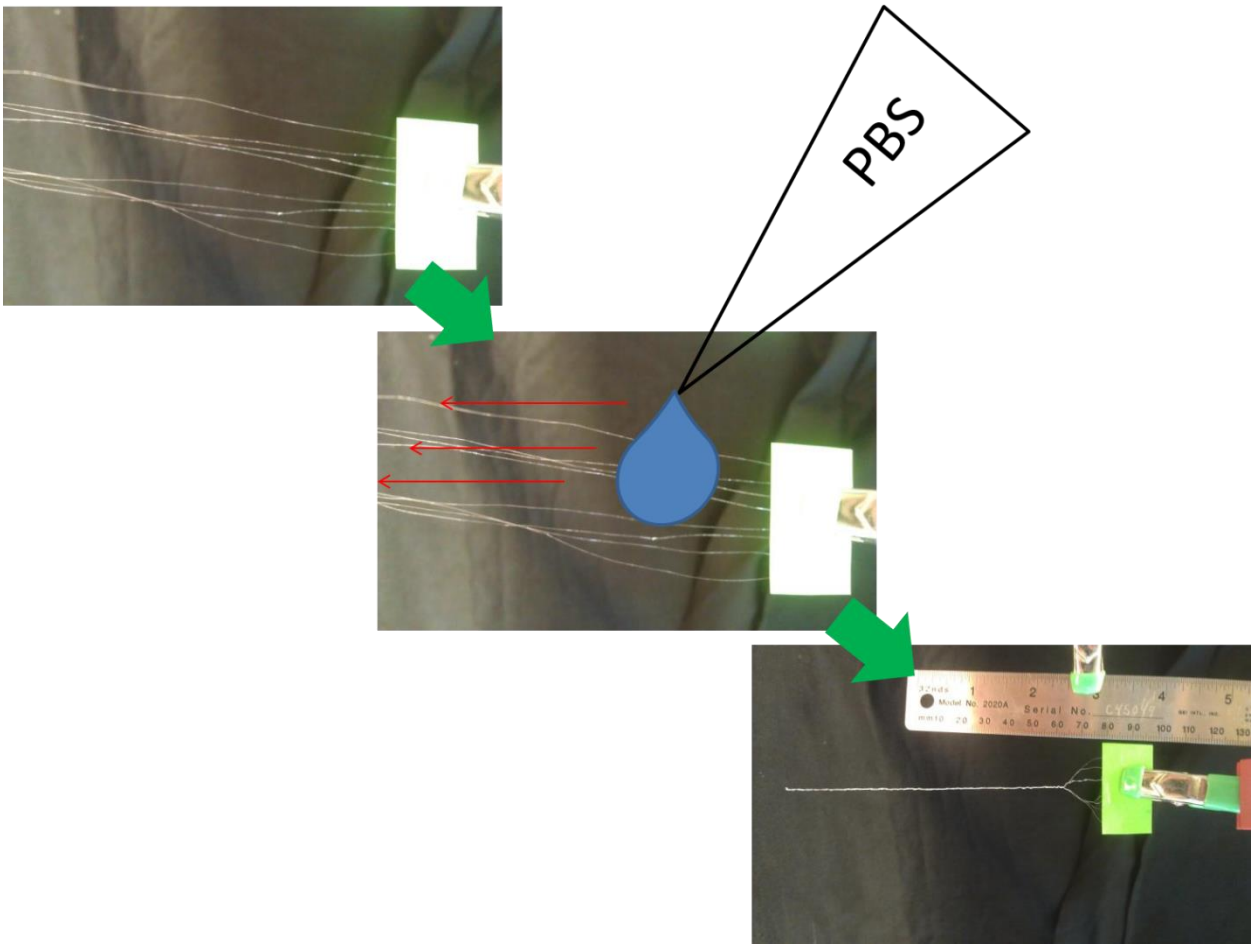

Figure 4: Microthreads to bundles. Using a drop of PBS, 12 separate fibrin microthreads are brought together and twisted to form a single bundle of 12 fibrin microthreads.

Microthread bundles were cut 4 cm lengths (8 cm lengths were used for mechanical testing), shown in Figure 5. Each cut microthread bundle was threaded through the eye of a surgical suture needle (size #20, 3/800 circle, tapered; Securos Surgical, Fiskdale, MA). With the needle placed in the center of the bundle, the bundle was hydrated for twenty minutes in DI water. After hydration the ends of the bundle were folded together, twisted, and dried to form a 2 cm suture (4 cm for mechanical testing) of twenty-four microthreads.

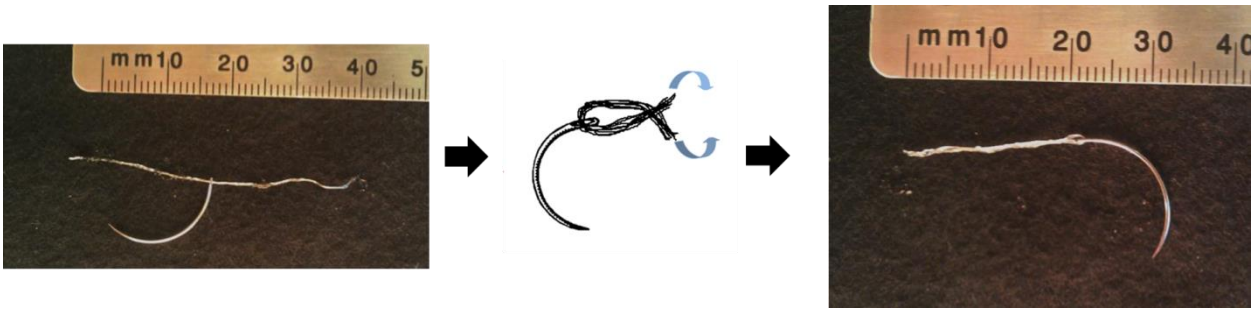

Figure 5: Suture Fabrication. 12 bundles of fibrin microthreads are cut to 4 cm, placed through the eye of a suture needle, hydrated in DI water, and twisted forming a 2 cm long suture.

To seed the sutures with cells a bioreactor was constructed around each suture, seen in Figure 6. A section of gas-permeable Silastic tubing (1.98-mm ID, Dow Corning, Midland, MI) approximately double the length of the suture was used to house the fibrin suture. A slide clamp was used to secure a 27-gaugue needle and the suture needle inside the bioreactor tubing and sterilized using a twelve hour cycle of ethylene oxide gas.

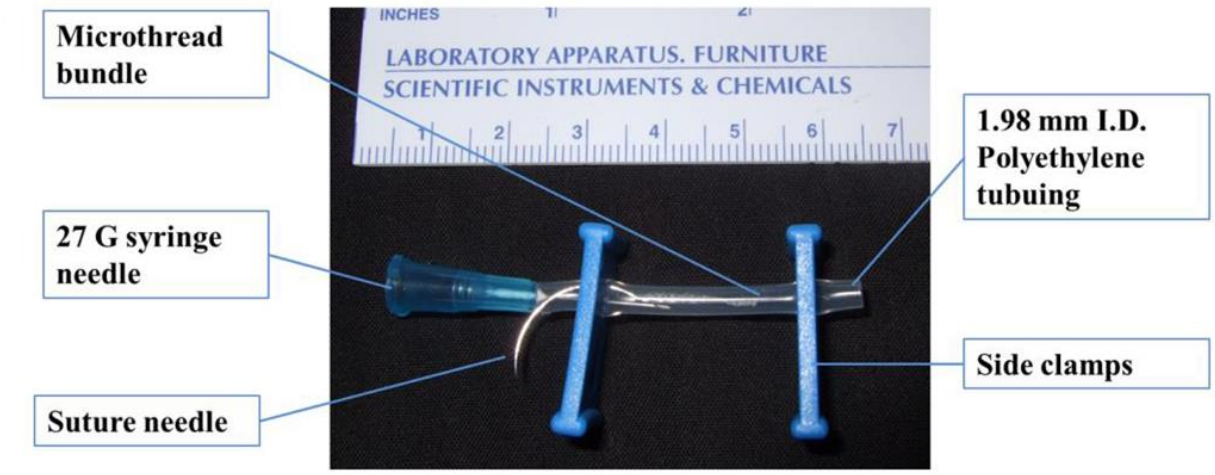

Figure 6: Suture housed inside bioreactor. Gas permeable polyethylene tubing is used to allow ethylene oxide sterilization to occur and to allow gas exchange when cells being seeded, the 27 Gauge syringe needle is used to deliver hMSCs, and the slide clamps holds the cellular suspension in the bioreactor.

After sterilization, the sutures were rehydrated in sterile Dulnecco's Phosphate Buffered Saline (DPBS, Mediatech Inc, Manassas VA) for twenty minutes. Sutures were seeded with a cellular suspension concentration of $1x10^6$ cells/mL and at 50,000 cells per 1 cm of suture. 100 µL of the cellular suspension was drawn up into a 1 mL syringe. The syringe, containing the cellular suspension, was attached to the 27 gauge needle of the bioreactor and used to inject the cellular

suspension. Bioreactors were then loaded into vented 50 mL conical tubes and placed on a rotator in a 37^{O}C incubator (5% CO2, atmospheric gas concentrations). Sutures were seeded for 24 hours.

Human mesenchymal stem cells (hMSCs; Lonza, Walkersville, MD; passage 5-8) were cultured in Mesenchymal Stem Cell Growth Medium (MSCGM; Lonza PT-3001, Walkersville, MD) in compliance with the manufacturer's instructions. Aprotinin was supplemented to complete MSCGM at a concentration of 100 µg/ml. Aprotinin supplemented media will be referred to as "Aprotinin" for the remainder of this paper, the concentration of aprotinin in MSCGM will be 100 µg/ml unless otherwise noted. This stock media was frozen in 10 mL aliquots and thawed as needed. After it was thawed it was used in less than two weeks; after this thaw media was not refrozen.

3.2 Preliminary Fibrin Degradation

Sutures (Aprotinin n=3 and MSCGM n=3) were seeded in a manner previously described. After seeding for 24 hours, sutures were plated in individual wells of a 12 well plate with 1 ml of either Aprotinin or MSCGM. Sutures were not disturbed. Media changes occurred every three days and light media swirling occurred every day. Sutures were not removed from the wells. Media changes took place until threads were degraded.

3.3 Fibrin Degradation Product ELISA

An FDP ELISA kit (NeoBioLab, Cambridge, MA) was used to determine the amount of FDP present in media used to culture seeded sutures. Sutures were created and seeded in the manner previously described. After cells were seeded, sutures were placed in wells of a twelve well plate and cultured in the following concentrations of aprotinin in MSCGM: 100, 50, 10, 5, 1 and 0 µg of aprotinin per mL of MSCGM (Aprotinin-100,-50,-10,-5,-1, and MSCGM, respectively), with controls being unseeded sutures in PBS, MSCGM, and Aprotinin-100. Media changes occurred every 3 days for 9 days. Media was removed and placed in 2 ml Eppendorf tubes and stored at -80^{o}C until all samples were collected. Sample and components of the FDP ELISA were allowed to thaw to room temperature. 100 µL of samples were added to wells of the ninety-six well microtiter plate and 10 µL of balance solution was added to each. The FDP ELISA kit includes dilutions of FDP, in order to create a standard curve, which were also placed in the microtiter plate; these dilutions were: 0, 0.5,

1, 2.5, 5, and 10 mg/mL. 50 µL of conjugate was added to well with samples or standards, and mixed well. After mixing, the plate was covered and incubated at 37°C for 1 hour. Wells were washed 5 times with 300 µL of wash solution and blotted dry. 50 µL of Substrates A and B were added to wells containing samples or standards. The plate was covered and incubated at room temperature for 15 minutes. 50 µL of stop solution was mixed into each well. The optical density (OD) at 450 nm was then measured on a Victor3 1420 Plate Reader.

A standard curve was created by plotting the optical densities of the included standards against the concentration of FDP. A best fit line was created in order to determine the concentration of FDP in the collected samples.

3.4 Suture Mechanics

4 cm sutures were seeding with 200,000 hMSCs per suture, in the manner previously described. After seeding, the sutures were plated in separate wells of a six well plate with 3 mL of either MSCGM or Aprotinin. After three days, sutures were removed from the media for diameter measurements and mechanical testing. Three days was used as the end point because after three days of culture, there is no significant increase in the number of cells on the suture (16), and after three days, the control sutures had little to no mechanical integrity and could not be loaded for mechanical testing. These sutures often broke while loading sutures into the Instron grips. Sutures were removed from media and rinsed and store in PBS until diameter measurement and mechanical testing the same day. Test groups for thread diameters and mechanical testing included: MSCGM, Aprotinin, MSCGM with no cells, Aprotinin with no cells, and sutures hydrated in PBS for twenty minutes.

3.4.1 Thread diameters

Before mechanical testing, sutures were placed on a glass slide and three images were acquired on Leica DM LB2 microscope at 5 x. Suture diameters were measured with no coverslip on top of the suture. Because the sutures are two bundles twisted together there is a large difference in diameter when looking at the threads on a two dimensional plane. In order to get a representative diameter over the 4 cm of the suture, three images were taken of each suture: one at the left end (in the first cm of the thread, proximal to the needle), center (approximately 2 cm

from the needle), and the right end (at the end of the thread distal to the needle). For each image the maximum and the minimum diameters were recorded. The average suture diameter determined by taking the average of the six diameters obtained for each suture.

3.4.2 Mechanical Testing

Mechanical testing was performed on an Instron E1000, using a 1N load cell. Sutures were secured in custom grips and loaded onto the Instron. Once loaded on the Instron, the sutures were hydrated using PBS from a dropper a final time before testing. A 10 mN load was applied to the sutures, and a ruler was used measure the distance between the grips (this value was used as the initial length of the suture). Using Bluehill software, a tensile test to failure was performed on each suture. The data output by BlueHill was in Force (N)/Displacement (mm). Using the average suture diameter and the gauge length, the Force-Displacement data was converted to Stress/Strain and plotted. From the Stress-Strain curve the Ultimate Tensile Strength (UTS), Modulus (E), and Strain at Failure (SAF) was calculated.

3.5 Cell Viability

To confirm hMSC viability, a LIVE/DEAD Viability/Cytoxicity Kit for mammalian cells (Invitrogen L-3244, Carlsbad, CA) was used. This kit uses two stains, calcein and ethidium. Calcein is absorbed by cells and fluoresces green when intracellular esterase activity occurs; which only occurs in live cells. Ethidium penetrates the nuclei of dead cells; and binds to nucleic acids, fluorescing red. Hoechst was used as a nuclei stain to identify cells.

hMSCs were seeded on glass coverslips at a seeding density of approximately 5000 cells/cm^2. Six coverslips were cultured in MSCGM and six were cultured in MSCGM or Aprotinin. Media was changed every 3 days until confluence was reached; this occurred in approximately seven days.

After the hMSCs on the coverslips had reached confluence, they were rinsed in PBS and incubated at 37^{O}C with a 1:1000 dilution of ethidum, 1:1000 dilution of calcein, and a 1:2000 dilution of Hoechst for 30 minutes. The coverslips were mounted on glass slides using Cytoseal, and images using a Leica DM LB2 microscope at 20x magnification. Images were acquired using a blue, red, and green fluorescent channels to acquire the hMSC nuclei, dead cells, and live cells,

respectively. Two sets of images were acquired from each coverslip and the average numbers of live and dead cells were determined.

Images were imported into ImageJ to quantify the numbers of live and dead cells. Using the blue channel, the Hoechst stain, the image was split into red, blue, and green channels; and the blue channel was thresholded until only the nuclei remained. From there the nuclei were counted using the Particle Analysis function on ImageJ, indicating the total number of cells. This was repeated for the ethidium and calcein stained images to determine the number of dead and live cells, respectively.

3.6 Ki-67 Proliferation

To determine if aprotinin affected hMSC growth a stain for Ki-67 was used. Ki-67 is a protein expressed during cellular proliferation, specifically during the G1, S, G2, and M phases. hMSCs were seeded on glass coverslips at a seeding density of approximately 5000 cells/cm^2. Six coverslips were cultured in MSCGM and 6 were cultured in Aprotinin.

After three days, the cover slips were rinsed with PBS, fixed for fifteen minutes in 4% paraformaldehyde in PBS, and then rinsed again with PBS. 0.25% Triton-X100 in DI water was used to permeabilize hMSCs for twenty minutes. After permeabilization, the coverslips were rinsed with PBS and blocked with 5% goat serum in PBS for thirty minutes. Coverslips were incubated at 4^oC with rabbit anti Ki-67 monoclonal at a dilution of 1:100 (Sigma,AB1667) in 3% goat serum in PBS for 10 hours, then rinsed in PBS. Alexa-fluor 568 goat anti-rabbit at a dilution of 1:400 (Invitrogen A11036) in 3% goat serum in PBS was used as the secondary antibody and incubated at room temperature for one hour. The coverslips were rinsed with PBS then counterstained with Hoechst at a concentration of 1:6000 for five minutes. Coverslips were again rinsed in PBS and mounted using Cytoseal. Fluorescent images were acquired using a Leica DM LB2 microscope. Two images were acquired from each coverslip and the average numbers of Ki-67 positive cells were counted.

The same thresholding technique used for the LIVE/DEAD analysis was used for determining the percent of Ki-67 positive cells. The Hoechst stain, viewed through the blue channel, was used to determine the number of cells. The Hoechst stained image was split into red, blue, and green channels. The blue channel was thresholded until only the nuclei remained and the remaining

nuclei were counted using the Particle Analysis function on ImageJ. This process was repeated on the Ki-67 stained image, which was taken using the red fluorescent cube on the Leica DM LB2 microscope. This image was split into the red, blue, and green channels, and the red was thresholded and analyzed, determining the number of Ki-67 positive cells.

3.7 Differentiation Assay

hMSCs are multipotent cells, meaning they have the ability to differentiate into multiple cells types. To ensure that aprotinin does not hinder the multipotency capacity of hMSCs a differentiation assay was performed. hMSCs were differentiated into the following three cell types: adipogenic, osteogenic, and chondrogenic.

3.7.1 Adipogenic Differentiation

For adipogenic differentiation, hMSCs were seeded at 5000 cells/cm^2 in 12 well plates and cultured in either MSCGM or Aprotinin. Media changes occurred every 3 days until cells were 100% confluence.

Adipogenic differentiation was completed using adipogenic kit from Lonza (Adipogenic Differentiation Medium, PT-3004). hMSCs were fed for three cycles of three days with Adipogenic Induction Medium followed by three days with Adipogenic Maintenance Medium. After the three cycles of Maintenance and Induction media, all cells were cultured for an additional cycle in Adipogenic Maintenance Medium. hMSCs were differentiated in three separate experiments with n = 3 in each experiment. The control group for adipogenic differentiation was n = 3 wells of a twelve well plate, grown to confluence in either Aprotinin or MSCGM.

3.7.2 Oil Red O Stain

To assess lipid vacuole formation, adipogenic cells were stained with Oil Red O. Cells were fixed using 4% paraformaldehyde in PBS for fifteen minutes, rinsed in distilled water for five minutes then dehydrated in 60% isopropanol for five minutes. 300 mg of Oil Red powder (Sigma Aldrich, St. Louis, MO) was dissolved into 100 mL of 100% isopropanol to make the Oil Red O stock solution. To create the working solution, three parts of the stock solution were combined with two parts of a 10% Dextrin-DI solution; then filtered using a 0.80 µm membrane syringe filter (Corning

Incorporated, Corning, NY). Cell cultures were stained with the Oil Red O working solution for five minutes and counterstained with Mayer's hematoxylin (Sigma Aldrich, St. Louis, MO) for one minute before rinsing with DI water. Stained images were acquired with a LEICA DMIL microscope.

3.7.3 Osteogenic Differentiation

hMSCs were seeded at 5000 cells/cm^2 in twelve well plates and cultured in either MSCGM or Aprotinin. Media changes occurred every three days until cells were 100% confluence. Cells were then fed Complete Osteogenic Differentiation Media (Lonza, Walkersville, MD). Media changes occurred every three days for three weeks. Over the course of the osteogenic differentiation, cells were observed under a LEICA DMIL microscope to confirm changes in cell morphology from spindle to cuboidal shaped. hMSCs were differentiated in three separate experiments with n = 3 in each experiment. The control group for osteogenic differentiation was n=3 wells of a twelve well plate, grown to confluence in either Aprotinin or MSCGM.

3.7.4 Alizarin Red S Stain

Alizarin Red S was used to assess calcium deposits. Cells were first rinsed with calcium free PBS (Invitrogen, Carlsbad, CA) for one minute and fixed in 4% paraformaldehyde in PBS for fifteen minutes. After fixing cultures were rinsed with PBS and DI water for 5 minutes each. The Alizarin Red stock solution was made by dissolving 2 grams of Alizarin Red Powder into 100 mL of DI water. The pH of the stock solution was adjusted to 4.1-4.3 using 10% ammonium hydroxide. Cultures were stained with Alizarin Red S working solution for five minutes then rinsed with DI water for five minutes. Osteocytes were imaged using a LEICA DMIL microscope after rinsing.

3.7.5 Chondrogenic Differentiation

hMSCs were cultures in t75s and media was changed every three days until confluence was reached. Once confluence was reached, cells were passaged placed into 15 mL conical tubes at 250,000 cells per. Cells were washed in incomplete chondrogenic media, by resuspending and centrifuging at 150G for five minutes. Complete condrogenic media was created by adding TGF-β3 (Lonza, Walkersville, MD) to incomplete condrogenic media (Lonza, Walkersville, MD). Cells were resuspended in 5 mL of complete condrogenic media and centrifuged at 150G for five minutes. The conical tube was incubated at 37°C, in a humidified atmosphere of 5% CO_2, with the cap of the

conical tube was not fully tightened to allow gas exchange. Media changes occurred every three days and after media change, ensure that the pellet is free-floating. Chondrocyte pellets were harvested after twenty days for sectioning. hMSCs were differentiated in three separate experiments with n = 3 in each experiment.

Chondrocyte pellets were fixed for three minutes in 4% paraformaldehyde in PBS, and rinsed in PBS before and after fixing. Pellets were prepped for section using an Automated Tissue Processor, on a delicate, no fix cycle**.** A 2 w/w% agarose gel was prepared using and heated using a hot plate until the solution of 1 gram of agarose into 49 grams of water, melted and dissolved. The melted agarose solution was poured over the chondrocyte pellet and placed cooled to 20^{o}C to solidify the agarose solution. The chondrocyte pellet was then embedded in paraffin and sectioned using a LIECA RM 2235 microtome, cutting 5 µm sections and fixed to charged glass slides.

3.7.6 Masson's Trichrome

Chondrogenic pellet sections were stained using Masson's Trichrome to detect Collagen II, produced by chondrocytes. Paraffin sections were first deparaffinized in: Xylene I, Xylene II, Xylene III, 100% EtOH, 95% EtOH, and 70% EtOH for three minutes each. Slides were then rinsed in running water for 10 minutes. Sections were mordanted in Bouin's solution (sigma HT10-1-128) for one hour at 60^{o}C then rinsed in running water for ten minutes. Weigert's hematoxylin, created by mixing equal parts of Solution A (sigma HT107-500mL) and Solution B (sigma HT109-500mL), was used to stain sections for ten minutes. Sections were rinsed with running water for ten minutes. Sections were stained for five minutes using a working Biebrich Scarlet-Acid Fuchsin Solution (1 gram of Biebrich Scarlett, 1 gram of Acid Fuchsin, and 198 mL of DI water), then rinsed for ten minutes in running water. Slides were then placed in Phosphomolybdic/phosphotungstic acid solution (1 Part Phosphomolybdic acid solution (HT156-250 mL), 1 Part Phosphotungstic acid solution (HT152-250 mL), and 2 Parts DI Water) for fifteen minutes. Slides were immediately stained in aniline blue solution (Aniline Blue 5g, 100% Glacial Acetic Acid 4 mL, and DI water 200 mL) for five minutes followed by a rinse in running water for two minutes. Slides were then placed in 1% acetic acid solution for five minutes. Sectioned chondrocytes were then dehydrated: in two, one minutes cycles in 95% EtOH; two, one minute cycles in 100% EtOH; one, five minute cycle in 100% EtOH; one, five minute cycle in Xylene IV; and one, five minute cycle in Xylene V. Following

dehydration, slides were mounted in cytoseal and coversliped and imaged using a Leica DM LB2 microscope. Masson's Trichrome stains Nuclei – black, collagen – blue, and cytoplasm and keratin – red.

3.7.7 Picro-sirius Stain

In addition to the Masson's Trichrome, a Picro-sirius Stain was used to identify collagen. After chondrocytes were paraffin embedded, sectioned 5 µm sections), and adhered to slides, deparaffinized in: Xylene I, Xylene II, Xylene III, 100% EtOH, 100% EtOH, and 90% EtOH for 2 minutes each, then placed in running water for five minutes. Slides were then stained in Harris Hematoxylin for two minutes and rinsed in running water for two minutes. A quick dip in acid alcohol, a quick rinse in water, and a dip in ammonia water (approximately thirty seconds) was completed before a rinse in tap water for ten minutes. Slides are then exposed to Picro-Sirius Red fast green for thirty minutes. The Picro-Sirius Red fast green is made by mixing 0.03 grams of Fast Green in 100 mL of Picric Acid. Slides are then dehydrated using: 80% EtOH (one minute), 95% EtOH (one minute), 95% EtOH (one minute), 100 % EtOH (one minute), 100% EtOH (five minutes), Xylene IV (two minutes), and Xylene V (five minutes).

3.8 CyQuant Assay

The CyQuant cell proliferation assay kit (Molecular Probes, Eugene, OR) uses a DNA stain to fluorescently label DNA and using a standard curve correlates the fluoresced DNA to a number of cells. To create the CyQuant lysis buffer used in the assay, 1 mL of Cell-lysis buffer and 50 µL of CyQuant GR fluorescent dye were added to 19 mL of DPBS.

Sutures were created, seeded, and sterilized in the manner previously described. After seeding the sutures were removed from the bioreactors and cut to 1 cm to standardize the length of sutures. Sutures were then placed in microcentrifuge tube with 500 µL of DPBS and centrifuged for 5 minutes at 2,000 RPM. After centrifuging, 400 µL of DPBS was removed and samples were placed in - 80^{o}C. The deionized water of the DPBS freezes and lyses the cells leaving the DNA in solution. After at least one hour at - 80^{o}C, samples were brought to room temperature.

Using a flat bottomed 96 well plate, 100 µL of the CyQuant lysis buffer were added to wells in Columns 1-4 and Rows B-H. In row A, columns 1-4, 30,000 hMSCs were added in 200 µL of DPBS.

Immediately afterwards, 100 µL was transferred from row A to row B, then from row B to row C…until row G, ensuing that each was thoroughly mixed. In columns 1-4 in row, H an additional 100 µL of CyQuant lysis buffer was added. Row H contained no cells served as blanks for the standard curve.

CyQuant lysis buffer was added at a volume of 400 µL to microcentrifuge tubes containing microthread sample at room temperature. A Vortex Genie was used to lightly mix the lysis buffer and microthread sample. The sutures was removed and stained with Hoechst (0.5 µL in 3000 µL of PBS for 5 minutes) to confirm all cells have been removed. Using a micropipette, 100 µL were added to four wells of a 96 well plate, these four samples were averaged to calculate the averge number of cells per cm of suture. This was repeated for all samples. The 96 well plate was placed in a Victor3 1420 Plate Reader to record the optical density at 480 nm. A standard curve was created using the optical densities and the know cell numbers in rows 1 through 4.

Chapter 4: Results

4.1 Aim 1

4.1.1 Preliminary Fibrin Degradation

Six seeded sutures were plated in a twelve well plate, three with Aprotinin and three with MSCGM. Media changes occurred every three days and plate was lightly swirled to move suture in plate and keep the sutures free floating. MSCGM sutures were degraded at Days 10, 13, and 15. Aprotinin sutured remained intact at these time points. This experiment was used to determine the ending time-point for the Fibrin Degradation ELISA. Day 9 was used so MSCGM sutures would not be completely degraded.

4.1.2 Fibrin Degradation ELISA

An FDP ELISA kit was used to determine the concentrations of FDP found in media after sutures had been cultured for 3, 6, and 9 days. A distinct decrease in FDP production was observed to correlate with an increase in the aprotinin concentration of the media. A two-way ANOVA was used to determine significant differences between groups ($p<0.05$). All FDP concentrations and standard deviations (µg/mL) are displayed in

Table 3. At Day 3, Aprotinin-0 had significantly higher concentrations of FDP when compared to all other groups (Aprotinin-50, Aprotinin-10, Aprotinin-5, Aprotinin-1, and Aprotinin-0; n = 6 within each group, $p<0.05$). Likewise at Day 3, Aprotinin-100 had significantly less FDP when compared to FDP concentrations observed in all other groups (Aprotinin-50, Aprotinin-10, Aprotinin-5, Aprotinin-1, and Aprotinin-0; n = 6 within each group, $p<0.05$). At Day 6, Aprotinin-100 had significantly less FDP than Aprotinin-50, Aprotinin-5, Aprotinin-1, and Aprotinin-0 (n = 6 for all groups, $p<0.05$). At Day 9, a significant decrease in FDP concentrations was observed between Aprotinin-100 and Aprotinin-50, Aprotinin-10, Aprotinin-1, and Aprotinin-0, with n = 6 in all groups ($p<0.05$). The comparison of FDP concentrations at each Day are depicted in Figure 7 and all groups and time points are shown in Figure 8.

Every three days media was collected and analyzed for FDP concentrations; however this only measures the amount of degradation that occurred during the previous days. Figure 9 (and

Table 3) depicts the cumulative masses of FDP over the nine days. Data separated by day is displayed in Figure 10. Statistics were determined using a two-way ANOVA, and significance was determined at $p = 0.05$. At Day 3, Aprotinin 0 had significantly more FDP mass when compared to Aprotinin-5, Aprotinin-10, Aprotinin-50, and Aprotinin-100 ($n=6$, $p>0.05$). At this same time point, Aprotinin-100 exhibited significantly less FDP mass when compared to all other groups (Aprotinin-0, Aprotinin-1, Aprotinin-5, Aprotinin-10, and Aprotinin-50). At Day 6, Aprotinin 0 had significantly more FDP mass when compared to Aprotinin-10, Aprotinin-50, and Aprotinin-100 ($n=6$, $p>0.05$). Aprotinin-100 exhibited significantly less FDP mass when compared to all other groups (Aprotinin-0, Aprotinin-1, Aprotinin-5, Aprotinin-10, and Aprotinin-50) at Day 6. Lastly, at Day 9 Aprotinin 0 had significantly more FDP mass when compared to Aprotinin-5, Aprotinin-10, Aprotinin-50, and Aprotinin-100 ($n=6$, $p>0.05$). At this same time point, Aprotinin-100 exhibited significantly less FDP mass when compared to all other groups (Aprotinin-0, Aprotinin-1, Aprotinin-5, Aprotinin-10, and Aprotinin-50).

Results from this experiment indicated that Aprotinin-100 had the least degradation. For all of the following experiments, only Aprotinin-100 was used. "Aprotinin" will now refer to Aprotinin-100, or 100 µg of Aprotinin per 1 ml of MSCGM. Likewise, Aprotinin-0 (0 µg of Aprotinin per 1 ml of MSCGM) will be referred to as MSCGM.

Table 3: Fibrin Degradation Product Concentrations (μg/mL) and Cumulative Mass (μg) at Days 3, 6, and 9

Time-point	Group (n=6, all groups)	FDP Concentration ± St Dev (μg/mL)	FDP Cumulative Mass ± St Dev (μg)
Day 3	Aprotinin-100	8.680 ± 1.062	8.680 ± 1.062
	Aprotinin-50	11.162 ± 1.103	11.162 ± 1.103
	Aprotinin-10	11.333 ± 1.785	11.333 ± 1.785
	Aprotinin-5	11.640 ± 0.964	11.640 ± 0.964
	Aprotinin-1	12.602 ± 0.780	12.602 ± 0.780
	Aprotinin-0	14.127 ± 1.577	14.127 ± 1.577
Day 6	Aprotinin-100	8.967 ± 0.734	17.647 ± 1.796
	Aprotinin-50	11.003 ± 0.711	22.165 ± 1.814
	Aprotinin-10	10.947 ± 1.656	22.280 ± 3.441
	Aprotinin-5	11.167 ± 0.565	23.587 ± 1.529
	Aprotinin-1	12.361 ± 0.583	24.963 ± 1.363
	Aprotinin-0	12.898 ± 1.836	27.025 ± 3.413
Day 9	Aprotinin-100	9.050 ± 0.534	26.697 ± 2.330
	Aprotinin-50	11.056 ± 1.315	33.221 ± 3.129
	Aprotinin-10	11.260 ± 1.806	33.54 ± 5.247
	Aprotinin-5	10.140 ± 0.929	33.727 ± 2.458
	Aprotinin-1	12.692 ± 1.221	37.655 ± 2.584
	Aprotinin-0	12.989 ± 1.356	40.014 ± 4.769

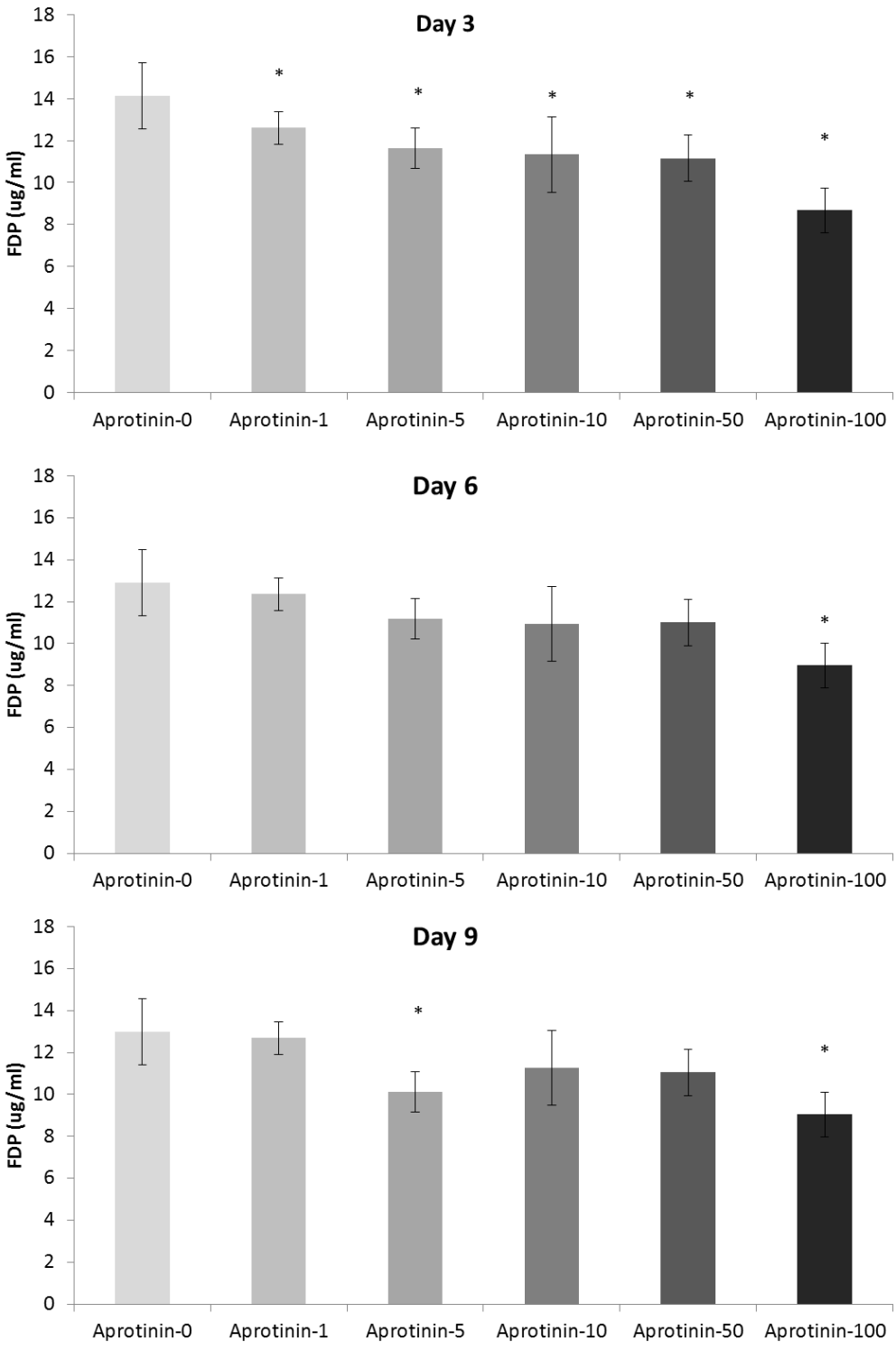

Figure 7: Fibrin Degradation Product Concentration (FDP) Data and Day Data. FDP data is reported in µg/mL. Bars of graph represent the average, and error bars represent standard deviations. Sample size was 6 sutures for each experimental group. * represents 0.05 significance as determined by an ANOVA.

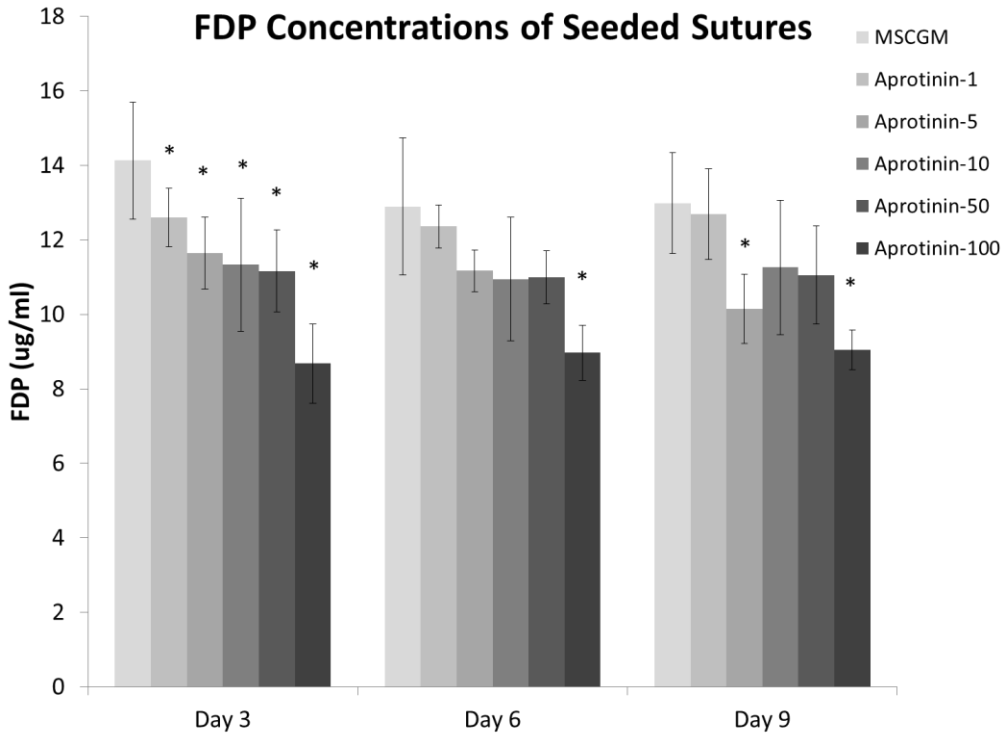

Figure 8: Fibrin Degradation Product (FDP) Data. Sutures were seeded at 100,000 cells for 24 hours and cultured for 9 days with media collections at Days 3, 6, and 9. Concentrations of FDP were used to quantify degrataion. Sample size of 6 sutures were used for each experimental group. * represents 0.05 significance as determined by a two way ANOVA.

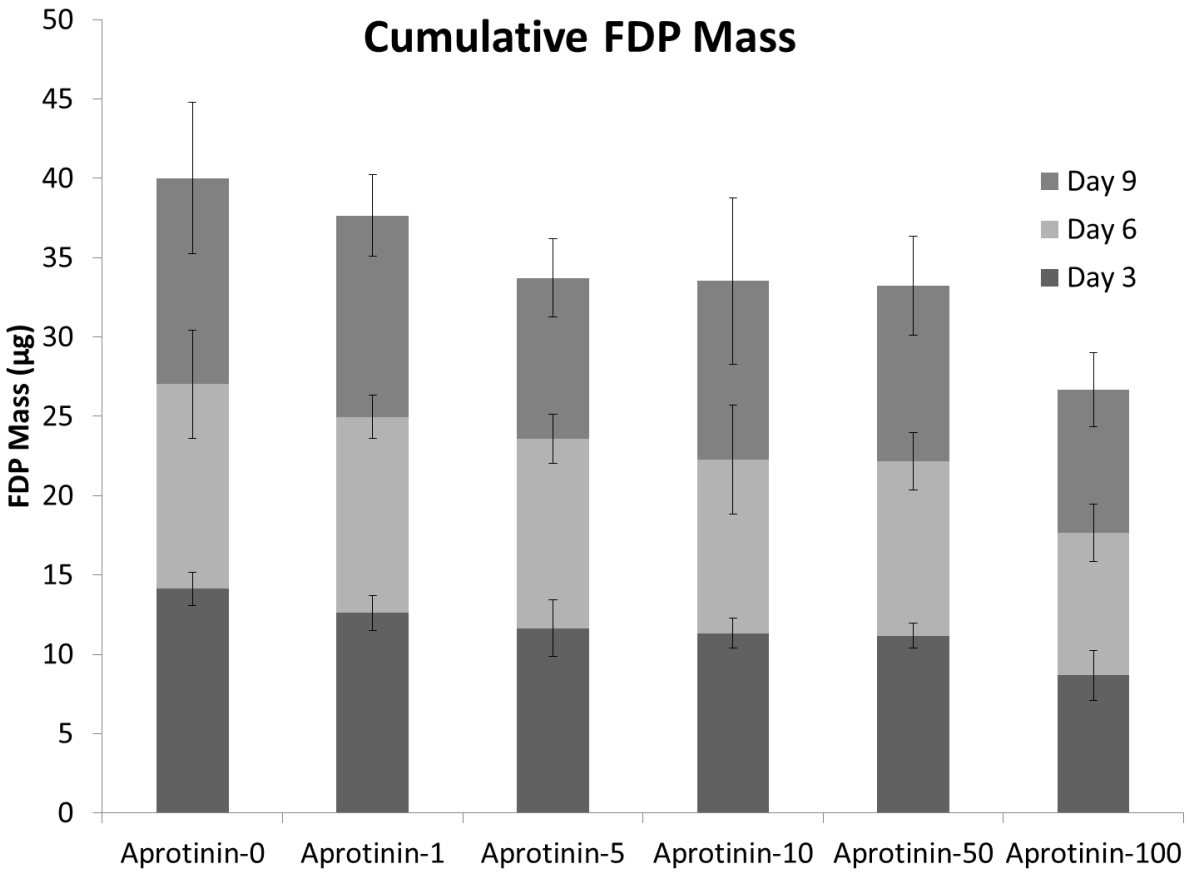

Figure 9: Cumulative FDP Mass. FDP masses were determined at each time-point and each bar displays the FDP mass at each day and the cumulative masses. The error bars depict the cumulative standard deviation at each time-point.

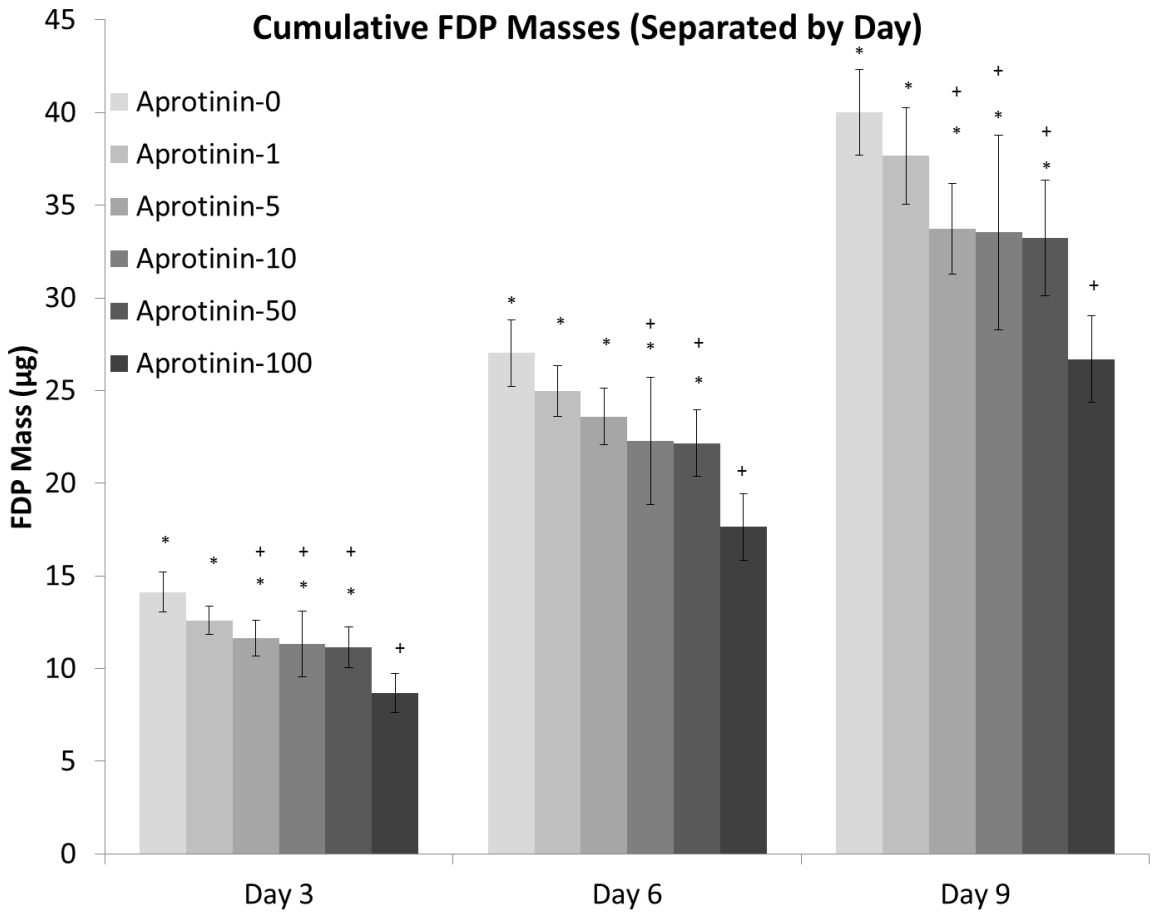

Figure 10: Cumulative FDP Mass at Days 3, 6, and 9. Bars represent average FDP mass in µg and error bars represent standard deviations. *represents a 0.05 significance level between Aprotinin-100 and + represents a 0.05 significance level between Aprotinin-0 (at each day).

Lastly, when examining the response of cumulative FDP production (in terms of cumulative mass) in response to aprotinin concentration. This data is displayed in Figure 11. Curves were fit using a logarithmic decay function. It appears that the around the 100 µg/ml aprotinin concentration that FDP production is nearing a limit.

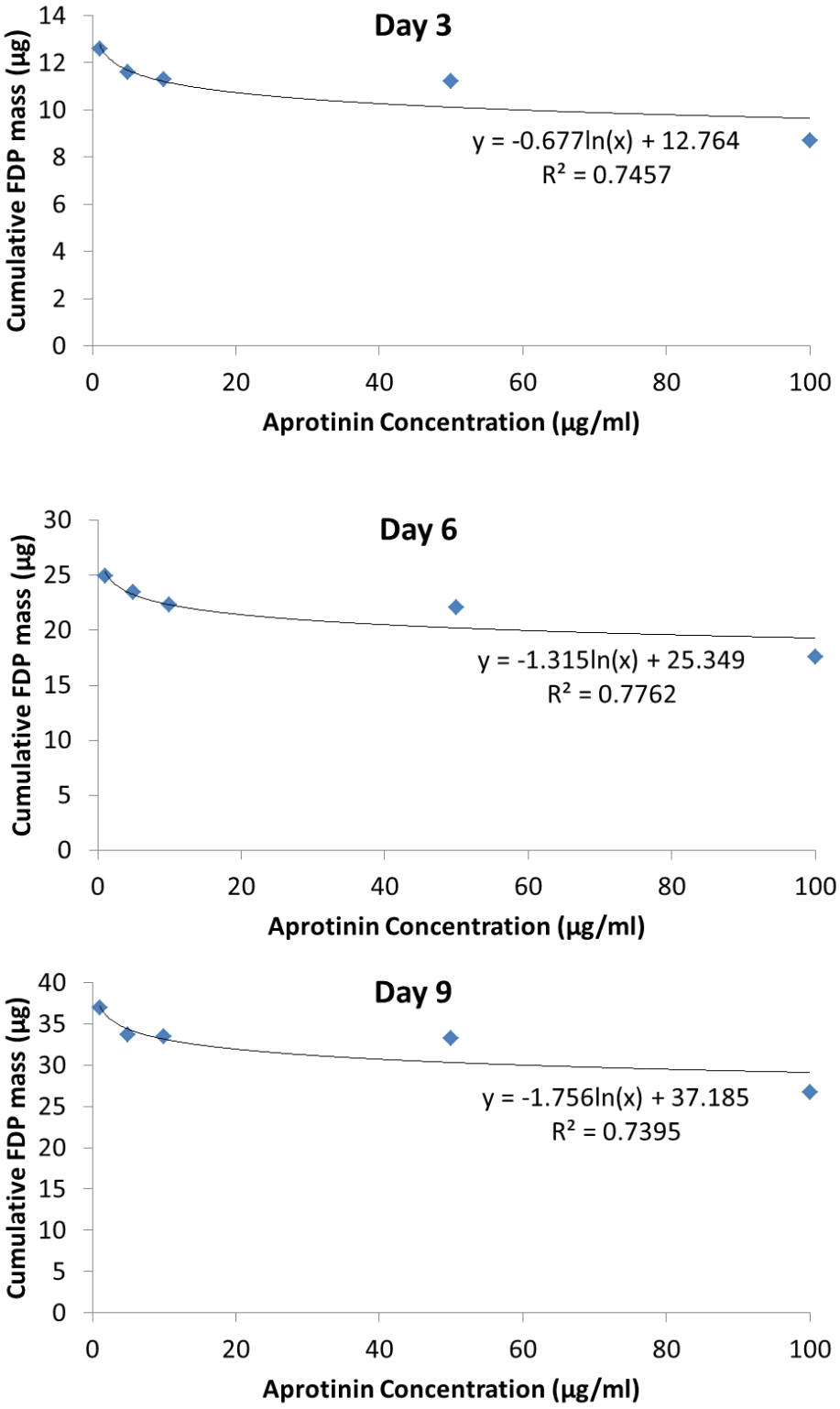

Figure 11: FDP mass production as a function of Aprotinin concentration. Data was fit using a logarithmic decay function and the fit curves are displayed on the graphs

4.1.3 Suture Mechanics

Thread diameters

Diameters of sutures were recorded at Day 3, prior to mechanical testing. Sutures were placed on a glass slide and images were acquired using a Leica DM LB2 microscope at 5 x. The diameters of sutures ± standard deviations (in mm) are displayed in Figure 12. The sample size for suture diameters are as follows Aprotinin (n=6), MSCGM (n=6), Aprotinin no cells (n=3), MCGM no cells (n=3), and PBS no cells (n=4). The average diameter and standard deviation of each group is depicted in

Table 4. An ANOVA was used to determine the significance between groups. Significant differences ($p<0.05$) were observed: between MSCGM and MSCGM-unseeded/Aprotinin/MSCGM unseeded/PBS unseeded and between Aprotinin and Aprotinin-unseeded/MSCGM/MSCGM unseeded (also depicted in Figure 12).

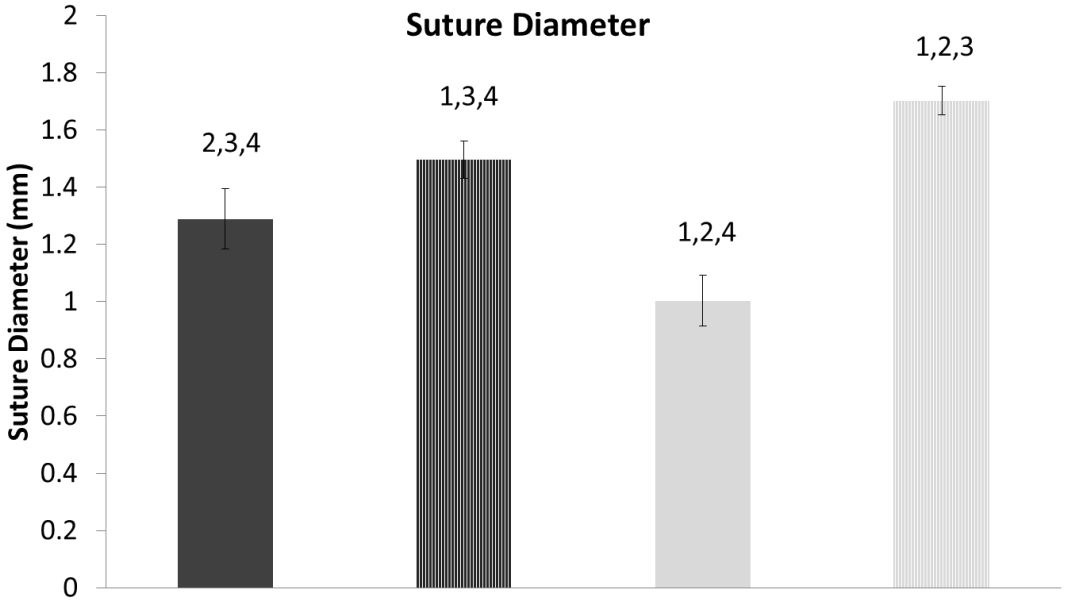

MSCGM	**+**	**+**	**+**	**+**
Aprotinin	**+**	**+**	**-**	**-**
Cells	**+**	**-**	**+**	**-**
Sample Size	**6**	**3**	**6**	**3**

Figure 12: Suture diameters of seeded and unseeded sutures. Sutures were plated (followed standard seeding) for 3 days. Diameters were recorded by placing the suture on a glass slide and imaging on a LEICA DM LB2 microscope and recording 6 diameters across the length of the suture and taking the average. 1 represents a

0.05 significance between seeded Aprotinin, 2 represents a 0.05 significance between non-seeded Aprotinin, 3 represents a 0.05 significance between seeded MSCGM, and 4 represents a 0.05 significance between non-seeded MSCGM. Significance was determined using a one way ANOVA.

Table 4: Suture Diameters after 3 days in culture (mm)

	Diameter	Standard Deviation
Aprotinin	1.288	0.106
MSCGM	1.003	0.088
Aprotinin-unseeded	1.496	0.065
MSCGM-unseeded	1.702	0.050
PBS-unseeded	1.289	0.092

Mechanical Data

Sutures were seeded with a 100,000 hMSC suspension for 24 hours. Following seeding, sutures were plated in either MSCGM or MSCGM supplemented with aprotinin for 3 days. Following suture diameter measurement, sutures were mechanically loaded to failure on an Instron. Force-displacement data was converted to stress-strain data (shown in Figure 13). The UTS was determined by the stress at which the suture failed, likewise this point was also the SAF. E was calculated by the linear region between the UTS and 0,0 starting point. If the curve was not linear to 0,0, the E was calculate in the linear portion of the curve.

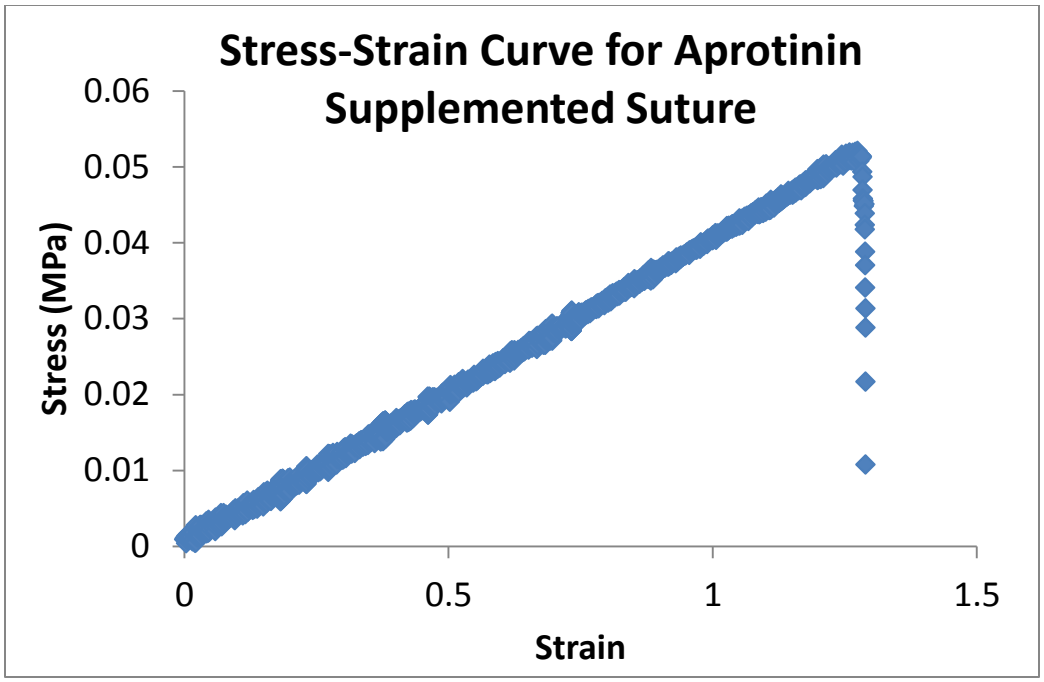

Figure 13: Stress-Strain Curve. After diameters were recorded, sutures were loaded into the Instron and mechanically loaded to failure. A Stress-Strain curve was calculated from the force-displacement data recorded by the Instron. The highest stress is the UTS, the strain value of the UTS is the SAF, and the slope of the linear region between the UTS and the starting 0,0 point is the E.

Figure 14 depicts the UTS data for seeded sutures. Seeded sutures exposed to aprotinin failed at a significnatly higher UTS when compared to sutures cultured in MSCGM alone ($n = 6$, $p < 0.05$, one-way ANOVA). Unseeded controls were also tested, this data is displayed in Figure 15. Unseeded sutures cultured in Aprotinin also exhibited a significantly higher UTS when compared to sutures cultured in MSCGM alone ($n = 3$, $p < 0.05$, one-way ANOVA). A significanct difference was observed between the Aprotinin and MSCGM seeded and their unseeded counterparts ($p < 0.05$, one way ANOVA). This and other sifnificant observations are shown in Figure 15. UTS values are shown in Table 5.

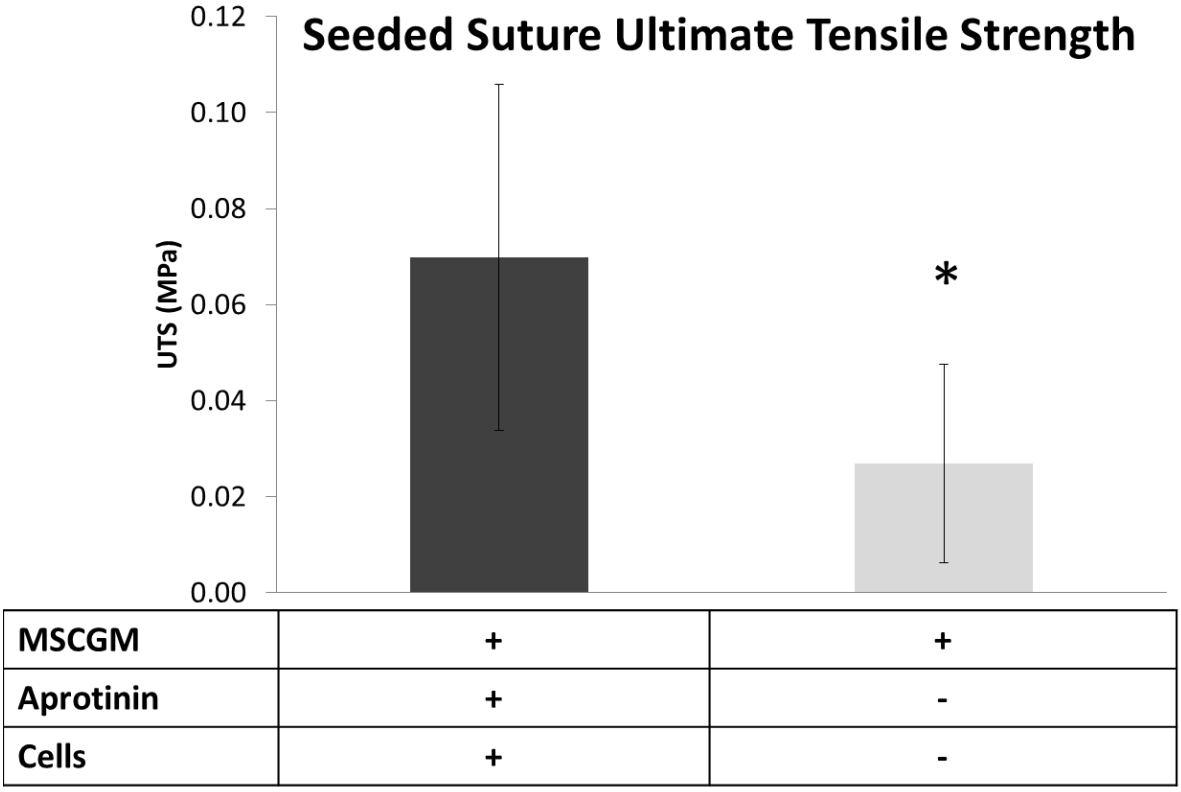

Figure 14: Ultimate Tensile Strength Data for seeded sutures. Sutures were seeded as previously described. Seeded sutures cultured in aprotinin supplemented media had a significant increase in UTS when compared to those cultured in MSCGM alone. * represents 0.05 significance level as determined by a one way ANOVA.

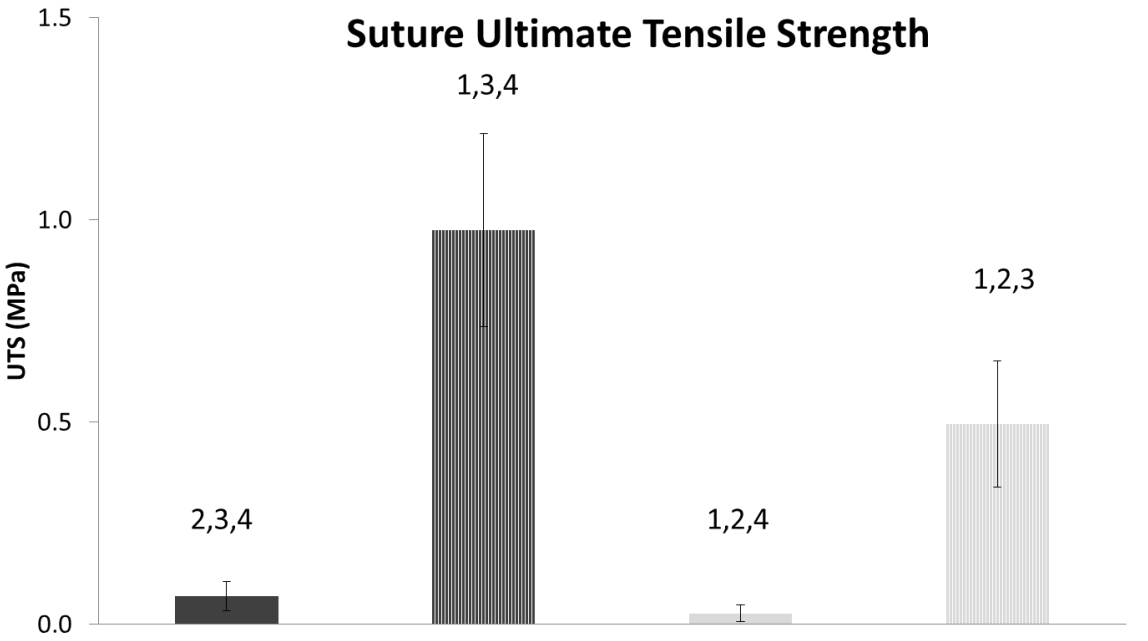

MSCGM	**+**	**+**	**+**	**+**
Aprotinin	**+**	**+**	**-**	**-**
Cells	**+**	**-**	**+**	**-**
Sample Size	**6**	**3**	**6**	**3**

Figure 15: Ultimate Tensile Strength Data for seeded and unseeded sutures. Sutures were seeded as previously described, while unseeded sutures underwent the same conditions, with no cells. Unseeded sutures had significantly higher UTS when compared to their seeded counterparts. 1 represents a 0.05 significant difference between seeded aprotinin sutures, 2 represents a 0.05 significant difference between non-seeded aprotinin sutures, 3 represents a 0.05 significant difference between seeded MSCGM sutures, 4 represents a 0.05 significant difference between non-seeded MSCGM sutures. Significance was determined using a one-way ANOVA.

Table 5: Ultimate Tensile Strength values for seeded and unseeded sutures

Group	UTS (MPa)	Standard Deviation (MPa)
Aprotinin – hMSCs	0.070	0.036
MSCGM – hMSCs	0.027	0.021
Aprotinin – Unseeded	0.975	0.239
MSCGM – Unseeded	0.495	0.155

A similar trend was also observed between the E values of seeded sutures. E data is shown in Table 6 had significantly higher than those observed in the MSCGM alone group; this is displayed in Figure 16: hMSC seeded suture modulus (E) Data. Sutures were seeded as previously described. Seeded sutures cultured in aprotinin supplemented media had a significant increase in modulus when compared to those cultured in MSCGM alone. * represents 0.05 significance level as determined by a one way ANOVA. ($p < 0.05$, one-way ANOVA). When examining the E values of seeded ($n = 6$) and unseeded ($n = 3$) sutures, the unseeded counterparts had a much higher E however, only Aprotinin exhibited a significant difference, shown in Figure 17: Suture Modulus (E) Data, seeded and unseeded controls. Sutures were seeded in a manner previously described and mechanically loaded to failure. Seeded sutures in both the 1 represents a 0.05 significant difference between seeded aprotinin sutures, 2 represents a 0.05 significant difference between non-seeded aprotinin sutures, 3 represents a 0.05 significant difference between seeded MSCGM sutures, 4 represents a 0.05 significant difference between non-seeded MSCGM sutures. Significance was determined using a two way ANOVA. ($p < 0.05$, one-way ANOVA).

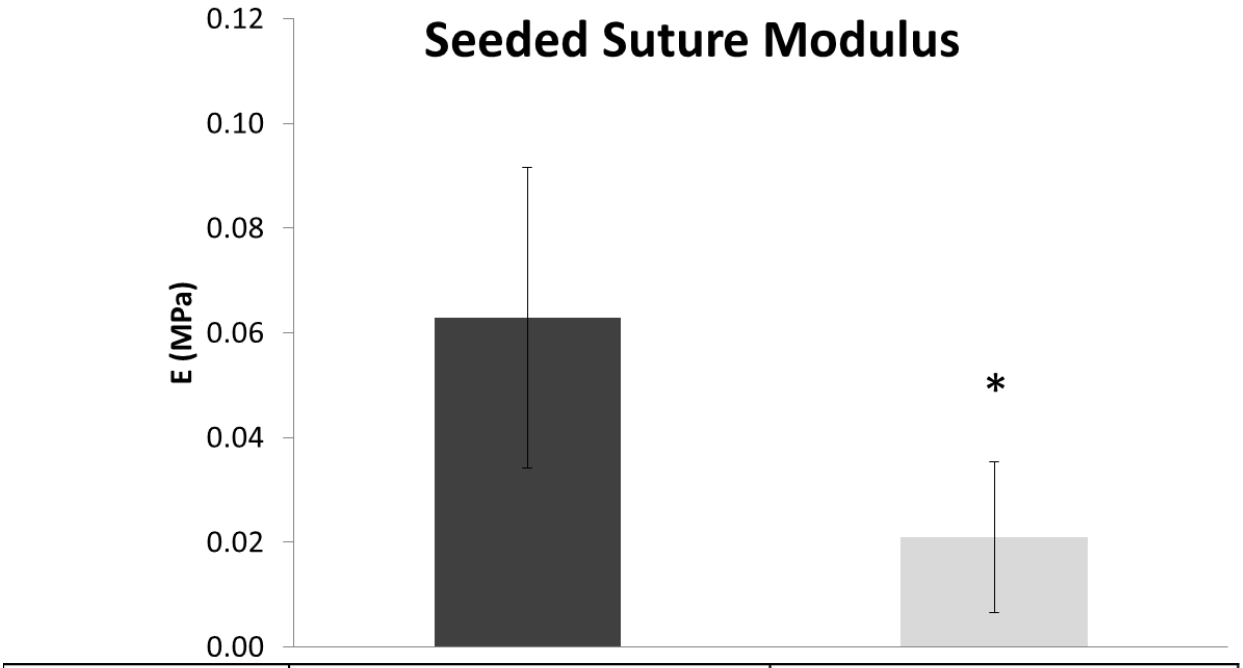

MSCGM	**+**	**+**
Aprotinin	**+**	**-**
Cells	**+**	**-**

Figure 16: hMSC seeded suture modulus (E) Data. Sutures were seeded as previously described. Seeded sutures cultured in aprotinin supplemented media had a significant increase in modulus when compared to those cultured in MSCGM alone. * represents 0.05 significance level as determined by a one way ANOVA.

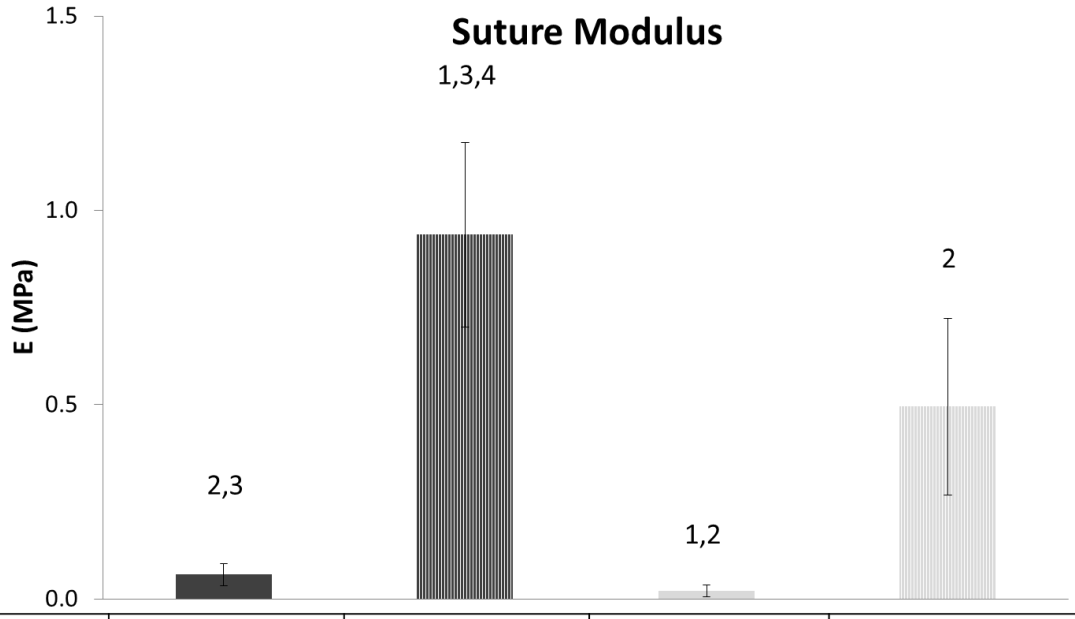

MSCGM	**+**	**+**	**+**	**+**
Aprotinin	**+**	**+**	**-**	**-**
Cells	**+**	**-**	**+**	**-**
Sample Size	**6**	**3**	**6**	**3**

Figure 17: Suture Modulus (E) Data, seeded and unseeded controls. Sutures were seeded in a manner previously described and mechanically loaded to failure. Seeded sutures in both the 1 represents a 0.05 significant difference between seeded aprotinin sutures, 2 represents a 0.05 significant difference between non-seeded aprotinin sutures, 3 represents a 0.05 significant difference between seeded MSCGM sutures, 4 represents a 0.05 significant difference between non-seeded MSCGM sutures. Significance was determined using a two way ANOVA.

Table 6: Modulus values for seeded and unseeded sutures.

Group	E (MPa)	Standard Deviation (MPa)
Aprotinin – hMSCs	0.063	0.029
MSCGM – hMSCs	0.021	0.014
Aprotinin – Unseeded	0.937	0.237
MSCGM – Unseeded	0.495	0.227

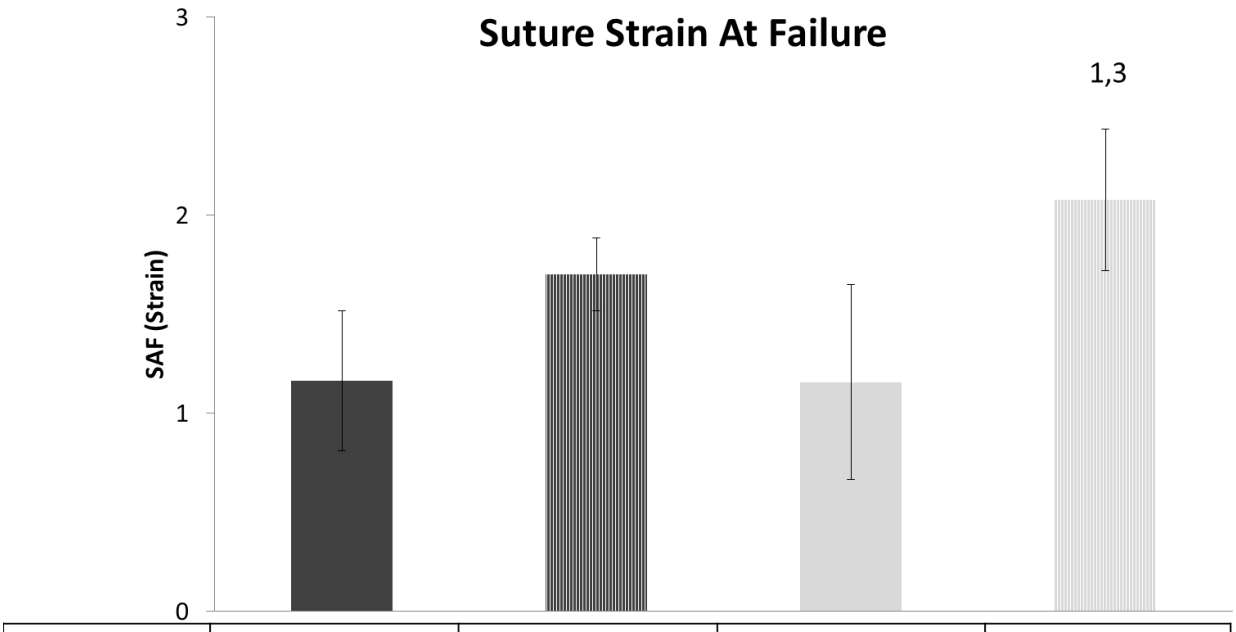

MSCGM	**+**	**+**	**+**	**+**
Aprotinin	**+**	**+**	**-**	**-**
Cells	**+**	**-**	**+**	**-**
Sample Size	**6**	**3**	**6**	**3**

Figure 18: Suture Strain at Failure (SAF). Sutures were seeded in a manner previously described and mechanically loaded to failure. Seeded sutures saw a slight decrease in SAF when compared to their unseeded counterparts. 1 represents a 0.05 significant difference between seeded aprotinin sutures, 3 represents a 0.05 significant difference between seeded MSCGM sutures. Significance was determined using a two-way ANOVA.

Table 7: Strain at Failure values for seeded and unseeded sutures

Group	SAF (Strain)	Standard Deviation (Strain)
Aprotinin – hMSCs	1.164	0.354
MSCGM – hMSCs	1.158	0.493
Aprotinin – Unseeded	1.702	0.183
MSCGM – Unseeded	2.079	0.358

4.2 Aim 2

4.2.1 Cell Viability

LIVE/DEAD stained images are shown in Figure 19. 5,600 hMSCs were seeded on each coverslip. The number of cells was quantified using ImageJ. Results from the LIVE/DEAD were recorded in percent live cells and are shown in Figure 20 box plot (data in Table 8) and Figure 20 bar chart. Cells cultured in media supplemented with Aprotinin had 97.08 ± 2.00% live cells, compared to the control media's 97.84 ± 1.33%. A student's T-test was used to test significance between MSCGM and Aprotinin groups (n = 6 within each group). No significant difference in the percent of live cells was observed between groups at the 0.05 significance level (with a statistical power of 0.29)

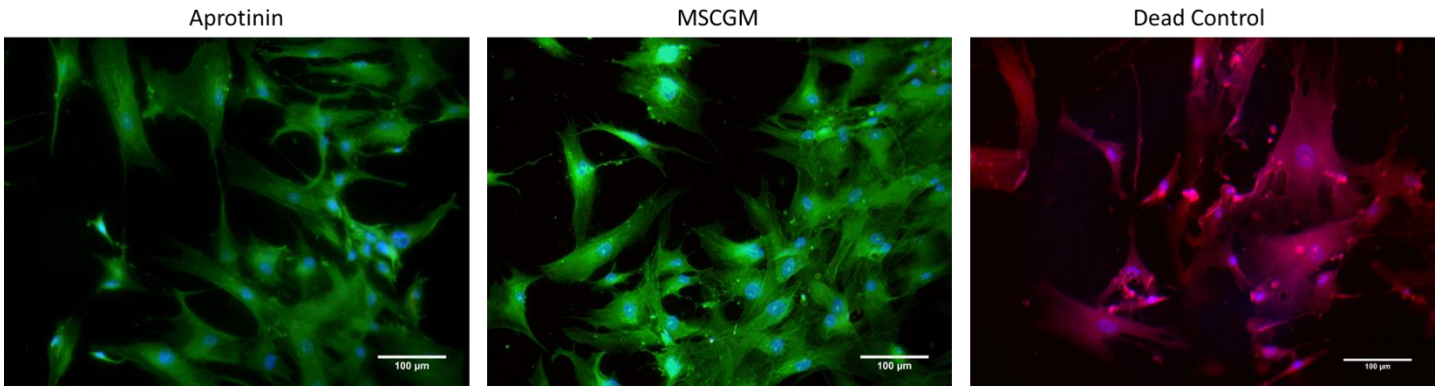

Figure 19: LIVE/DEAD stained hMCS on coverslips. The first image depicts hMSCs cultured in MSCGM 0+aprotinin, the second image depicts cells cultured in standard MSCGM. The third image depicts dead controls; cells were cultured in MSCGM and killed using 70% ethanol. Nuclei are stained with Hoechst and fluoresce blue, calcein fluoresces green indicating live cells, and ethidium stains dead cells red.

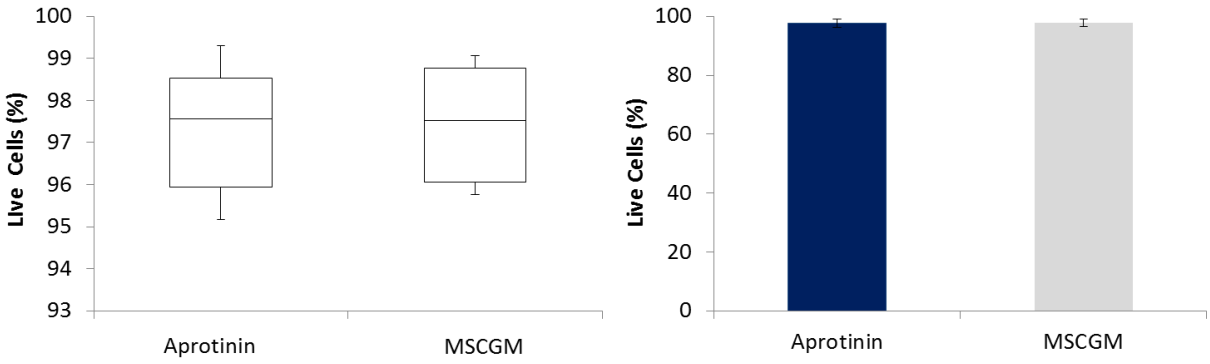

Figure 20: LIVE/DEAD analysis. A is a boxplot shows the depicting the spread of the live percentages, B depicts the average percentage of live cells (Aprotinin: 97.78 ±1.43%, SCGM 97.87±1.25%). hMSCs were cultured in either MSCGM or MSCGM -100. There was no significant difference between the two data sets at the 0.05 significance level.

Table 8: LIVE/DEAD boxplot data

Live cells (%)	Aprotinin	MSCGM
Minimum	94.16	95.50
Quartile 1	95.47	97.00
Median	97.29	98.06
Quartile 3	98.73	98.90
Maximum	99.30	99.07

4.2.2 Cell Proliferation

Proliferation was assessed using a stain for the proliferation marker Ki-67, Figure 21. 5,600 hMSCs were seeded on each coverslip. Like the LIVE/DEAD analysis, hMSCs were counted using ImageJ. hMSC nuclei fluoresce blue and Ki-67 fluoresce red, making Ki-67 positive cells appear a red/purple color. Figure 22 show the spread percentages of Ki-67+**Error! Reference source not found.** hMSCs. Figure 22 displays the average percentage of Ki-67 positive cells between hMSCs cultured in either MSCGM (19.16 ± 14.78%) or Aprotinin (19.65 ± 5.86%), Table 9: Percent Ki-67 positive hMSCs on glass coverslips displays additional statistical information. A student's t-test was used to compare the two data sets; and at the 0.05 significance level, no differences were observed (with a statistical power of 0.03).

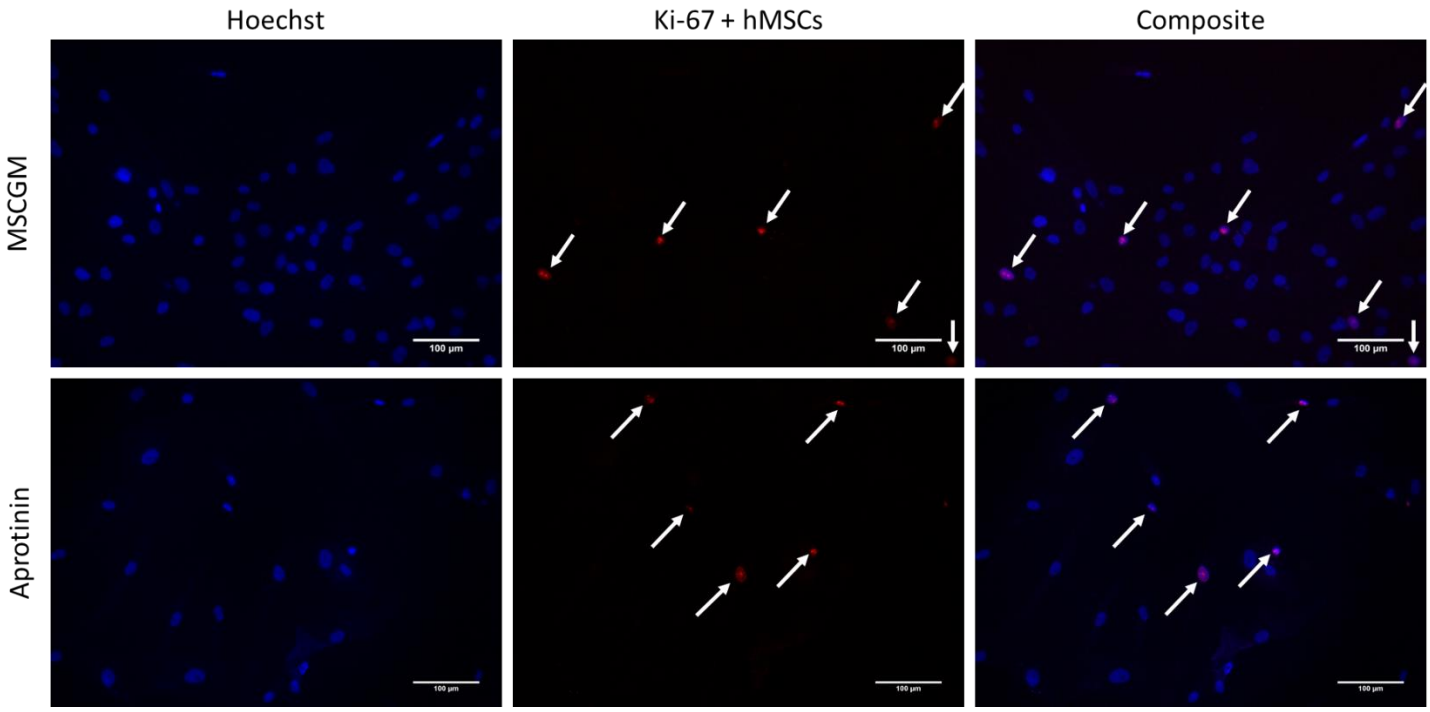

Figure 21: Ki-67 stain on hMSCs. hMSCs were cultured in aprotinin supplemented MSCGM or MSCGM alone. hMSCs were stained with Hoechst and anti-Ki-67. Nuclei are stained blue (first column0. Ki-67, a proliferation marker is stained red (second column). White arrows indicate Ki-67+hMSCs. A composite of the two images is shown in the third column.

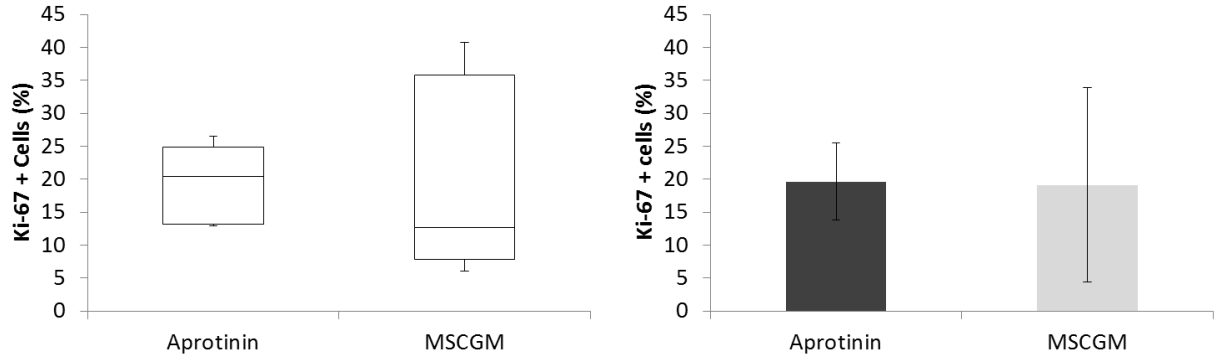

Figure 22: Ki-67 analysis. A is a boxplot shows the depicting the spread of percentages of Ki-67 + cells, B depicts the average percentage of Ki-67+ cells. hMSCs were cultured in either MSCGM or Aprotinin There was no significant difference between the Aprotinin (17.54 ± 6.32%) and MSCGM (16.73 ± 13.27%) at the 0.05 significance level.

Table 9: Percent Ki-67 positive hMSCs on glass coverslips

Ki-67+ hMSCs (%)	Aprotinin	MSCGM
Minimum	12.93	6.12
Quartile 1	13.21	7.83
Median	20.38	12.69
Quartile 3	24.90	35.87
Maximum	26.57	40.83

4.2.3 hMSC Differentiation

After confluence was reached in either Aprotinin or MSCGM, hMSCs underwent differentiation. hMSCs were exposed to three different medias to induce adipogenic, osteogenic, and chondrogenic differentiations. hMSCs were differentiated in three separate experiments; within each experiment, osteocytes and adipocytes with n = 3 and n = 1 for chondrocytes. Within each experimental group, cells were stained to for visualization of differentiation; adipocytes with Oil Red O, osteocytes with Alizarin Red S, and chondrocytes with Masson's Trichrome and Picro-sirius. Images were acquired of each cell type, confirming that differentiation occurred after hMSCs were cultured in Aprotinin and MSCGM.

Adipogenic Differentiation

The presence of lipid vacuoles is a positive confirmation of adipogenic differentiation. Images of differentiated hMSCs stained with Oil Red S are shown in Figure 23. These cells were imaged after 14 of culture, undergoing adipogenic differentiation. Adipogenic differentiation consisted of alternating (every 3 days) Induction and Maintenance media for adipocyte. After an additional week of differentiation, cells were stained with Oil Red O which stains lipid vacuoles red, as shown in Figure 24.

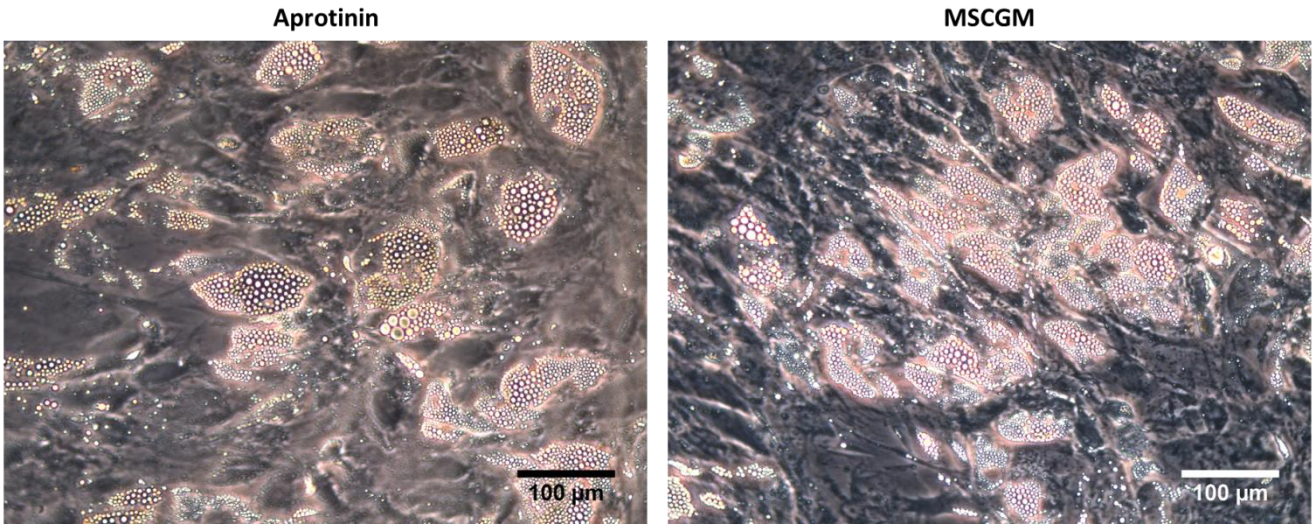

Figure 23: Adipogenic Differentiation. hMSC differentiation into adipocytes at week 2. hMSCs were cultured in media (MSCGM or Aprotinin) until 100 % confluent then differentiated. Both groups exhibit lipid vacuole formation, a sign of adipocyte differentiation

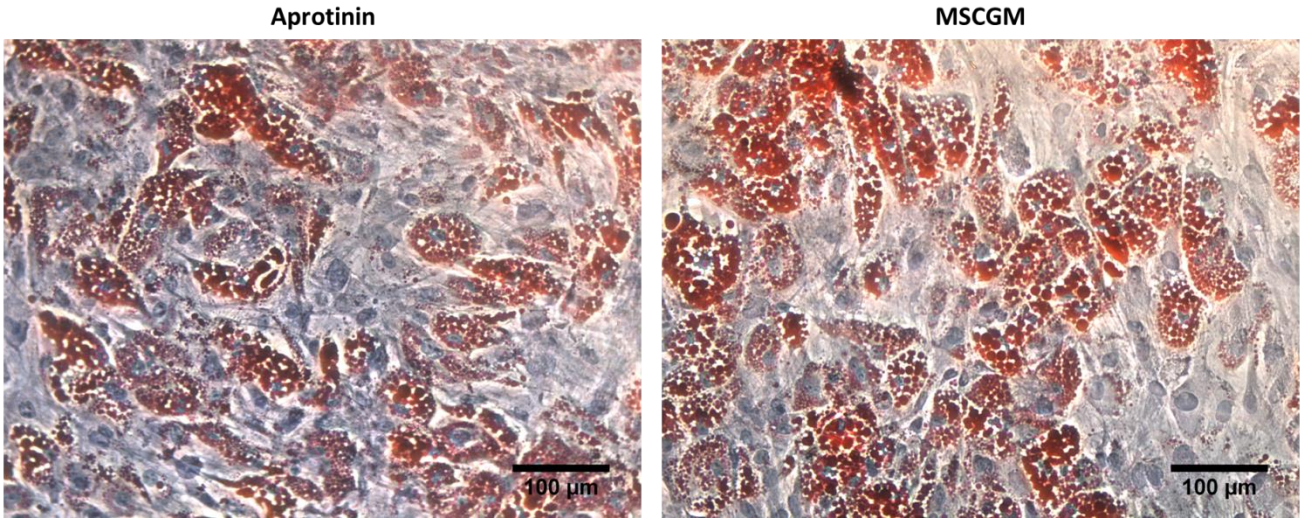

Figure 24: Oil Red O stained adipogenic differentiated hMSCs. Lipid vacuoles are stained red and nuclei are stained blue.

The control group, hMSCs grown to confluence then cultured for three weeks in either MSCGM or Aprotinin, was also stained with Oil Red to determine if any adipogenic differentiation occurred. Lipid vacuoles within adipocytes are stained red, while non-differentiated cells retain none of the red stain as see in Figure 25.

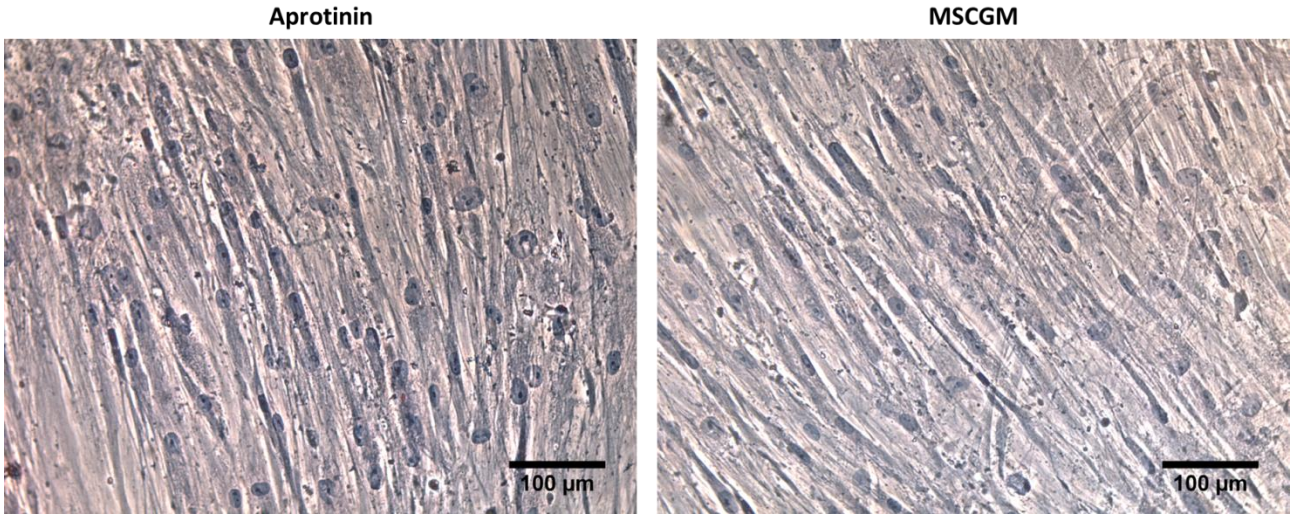

Figure 25: Oil Red Stain of hMSCs. hMSCs were cultured (in Aprotinin or MSCGM) for 3 weeks. Lipid vacuoles are stained red and nuclei are stained blue, however no lipid vacuoles were observed.

Osteogenic Differentiation

hMSCs were cultured in either Aprotinin or MSCGM until confluence was reached; then osteogenic differentiation media was fed to cells. During osteogenic differentiation hMSC exhibit a more cuboidal morphology, as shown in Figure 26.

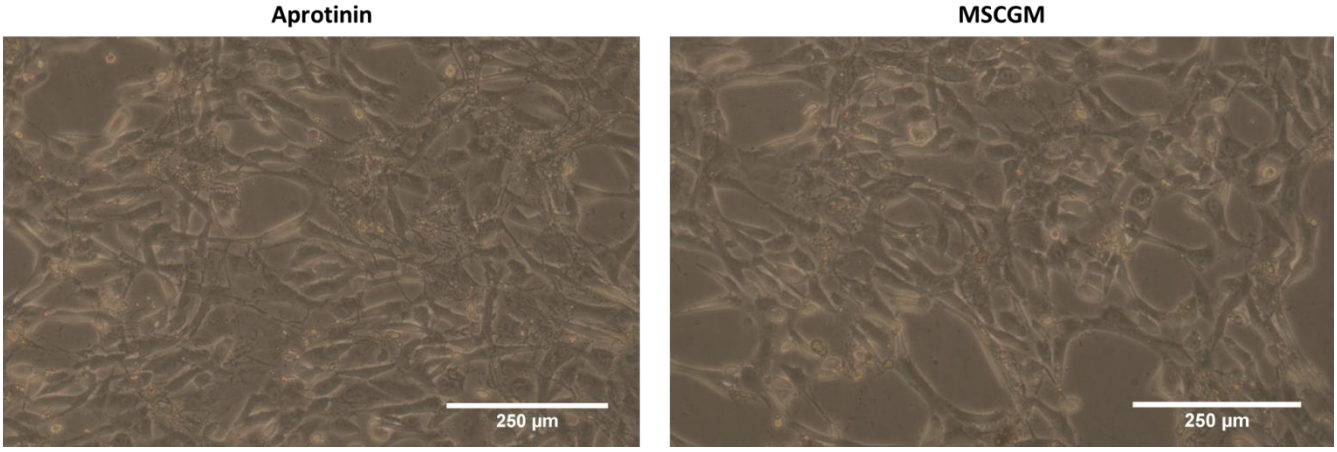

Figure 26: hMSC osteogenic differentiation – week 2, hMSCs begun to exhibit more cuboidal shape in both the aprotinin and MSCGM groups.

hMSCs were exposed to aprotinin or MSCGM then differentiated for 21 day in osteogenic induction media. Following differentiation, wells were stained with alizarin red, which stains for calcium deposits. Figure 27 shows images stained calcium deposits of differentiated hMSCs.

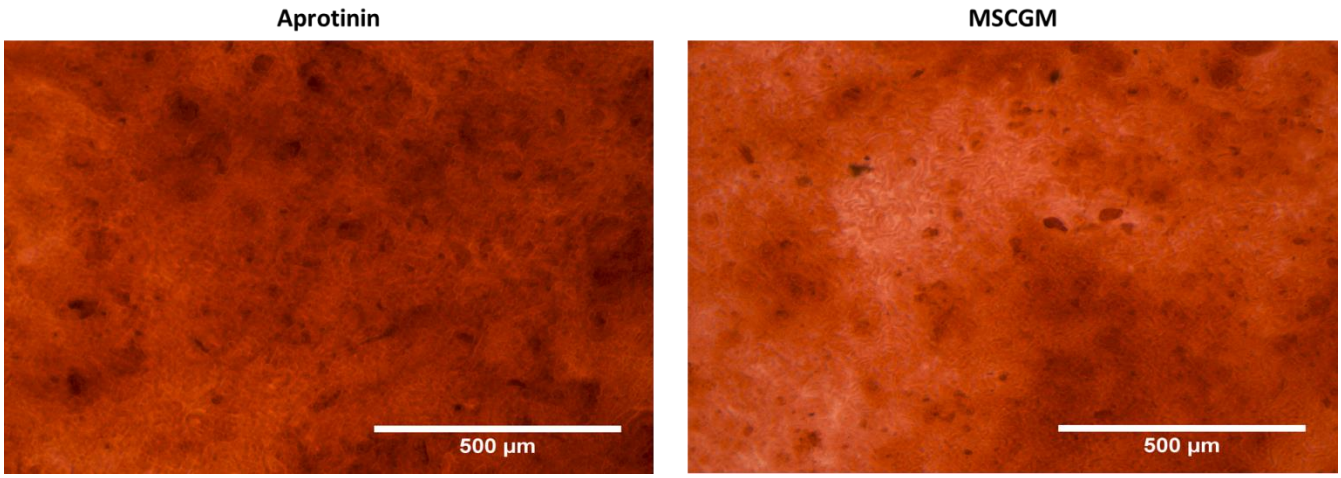

Figure 27: Alizarin Red S Stain – Stains calcium deposits red. hMSCs were cultured in either aprotinin or standard MSCGM until confluence, then differentiated for 21 days.

In addition to the hMSC differentiated osteocytes, hMSCs were cultured for 3 weeks at confluence in either MSCGM or Aprotinin. These hMSCs were also stained with Alizarin Red to determine if there was any calcium production. The undifferentiated hMSCs stained with alizarin red are shown in Figure 28.

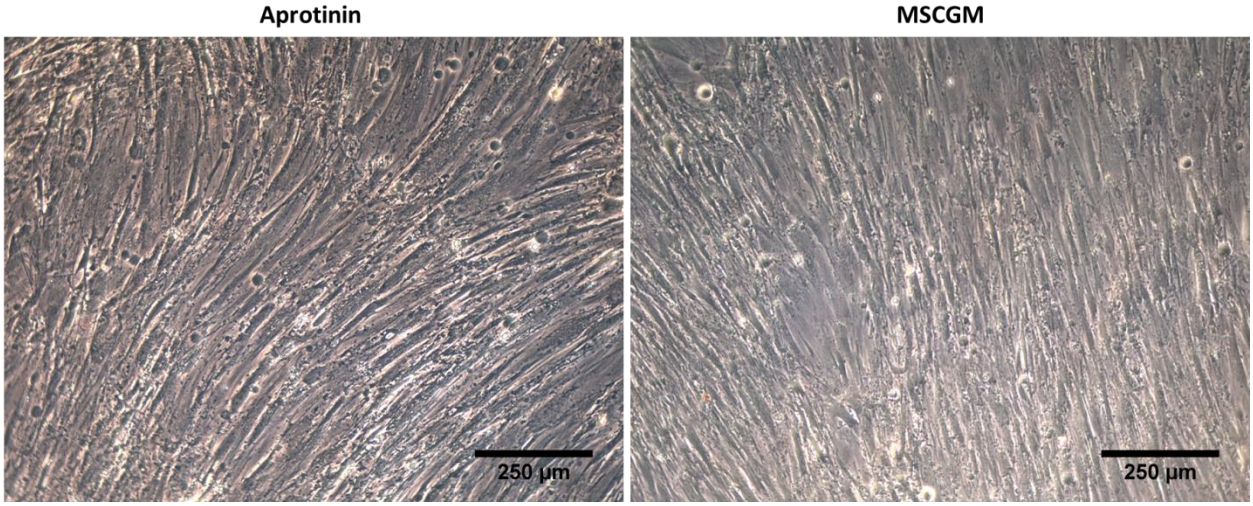

Figure 28: hMSCs stained with Alizarin Red. No calcium deposit formation, shown by no red stain detection, or the cuboidal cell morphology, indicating no osteogenic differentiation

Chondrogenic Differentiation

hMSCs were grown using aprotinin or MSCGM. Once 250,000 hMSCs were grown; cells were pelleted and fed chondrogenic media supplemented with TGF-β. After twenty-one days of differentiation, pellets were fixed, paraffin embedded, and sectioned. Chondrocyte sections were stained for collagen using Masson's Trichrome shown in Figure 29. Collagen is stained blue, nuclei are stained black and cytoplasm and keratin are both stained red.

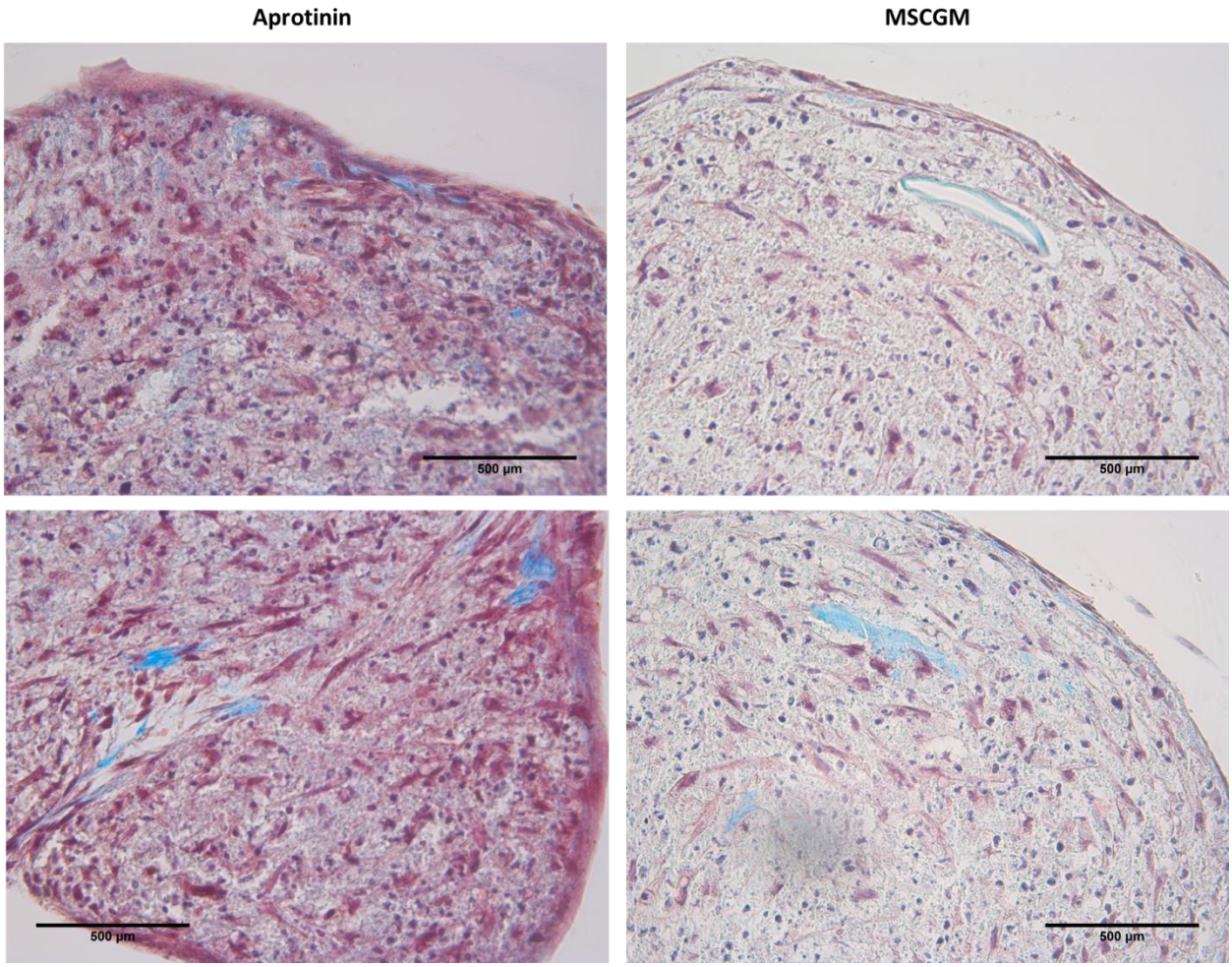

Figure 29: Chondrocyte Pellets stained with Masson's Trichrome. Collagen is stained blue, neucli are black, and cytoplasm and keratin are red. Both the aprotinin and MSCGM pellets expressed collagen formation.

A picro-sirius collagen stain was also performed to detect collagen. Picro-sirius is more efficient at collagen detection than Masson's Trichrome [78, 79]. Figure 30 shows a picro-sirius stain of the hMSC differentiated chondrocyte pellets.

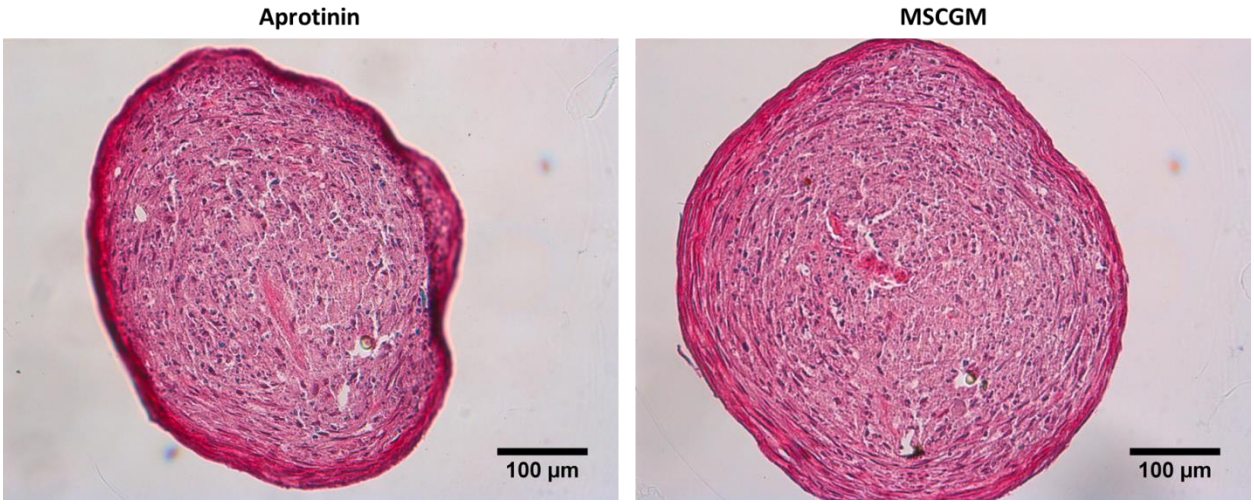

Figure 30: Picro-sirius Stain of Chondrocyte Pellets. Collagen is stained red, while nuclei are stained black. hMSCs exposed to either Aprotinin and MSCGM differentiated into collagen producing chondrocytes.

4.3 Aim 3

4.3.1 hMSC Quantities on Fibrin Sutures

The CyQuant Assay uses a DNA stain and correlates the optical density of stained DNA to the quantity of cells. Sutures were seeded for twenty four hours and plated with Aprotinin or MSCGM, for 0, 1, 2, 3, and 5 days. Each experimental group had a sample size of six. A two-way ANOVA was used to determine significance between groups. All data, including optical densities, cell quantities, standard curves, and ANOVA tables are listed in Appendix H: Cell

All cell quantity data is reported as average ± SEM and displayed in Table 10. At Day 0, sutures seeded in Aprotinin had 11,399 ± 1,133 cells, while MSCGM had 13,838 ± 2,764 cells. Aprotinin supplemented sutures had 14,696 ± 2,560 hMSCs compared to the 12,810 ± 1,153 found on MSCGM sutures at Day 1. When comparing sutures at Day 2, Aprotinin sutures (24,355 ± 3,516) had significantly more hMSCs attached to the suture surface when compared to MSCGM sutures (12,435 ± 1,495). Sutures cultured in aprotinin for three days were shown to have 28,508 ± 4,570 hMSCs, significantly more than those adhered to the surface MSCGM sutures, 13,949 ± 3,030. At Day 5 sutures cultured in the Aprotinin supplemented media showed a significant increase in the number of hMSCs on the sutures surface (31,648 ± 3,899 and 20,643 ± 4,314, respectively). Figure 31 depicts the quantity of hMSCs attached to fibrin suture surface.

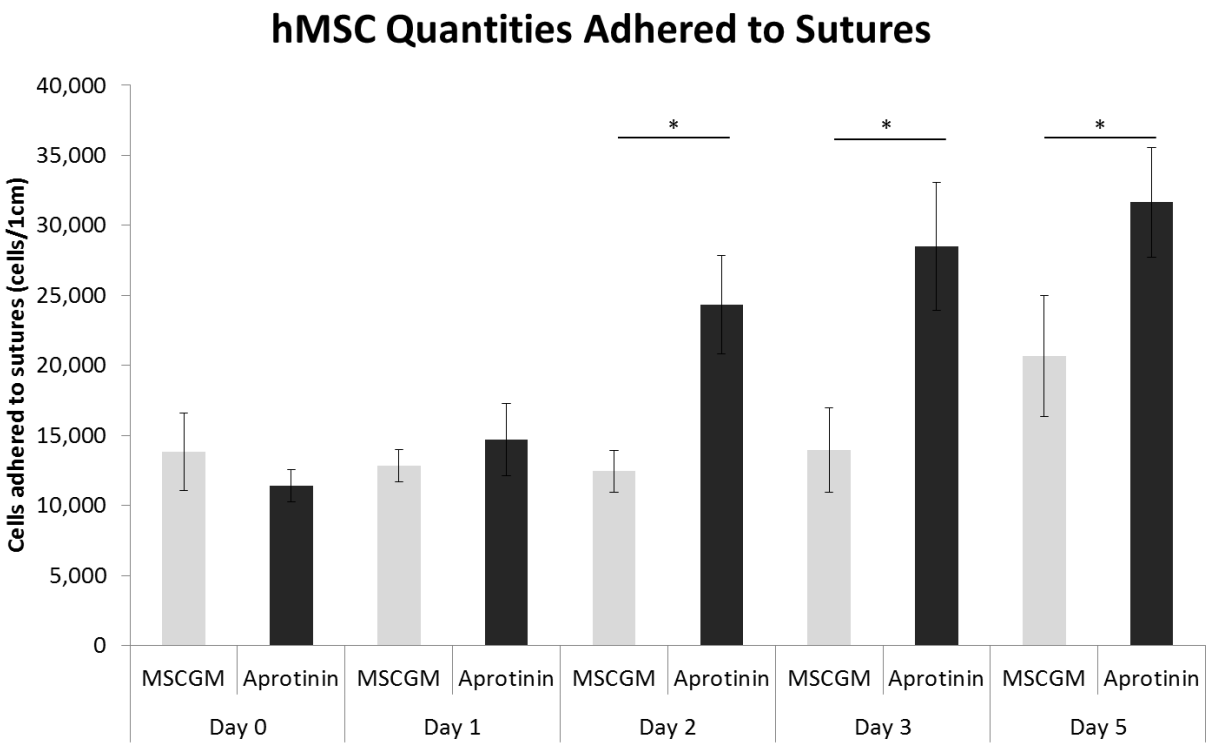

Figure 31: CyQuant Data. Number of cells adhered to fibrin sutures at Days 0, 1, 2, 3, and 5 when cultured in MSCGM or Aprotinin. On Days 2, 3, and 5 sutures cultured in Aprotinin has significantly more hMSCs on the sutures surface when compared to MSCGM alone. * represents a significant difference between groups, as determined by an ANOVA.

Table 10: Cell quantities adhered to the fibrin suture surface

Time-Point	Group	Number of hMSCs	SEM (# of cells)
Day 0	Aprotinin	11,399	1,133
	MSCGM	13,838	2,764
Day 1	Aprotinin	14,696	2,560
	MSCGM	12,810	1,153
Day 2	Aprotinin	24,355	3,516
	MSCGM	12,435	1,495
Day 3	Aprotinin	28,508	4,570
	MSCGM	13,949	3,030
Day 5	Aprotinin	31,648	3,899
	MSCGM	20,643	4,314

When examining the sutures cultured in aprotinin-supplemented MSCGM, Days 2 (24,355 ± 3,516), 3 (28,508 ± 4,570), and 5 (31,648 ± 3,899) each showed a significant increase in the number of cells adhered to the suture's surface when compared to both Day 0 (11,399 ± 1,133) and Day 1 (14,696 ± 2,560). Figure 32 depicts the number of hMSCs on the suture surface of sutures cultured in Aprotinin.

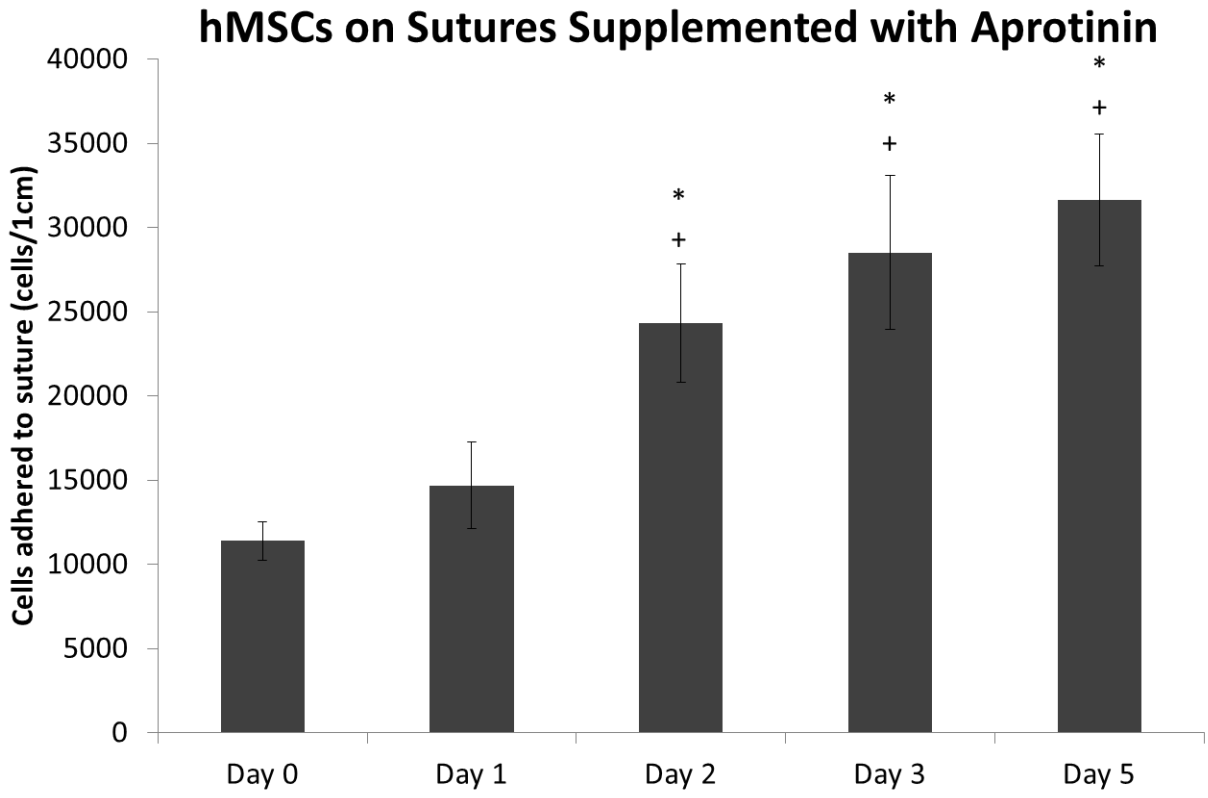

Figure 32: Cell Quantities adhered to sutures (Aprotinin only). An increase in the number of cells on the suture's surface was observed. * represents a 0.05 significance level difference between Day 0, + * represents a 0.05 significance level difference between Day 1.

Looking at the number of cells attached to the sutures, a large jump (approximately 10,000) occurred between days 1 and 2, almost double the number of cells. Knowing the passage doubling time of hMSCs is around 5 to 7 days, an increase of almost double warrants further experimentation. To investigate this increase in hMSCs, sutures were seeded and plated for 0, 1, or 2 Days, with an n = 3 in each group, and stained of Ki-67. This experiment determined the percentage of proliferating cells on sutures. The number of proliferating cells is depicted in Table 11Table 11. At Day 2, sutures cultured in aprotinin showed a significant increase in ki-67 positive cells, when compared to sutures cultured in aprotinin at Days, 0 and 1. This same trend was also observed in sutured cultured in MSCGM alone, with

a significant increase between Day 2 and both Days 0 and 1. Additionally at Day 2, sutures cultured in aprotinin had a significant increase in the number of Ki-67 positive cells when compared to MSCGM alone sutures. Significance was determined using a two way ANOVA, at 0.05 significance level.

Table 11: Percent of Ki-67 positive hMSCs on fibrin sutures.

Time-point	Group	Proliferating hMSCs (% Ki-67 +)	Standard Deviation (% Ki-67 +)
Day 0	Aprotinin	7.37	2.97
	MSCGM	4.82	0.98
Day 1	Aprotinin	9.58	1.36
	MSCGM	6.18	1.33
Day 2	Aprotinin	42.05	11.44
	MSCGM	29.24	2.46

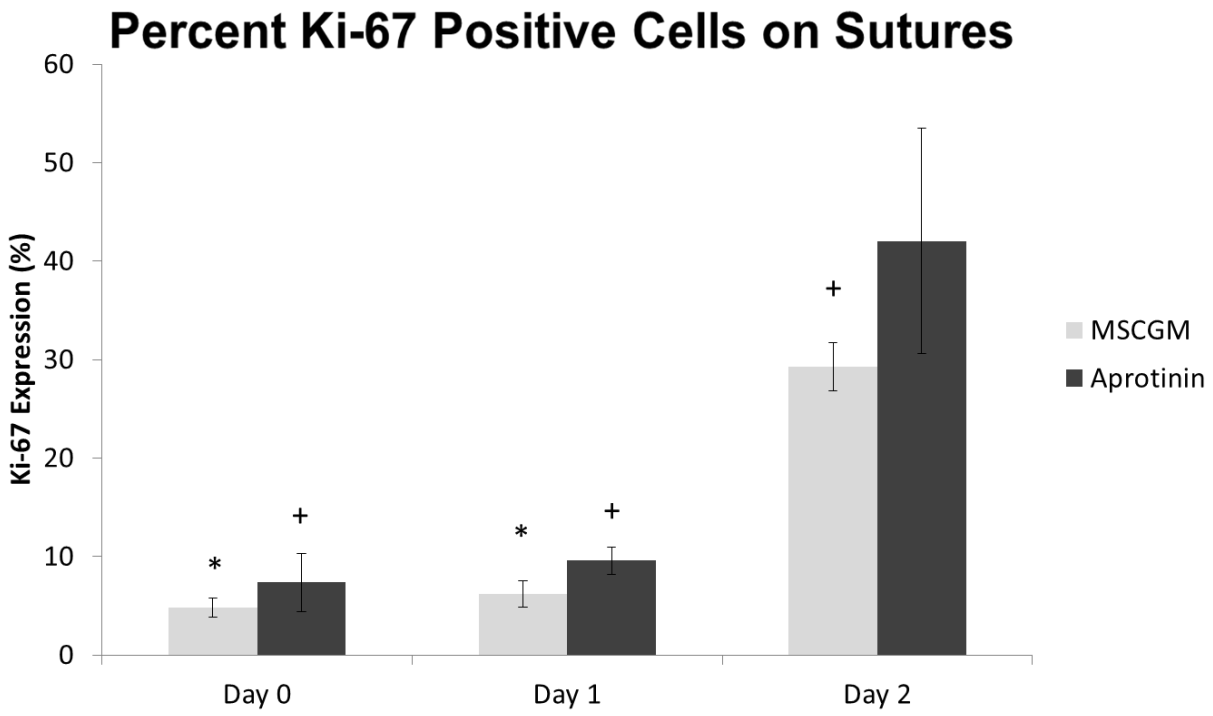

Figure 33: Ki-67 on Sutures (Days 0, 1, 2). At Day 2, Aprotinin sutures showed significant increase in proliferating cells when compared to MSCGM alone sutures. Both groups at Day 2 (Aprotinin and MSCGM), had a significant increase in proliferating cells when compared to both Days 0 and 1 (when compared within each media group). * represents a 0.05 significance level between Day 2 MSCGM and + represents a 0.05 significance level between Day 2 Aprotinin.

Chapter 5: Discussion

This project determined the effects of aprotinin on sutures by quantifying degradation by FDP concentrations in media and determining suture mechanics. Aprotinin supplementation did not seem to affect hMSC viability, determined by LIVE/DEAD, hMSC proliferation, quantified by Ki-67 stain, and hMSC differentiation capacity, by differentiating hMSCs into adipocytes, osteocytes, and chondrocytes and staining to confirm differentiation. Lastly, the number of hMSCs that were adhered to fibrin sutures was determined.

5.1 Alternatives to Aprotinin

In addition to aprotinin, there are two primary antifibrinolytic drugs that could be considered instead of aprotinin to use to control fibrinolysis. These two drugs are Tranexamic acid (TA) and Ɛ-aminocaproic acid (AA) and similar to aprotinin have been used in cardiac surgery to reduce bleeding [80]. If TA and AA were added to MSCGM, like aprotinin in this study, these acids may alter the pH of the MSCGM and growth factors found in the media. The addition of aprotinin did not appear to affect the pH of MSCGM in this study.

When compared to aprotinin, TA controls *in vivo* degradation extremely similar, if not better than aprotinin [80-82]. When investigated in an *in vitro* environment however, TA was shown to be less effective at control fibrin degradation when compared to aprotinin. Fibrin degradation was quantified in terms of thrombus mass, which thrombi formed when aprotinin was used had a significantly lower mass when compared to TA [81]. Both aprotinin and TA appear to have differences in terms of the method and potential to inhibit coagulation; *in vitro,* aprotinin is an effective inhibitor of the intrinsic (contact) coagulation pathway, while TA acid does not inhibit this coagulation pathway [81].

Similar to TA, AA showed similar reductions on fibrinolysis *in vivo* when compared to aprotinin [80]. In addition to investigating the effect on fibrinolysis, the plasma levels of proinflammatories and anti-inflammatories have also been investigated [83]. When compared to aprotinin, AA showed increased levels of plasma proinflammatory [interleukin-6 (IL-6)] and anti-inflammatory [interleukin-10 (IL-10)] cytokines [83]. While it has yet to be determined if this

increase in IL-6 and IL-10 has any effect on clinical outcome, it seems to indicate that aprotinin has less of an immune response when compared to AA.

5.2 Maximum Aprotinin Dosages

We observed a decrease in fibrin degradation, with an increase in aprotinin concentrations up to 100 µg/ml of aprotinin. There were several factors influence the 100 µg/ml cap. When looking at aprotinin concentrations in clinical settings aprotinin concentrations are measure in units of Kallikrein Inhibitor Units (KIU) per mL. One milligram of aprotinin is equivalent to 7,143 KIU [84, 85]. The 100 µg/ml of aprotinin concentration equates to approximately 700 KIU/ml. In a study, a full dose of aprotinin constitutes of: an initial 2 injections of 2,000,000 KIU, a constant infusion 500,000 KIU/hr, followed by a cardio-pulmonary bypass prime of 2 injections of 2,000,000 KIU. Following a full dose administration, patients showed aprotinin levels of 401 ± 91 KIU/ml, with a patient high of approximately 550 KIU/ml [86]. Other studies have also investigated the effect of aprotinin on fibrin scaffold degradation. These studies had aprotinin concentrations between 0 and 50 µg/ml [87-89]. Lastly, inhibition of plasmin and kallikrein have been shown *in vitro* to be 125 KIU/ml and 500 KIU/ml, respectively [90], much higher than the reported 50 KIU/ml for plasmin and 200 KIU/ml for kallikrein reported in patients [91]. Our concentration of 100 µg/ml of aprotinin (or approximately 700 KIU/ml) was slightly higher than the highest levels observed in patients, high enough to inhibit both plasmin and kallikrein, and was comparable to other *in vitro* studies.

5.3 Fibrin Degradation

When using the FDP ELISA to determine the concentrations of FDP, non-seeded controls were used to establish baseline degradations. Aprotinin, MSCGM, and PBS were used as media for culture in these controls. Sutures that were exposed to PBS seemed to degrade differently than other sutures. It appeared that fibrin degraded as a mix of bulk and surface degradation, when seeded with hMSCs in either aprotinin or MSCGM. Sutures became more transparent as time went on, which would seem to indicate bulk degradation. However the diameter also decreased, this may indicate the hMSCs were eating away at the surface of the suture, and therefore surface degradation. With unseeded PBS sutures neither of these two things occurred. It appeared as if the sutures were minced up using scissors, in addition, the fragments of suture that were remaining

did not appear transparent like the other sutures. This seems to indicate another method of fibrin degradation as opposed to the enzymatic degradation that occurred. This has been reported in literature; that fibrin gels placed in PBS have rapidly degraded, quantified by a loss of scaffold mass [92]. One possible explanation for this is that being placed in a salt solution; the ionic bonds of the PBS were strong enough to dissociate the bonds holding the fibrin microthreads together. Another possible explanation is that PBS is a very "blank" solution, meaning that there are no proteins in solution. Complete medias, including MSCGM and MSCGM supplemented with aprotinin, have proteins in solution which may make the fibrin more stable.

5.4 hMSC Differentiation

In this experiment, we demonstrated that hMSCs that were exposed to aprotinin, differentiated into adipocytes, osteocytes, and chondrocytes. While we did not quantify the amount of cells that differentiated, differentiation was observed in both the MSCGM and Aprotinin groups. Our data indicated that aprotinin did not significantly affect the differentiation capacity of hMSCs.

When examining the chondrogenic differentiation, Masson's Trichrome was initially used. Masson's Trichrome is a common stain used in histology to identify keratin, muscle fibers, connective tissue, cellular cytoplasm, and cell nuclei. It was chosen for use in this study because it identifies collagen and is commonly used in histology. Upon further literature review, one study compared a Masson's Trichrome and a Picro-sirius Red stain, and found that the Picro-sirius stain identified collagen more consistently in detecting renal fibrosis than Masson's Trichrome [93]. A different study concluded that Picro-sirius Red was able to provide a more detailed insight on the structure and composition of collagen networks in cardiac tissue when compared to Masson's Trichrome [78, 79]. Because of the slight amounts of collagen detected in this study using Masson's Trichrome, and the ability of Picro-sirius to more easily identify collagen, a Picro-sirius stain was used in addition to Masson's Trichrome to identify collagen in chondrocyte pellets. Additionally, Alcian Blue may be an additional stain that could be used. Alcian Blue stains acidic polysaccharides, which includes glycosaminoglycans that are found in collagen. Alcian Blue may be a better stain to use for collagen detection, because rather than stain specific types of collagen (like Masson's

Trichrome and Picro-sirius), Alcian blue stains the glycosaminoglycans which can be found in any type of collagen.

5.5 Cellular Proliferation on Sutures

When examining the number of hMSCs adhered to fibrin sutures, an increase was seen in the number of adhered cells, in both the MSCGM and Aprotinin groups (as seen in Figure 31 and Figure 32). It is known that the passage doubling time of bone derived hMSCs at low passages is typically around 5 to 7 days [94, 95]. The passage doubling has been known to decrease depending on the growth factors in media [94]. In this experiment there was a large increase (approximately double) between days 1 and 2 of the Aprotinin, seeded sutures. A proliferation stain was performed on sutures between days 0 and 2 to determine if there was any change in proliferation across these time points that could explain the large increase in hMSCs adhered to the sutures. We did see a large increase in proliferation at Day 2 (Figure 33), which corresponds to the increase in adhered cells on sutures. It may be possible that in the 3D environment of being seeded on the suture is somehow stimulating hMSC proliferation. Aprotinin further stimulated proliferation of the hMSCs seeded on fibrin sutures for two days. We did not investigate the mechanism in which aprotinin affected hMSC proliferation, but we clearly observed a large increase in proliferation, indicating that some form of stimulation in proliferation occurred when seeded sutures were cultured for two days in aprotinin.

The seeding procedure is very manual and has a substantial learning curve. Because of this there will be a degree of variability between people seeding sutures and even different batches seeded by the same person. The Cyquant assay is terminal, meaning the cells and sutures are destroyed during the analysis. This prevents the investigation of the number of cells adhered to a single suture over various time points.

Chapter 6: Future Work and Implications

The use of fibrin sutures is a novel method of delivery hMSCs to the infarcted heart used by the Gaudette Lab. It has improved engraftment and localization when compared to traditional IM injections [53]. In addition to these benefits, it is a simple method that surgeons could use to delivery hMSCs to patients without any additional training. Multiple sutures could be used to deliver a desired amount of cells to a particular patient depending on the size of the infarct. Additionally we demonstrated that the use of aprotinin can increase the number of hMSCs when compared to MSCGM alone, while also retaining more of the integrity of the suture. This can be used to increase the number of cells delivered to the infarct zone requiring less sutures. Currently our lab uses seeded sutures to deliver hMSCs to infarcts in rat hearts. Sutures in these experiments are only seeded for 24 hours then delivered to the heart and no further culturing (past the initial twenty-four hours of seeding) is performed. If these sutures were cultured in Aprotinin for even two days before delivery to rat hearts could drastically increase the number of hMSCs delivered to the infarcted heart. Without using Aprotinin, further culture of sutures after seeding was not possible; because the hMSCs degraded the fibrin sutures. Using Aprotinin slowed the hMSC degradation of fibrin and would allow for culture before implantation. Not only does this broaden the range of when seeding needs to occur, further culture after seeding has the potential to deliver more cells.

This experiment did not investigate the adhesion strength of hMSCs cultured in either aprotinin or MSCGM. It is possible that aprotinin may affect the adhesion strength of hMSCs to fibrin sutures. In addition to how well the hMSCs adhere to the suture, how the hMSCs travel after delivery is also a question that can be raised. Future studies could investigate the engraftment rates and where delivered hMSCs are located after suture delivery. Additionally, adhesion molecules including poly-lysine, fibronectin, and laminin may alter the adhesion of hMSCs on fibrin sutures. It is possible that use of an adhesion molecule coupled with culturing in aprotinin-supplemented media may further increase the number of adhered hMSCs, due to increased adhesion and an elongated time in culture. More hMSCs adhered to the sutures may alter suture degradation. Additional FDP ELISAs would need to be performed to assess the degradation of protein coated sutures.

Aprotinin inhibits binding of enzymatic molecules. All of the experiments performed in this study were performed *in vitro*. If the binding of enzymatic molecule binding sites were blocked on the sutures, it is possible that the suture may take more time to degrade *in vivo*. *In vivo* studies could be able to determine if aprotinin supplemented fibrin sutures affect the degradation time following implantation.

hMSCs have been shown to aid in the healing process, but will not differentiate into contracting cardiomyocytes. Induced pluripotent stem cells (iPSC), are cells that have had genes altered to become stem cells. The initial cells are often fibroblasts. Efforts have been made to seed iPSCs on fibrin sutures, and the effect of aprotinin on iPSC cells and seeding on fibrin sutures is currently unknown.

All studies done on seeded fibrin suture delivery to infarcted hearts have been performed on rat models. Before this technology can be applied clinically, it must be further and extensively studied in both small and large animal models. Aspects that would need investigation include an autologous cell isolation and expansion (to eliminate immune response to cells), mechanical function of the heart, engraftment rates of delivered cells, degradation of sutures *in vivo,* and long term effects of delivery fibrin. The type of fibrin used is another area that may require further investigation. Currently, our lab uses bovine components when extruding fibrin microthreads. Determining tissue and immune response of interspecies protein implantation would need to be investigated. Following successful safety and efficacy trials in all animal trials, isolated clinical trials may begin. Success in isolated clinical trials may lead to further use.

Conclusion

The goal of this project was to characterize and explore the effects of aprotinin supplementation on both hMSCs and hMSC seeded biological sutures. Exposing sutures to aprotinin, exhibited low levels of FDP as well as higher suture mechanical strength and modulus. Aprotinin did not appear to effect hMSC viability, proliferation, or differentiation. Lastly, when cultured in Aprotinin, the number of hMSCs adhered to the fibrin sutures was increased compared to MSCGM alone. When supplemented with 100 μg/ml of aprotinin, we observed a 33% reduction in FDP mass over nine days, a 2.6 x increase in suture UTS, up to a 2.0 increase in the number of hMSCs adhered to sutures, and an increase of up to 1.4x the proliferation of hMSCs on sutures. The use of aprotinin will allow hMSC seeded sutures to remain in culture for more extended periods of time (when compared to MSCGM alone) while increasing the number of adhered hMSCs while extending the window of use for hMSC seeded fibrin biological sutures.

References

1. Murphy, M.K., *Fibrin Microthreads Promote Stem Cell Growth for Localized Delivery in Regenerative Therapy*, in *Biomedical Engineering, Worcester Polytechnic Institute*. 2008, WPI: Worcester.
2. Humphrey, J., *Cardiovascular Soild Mechanics: Cells, Tissues, and Organs*. 2001, New York, New York: Springer-Verlag.
3. Marieb, E.N.K., K., *Human Anatomy and Physiology*, ed. Pearson. 2011.
4. Sherwood, L., *Human Physiology: from cells to systems*. 4th ed, ed. Brooks/Cole. 2001, Pacific Grove, CA.
5. Bers, D.M., *Cardiac excitation-contraction coupling.* Nature, 2002. **415**(6868): p. 198-205.
6. Ferrero Jr, J., *Wiley Encyclopedia of Biomedical Engineering*. 2006: John Wiley and Sons Inc.
7. Kloner, R.A. and R.B. Jennings, *Consequences of brief ischemia: stunning, preconditioning, and their clinical implications: part 1.* Circulation, 2001. **104**(24): p. 2981-9.
8. Sutton, M.S.N., *Left Ventricle Remodeling After Myocardial Infarction: Pathophysiology and Therapy.* Circulation, 2000(101): p. 2981-2988.
9. Pagidipati, N.J. and T.A. Gaziano, *Estimating deaths from cardiovascular disease: a review of global methodologies of mortality measurement.* Circulation, 2013. **127**(6): p. 749-56.
10. Go, A.S., et al., *Heart disease and stroke statistics--2014 update: a report from the American Heart Association.* Circulation, 2014. **129**(3): p. e28-e292.
11. Mozaffarian, D., et al., *Heart disease and stroke statistics--2015 update: a report from the American Heart Association.* Circulation, 2015. **131**(4): p. e29-322.
12. Laflamme, M.A. and C.E. Murry, *Regenerating the heart.* Nat Biotechnol, 2005. **23**(7): p. 845-56.
13. *Heart and Stroke Statistics*. 2015 [cited 2015.
14. Pfeffer, M.A. and E. Braunwald, *Ventricular remodeling after myocardial infarction. Experimental observations and clinical implications.* Circulation, 1990. **81**(4): p. 1161-72.
15. Athanasuleas, C.L., et al., *Surgical ventricular restoration in the treatment of congestive heart failure due to post-infarction ventricular dilation.* J Am Coll Cardiol, 2004. **44**(7): p. 1439-45.
16. Buckberg, G., *Ventricular structure and surgical history.* Heart Fail Rev, 2004. **9**(4): p. 255-68; discussion 347-51.
17. Tonnessen, T. and C.W. Knudsen, *Surgical left ventricular remodeling in heart failure.* Eur J Heart Fail, 2005. **7**(5): p. 704-9.
18. Fang, J.C.G., *Surgical Management of Congestive Heart Failure*. 2005, Totowa, NJ: Humana Press Inc.
19. Kochupura, P.V., et al., *Tissue-engineered myocardial patch derived from extracellular matrix provides regional mechanical function.* Circulation, 2005. **112**(9 Suppl): p. I144-9.
20. Taylor, D.A., et al., *Regenerating functional myocardium: improved performance after skeletal myoblast transplantation.* Nat Med, 1998. **4**(8): p. 929-33.
21. Kolossov, E., et al., *Engraftment of engineered ES cell-derived cardiomyocytes but not BM cells restores contractile function to the infarcted myocardium.* J Exp Med, 2006. **203**(10): p. 2315-27.
22. Beltrami, A.P., et al., *Adult cardiac stem cells are multipotent and support myocardial regeneration.* Cell, 2003. **114**(6): p. 763-76.
23. Schuldt, A.J., et al., *Repairing damaged myocardium: evaluating cells used for cardiac regeneration.* Curr Treat Options Cardiovasc Med, 2008. **10**(1): p. 59-72.
24. Reffelmann, T. and R.A. Kloner, *Cellular cardiomyoplasty--cardiomyocytes, skeletal myoblasts, or stem cells for regenerating myocardium and treatment of heart failure?* Cardiovasc Res, 2003. **58**(2): p. 358-68.

25. Christman, K.L. and R.J. Lee, *Biomaterials for the treatment of myocardial infarction.* J Am Coll Cardiol, 2006. **48**(5): p. 907-13.
26. Rane, A.A. and K.L. Christman, *Biomaterials for the treatment of myocardial infarction: a 5-year update.* J Am Coll Cardiol, 2011. **58**(25): p. 2615-29.
27. Pittenger, M.F. and B.J. Martin, *Mesenchymal stem cells and their potential as cardiac therapeutics.* Circ Res, 2004. **95**(1): p. 9-20.
28. Barry, F.P. and J.M. Murphy, *Mesenchymal stem cells: clinical applications and biological characterization.* Int J Biochem Cell Biol, 2004. **36**(4): p. 568-84.
29. Tae, S.K., et al., *Mesenchymal stem cells for tissue engineering and regenerative medicine.* Biomed Mater, 2006. **1**(2): p. 63-71.
30. Toma, C., et al., *Human mesenchymal stem cells differentiate to a cardiomyocyte phenotype in the adult murine heart.* Circulation, 2002. **105**(1): p. 93-8.
31. Hou, M., et al., *Transplantation of mesenchymal stem cells from human bone marrow improves damaged heart function in rats.* Int J Cardiol, 2007. **115**(2): p. 220-8.
32. Orlic, D., et al., *Mobilized bone marrow cells repair the infarcted heart, improving function and survival.* Proc Natl Acad Sci U S A, 2001. **98**(18): p. 10344-9.
33. Behfar, A., et al., *Guided cardiopoiesis enhances therapeutic benefit of bone marrow human mesenchymal stem cells in chronic myocardial infarction.* J Am Coll Cardiol, 2010. **56**(9): p. 721-34.
34. Potapova, I.A., et al., *Enhanced recovery of mechanical function in the canine heart by seeding an extracellular matrix patch with mesenchymal stem cells committed to a cardiac lineage.* Am J Physiol Heart Circ Physiol, 2008. **295**(6): p. H2257-63.
35. Mauritz, C., et al., *Generation of functional murine cardiac myocytes from induced pluripotent stem cells.* Circulation, 2008. **118**(5): p. 507-17.
36. Kreutziger, K.L. and C.E. Murry, *Engineered human cardiac tissue.* Pediatr Cardiol, 2011. **32**(3): p. 334-41.
37. Tomita, S., et al., *Autologous transplantation of bone marrow cells improves damaged heart function.* Circulation, 1999. **100**(19 Suppl): p. II247-56.
38. Kamihata, H., et al., *Implantation of bone marrow mononuclear cells into ischemic myocardium enhances collateral perfusion and regional function via side supply of angioblasts, angiogenic ligands, and cytokines.* Circulation, 2001. **104**(9): p. 1046-52.
39. Tang, Y.L., et al., *Autologous mesenchymal stem cell transplantation induce VEGF and neovascularization in ischemic myocardium.* Regul Pept, 2004. **117**(1): p. 3-10.
40. Zhang, S., et al., *Long-term effects of bone marrow mononuclear cell transplantation on left ventricular function and remodeling in rats.* Life Sci, 2004. **74**(23): p. 2853-64.
41. Tang, J., et al., *Mesenchymal stem cells participate in angiogenesis and improve heart function in rat model of myocardial ischemia with reperfusion.* Eur J Cardiothorac Surg, 2006. **30**(2): p. 353-61.
42. Mazo, M., et al., *Transplantation of adipose derived stromal cells is associated with functional improvement in a rat model of chronic myocardial infarction.* Eur J Heart Fail, 2008. **10**(5): p. 454-62.
43. Orlic, D., et al., *Bone marrow cells regenerate infarcted myocardium.* Nature, 2001. **410**(6829): p. 701-5.
44. Kudo, M., et al., *Implantation of bone marrow stem cells reduces the infarction and fibrosis in ischemic mouse heart.* J Mol Cell Cardiol, 2003. **35**(9): p. 1113-9.
45. Kajstura, J., et al., *Bone marrow cells differentiate in cardiac cell lineages after infarction independently of cell fusion.* Circ Res, 2005. **96**(1): p. 127-37.

46. Rota, M., et al., *Bone marrow cells adopt the cardiomyogenic fate in vivo.* Proc Natl Acad Sci U S A, 2007. **104**(45): p. 17783-8.
47. Shake, J.G., et al., *Mesenchymal stem cell implantation in a swine myocardial infarct model: engraftment and functional effects.* Ann Thorac Surg, 2002. **73**(6): p. 1919-25; discussion 1926.
48. Amado, L.C., et al., *Cardiac repair with intramyocardial injection of allogeneic mesenchymal stem cells after myocardial infarction.* Proc Natl Acad Sci U S A, 2005. **102**(32): p. 11474-9.
49. Valina, C., et al., *Intracoronary administration of autologous adipose tissue-derived stem cells improves left ventricular function, perfusion, and remodelling after acute myocardial infarction.* Eur Heart J, 2007. **28**(21): p. 2667-77.
50. Silva, G.V., et al., *Mesenchymal stem cells differentiate into an endothelial phenotype, enhance vascular density, and improve heart function in a canine chronic ischemia model.* Circulation, 2005. **111**(2): p. 150-6.
51. Muller-Ehmsen, J., et al., *Survival and development of neonatal rat cardiomyocytes transplanted into adult myocardium.* J Mol Cell Cardiol, 2002. **34**(2): p. 107-16.
52. Hou, D., et al., *Radiolabeled cell distribution after intramyocardial, intracoronary, and interstitial retrograde coronary venous delivery: implications for current clinical trials.* Circulation, 2005. **112**(9 Suppl): p. I150-6.
53. Guyette, J.P., et al., *A novel suture-based method for efficient transplantation of stem cells.* J Biomed Mater Res A, 2013. **101**(3): p. 809-18.
54. Zhang, M., et al., *Cardiomyocyte grafting for cardiac repair: graft cell death and anti-death strategies.* J Mol Cell Cardiol, 2001. **33**(5): p. 907-21.
55. Clark, R.A., *Fibrin and wound healing.* Ann N Y Acad Sci, 2001. **936**: p. 355-67.
56. Kofidis, T., et al., *Injectable bioartificial myocardial tissue for large-scale intramural cell transfer and functional recovery of injured heart muscle.* J Thorac Cardiovasc Surg, 2004. **128**(4): p. 571-8.
57. Ryu, J.H., et al., *Implantation of bone marrow mononuclear cells using injectable fibrin matrix enhances neovascularization in infarcted myocardium.* Biomaterials, 2005. **26**(3): p. 319-26.
58. Mol, A., et al., *Fibrin as a cell carrier in cardiovascular tissue engineering applications.* Biomaterials, 2005. **26**(16): p. 3113-21.
59. Ahmed, T.A., E.V. Dare, and M. Hincke, *Fibrin: a versatile scaffold for tissue engineering applications.* Tissue Eng Part B Rev, 2008. **14**(2): p. 199-215.
60. Buchta, C., et al., *Biochemical characterization of autologous fibrin sealants produced by CryoSeal and Vivostat in comparison to the homologous fibrin sealant product Tissucol/Tisseel.* Biomaterials, 2005. **26**(31): p. 6233-41.
61. Leo, A.J. and D.A. Grande, *Mesenchymal stem cells in tissue engineering.* Cells Tissues Organs, 2006. **183**(3): p. 112-22.
62. Gruber, H.E., et al., *Cell-based tissue engineering for the intervertebral disc: in vitro studies of human disc cell gene expression and matrix production within selected cell carriers.* Spine J, 2004. **4**(1): p. 44-55.
63. Ringe, J., et al., *Stem cells for regenerative medicine: advances in the engineering of tissues and organs.* Naturwissenschaften, 2002. **89**(8): p. 338-51.
64. Schense, J.C. and J.A. Hubbell, *Cross-linking exogenous bifunctional peptides into fibrin gels with factor XIIIa.* Bioconjug Chem, 1999. **10**(1): p. 75-81.
65. Cornwell, K.G. and G.D. Pins, *Discrete crosslinked fibrin microthread scaffolds for tissue regeneration.* J Biomed Mater Res A, 2007. **82**(1): p. 104-12.
66. Kowaleski, M., *Increasing Cell Attachment and Adhesion on Fibrin Microthread Sutures for Cell Delivery*, in *Biomedical Engineering*. 2012, Worcester Polyetchnic Institute: Worcester, MA.
67. Neuss, S., et al., *Secretion of fibrinolytic enzymes facilitates human mesenchymal stem cell invasion into fibrin clots.* Cells Tissues Organs, 2010. **191**(1): p. 36-46.

68. Cesarman-Maus, G. and K.A. Hajjar, *Molecular mechanisms of fibrinolysis.* Br J Haematol, 2005. **129**(3): p. 307-21.
69. Hajjiar, K.A., *The molecular basis of fibrinolysis*. Hematology of Infancy and Childhood. 2003, Philadelphia, USA: W.B. Saunders Co.
70. Mannucci, P.M., *Hemostatic drugs.* N Engl J Med, 1998. **339**(4): p. 245-53.
71. Richardson, J.S., *The anatomy and taxonomy of protein structure.* Adv Protein Chem, 1981. **34**: p. 167-339.
72. Kassell, B., et al., *The Basic Trypsin Inhibitor of Bovine Pancreas. Iv. The Linear Sequence of the 58 Amino Acids.* Biochem Biophys Res Commun, 1965. **18**: p. 255-8.
73. Hewlett, G., *Apropos aprotinin: a review.* Biotechnology (N Y), 1990. **8**(6): p. 565-6, 568.
74. Mangano, D.T., et al., *The risk associated with aprotinin in cardiac surgery.* N Engl J Med, 2006. **354**(4): p. 353-65.
75. Mangano, D.T., et al., *Mortality associated with aprotinin during 5 years following coronary artery bypass graft surgery.* JAMA, 2007. **297**(5): p. 471-9.
76. *Bayer Temporarily Suspends Global Trasylol Marketing*, Bayer, Editor. 2007: Trasylol.com.
77. Benstetter, M.H., S, *European Medicines Agency recommends lifting suspension of aprotinin*. 2012, European Medicines Agency.
78. de Jong, S., et al., *Monitoring cardiac fibrosis: a technical challenge.* Neth Heart J, 2012. **20**(1): p. 44-8.
79. Whittaker, P., et al., *Quantitative assessment of myocardial collagen with picrosirius red staining and circularly polarized light.* Basic Res Cardiol, 1994. **89**(5): p. 397-410.
80. Schouten, E.S., et al., *The effect of aprotinin, tranexamic acid, and aminocaproic acid on blood loss and use of blood products in major pediatric surgery: a meta-analysis.* Pediatr Crit Care Med, 2009. **10**(2): p. 182-90.
81. Sperzel, M. and J. Huetter, *Evaluation of aprotinin and tranexamic acid in different in vitro and in vivo models of fibrinolysis, coagulation and thrombus formation.* J Thromb Haemost, 2007. **5**(10): p. 2113-8.
82. Cholewinski, E., et al., *Tranexamic acid--an alternative to aprotinin in fibrin-based cardiovascular tissue engineering.* Tissue Eng Part A, 2009. **15**(11): p. 3645-53.
83. Greilich, P.E., et al., *Aprotinin but not epsilon-aminocaproic acid decreases interleukin-10 after cardiac surgery with extracorporeal circulation: randomized, double-blind, placebo-controlled study in patients receiving aprotinin and epsilon-aminocaproic acid.* Circulation, 2001. **104**(12 Suppl 1): p. I265-9.
84. *Pediatric Anesthesia: Basic Principles - State of the Art - Future*. 2011, Shelton, CN: People's Medical Publishing House.
85. *Blood Use in Cardiac Surgery*, ed. F.H. Friedel, R. Royston, D. 1991, Steinkopff, NY: Steinkopff.
86. Beath, S.M., et al., *Plasma aprotinin concentrations during cardiac surgery: full- versus half-dose regimens.* Anesth Analg, 2000. **91**(2): p. 257-64.
87. Ye, Q.Z., G. Benedikt, P. Jockenhovel, S. Hoestrup, S. Sakyama, S. Hubbell, J. Turina, M., *Fibrin gel as a three dimensional matrix in cardiovascular tissue engineering.* European Journal of Cardio-Thoratic Surgery, 2000. **17**(6): p. 587-591.
88. Jockenhoevel, S., et al., *Fibrin gel -- advantages of a new scaffold in cardiovascular tissue engineering.* Eur J Cardiothorac Surg, 2001. **19**(4): p. 424-30.
89. Willerth, S.M., et al., *Optimization of fibrin scaffolds for differentiation of murine embryonic stem cells into neural lineage cells.* Biomaterials, 2006. **27**(36): p. 5990-6003.
90. Fritz, H. and G. Wunderer, *Biochemistry and applications of aprotinin, the kallikrein inhibitor from bovine organs.* Arzneimittelforschung, 1983. **33**(4): p. 479-94.

91. Levy, J.H., J.M. Bailey, and M. Salmenpera, *Pharmacokinetics of aprotinin in preoperative cardiac surgical patients.* Anesthesiology, 1994. **80**(5): p. 1013-8.
92. Zhao, H., et al., *Fabrication and physical and biological properties of fibrin gel derived from human plasma.* Biomed Mater, 2008. **3**(1): p. 015001.
93. Street, J.M., et al., *Automated quantification of renal fibrosis with Sirius Red and polarization contrast microscopy.* Physiol Rep, 2014. **2**(7).
94. Ben Azouna, N., et al., *Phenotypical and functional characteristics of mesenchymal stem cells from bone marrow: comparison of culture using different media supplemented with human platelet lysate or fetal bovine serum.* Stem Cell Res Ther, 2012. **3**(1): p. 6.
95. Bruder, S.P., N. Jaiswal, and S.E. Haynesworth, *Growth kinetics, self-renewal, and the osteogenic potential of purified human mesenchymal stem cells during extensive subcultivation and following cryopreservation.* J Cell Biochem, 1997. **64**(2): p. 278-94.

Appendix A: Fibrin Degradation ELISA Results

		Exp 1	Exp 2	AVG	STDEV
Day 3	100	7.622936	9.228964		
		9.910392	9.570009		
		7.319273	8.425706	8.679547	1.062165
	50	10.88719	11.90369		
		9.457667	12.65799		
		10.66005	11.406	11.1621	1.102712
	10	13.23196	11.71343		
		7.956207	11.73842		
		11.24472	12.11063	11.33256	1.784957
	5	9.951722	11.55223		
		12.82803	11.79074		
		12.21712	11.49912	11.63983	0.96385
	1	13.65471	11.88366		
		13.30805	12.61517		
		12.50133	11.64742	12.60172	0.780287
	0	11.43684	15.76576		
		15.37414	14.77188		
		13.40549	14.00589	14.12667	1.576638

		Exp 1	Exp 2	AVG	STDEV
Day 6	100	8.790885	8.30922		
		10.21902	8.55726		
		8.464757	9.462697	8.967307	0.732059
	50	11.04145	11.2841		
		10.61389	12.2332		
		10.18633	10.66074	11.00328	0.711249
	10	12.55242	11.8652		
		7.824913	11.00254		
		11.66233	10.7725	10.94665	1.656087

	5	11.3138	11.16072		
		10.95394	10.48661		
		12.1703	10.91923	11.16743	0.565316
	1	13.02423	11.78728		
		12.51723	12.9435		
		12.27846	11.61284	12.36059	0.582975
	0	10.36769	12.81272		
		14.66589	14.47927		
		11.02304	14.03639	12.8975	1.835592

		Exp 1	Exp 2	AVG	STDEV
Day 9	100	8.434686	8.965305	9.050344	0.533658
		9.601762	9.756725		
		8.572459	8.971127		
	50	10.49048	11.99466	11.05617	1.314928
		9.474227	11.71798		
		9.854351	12.80531		
	10	13.65471	9.984784	11.25988	1.805767
		8.563633	11.04292		
		12.06238	12.25087		
	5	11.43684	10.14689	10.1396	0.929126
		8.596397	10.02761		
		10.01662	10.61324		
	1	13.67827	12.13779	12.69296	1.22134
		11.93878	11.44764		
		14.66681	12.28848		
	0	13.90932	12.21685	12.98867	1.355564
		13.34402	14.7018		
		10.82523	12.93479		

Appendix B: Fibrin Degradation ELISA ANOVA

Two Way Analysis of Variance Thursday, April 16, 2015, 10:23:49 AM

Data source: Data 2 in FDP ELISA

General Linear Model

Dependent Variable: Col 3

Normality Test (Shapiro-Wilk) Passed (P = 0.068)

Equal Variance Test: Passed (P = 0.530)

Source of Variation	DF	SS	MS	F	P
Col 1	7	234.655	33.522	24.588	<0.001
Col 2	2	1.106	0.553	0.406	0.668
Col 1 x Col 2	14	19.333	1.381	1.013	0.447
Residual	102	139.063	1.363		
Total	125	390.679	3.125		

The difference in the mean values among the different levels of Col 1 is greater than would be expected by chance after allowing for effects of differences in Col 2. There is a statistically significant difference (P = <0.001). To isolate which group(s) differ from the others use a multiple comparison procedure.

The difference in the mean values among the different levels of Col 2 is not great enough to exclude the possibility that the difference is just due to random sampling variability after allowing for the effects of differences in Col 1. There is not a statistically significant difference (P = 0.668).

The effect of different levels of Col 1 does not depend on what level of Col 2 is present. There is not a statistically significant interaction between Col 1 and Col 2. (P = 0.447)

Power of performed test with alpha = 0.0500: for Col 1 : 1.000
Power of performed test with alpha = 0.0500: for Col 2 : 0.0500
Power of performed test with alpha = 0.0500: for Col 1 x Col 2 : 0.0537

Least square means for Col 1 :

Group	Mean	SEM
MSCGM-100	8.899	0.275
MSCGM-50	11.074	0.275
MSCGM-10	11.180	0.275
MSCGM-5	10.982	0.275
MSCGM-1	12.496	0.269
MSCGM	13.517	0.284
MSCGM-NC	9.890	0.389
MSCGM-100-NC	10.977	0.389

Least square means for Col 2 :

Group	Mean	SEM
Day 3	11.265	0.189
Day 6	11.069	0.188
Day 9	11.047	0.188

Least square means for Col 1 x Col 2 :

Group	Mean	SEM
MSCGM-100 x Day 3	8.680	0.477
MSCGM-100 x Day 6	8.967	0.477
MSCGM-100 x Day 9	9.050	0.477
MSCGM-50 x Day 3	11.162	0.477
MSCGM-50 x Day 6	11.003	0.477
MSCGM-50 x Day 9	11.056	0.477
MSCGM-10 x Day 3	11.333	0.477
MSCGM-10 x Day 6	10.947	0.477
MSCGM-10 x Day 9	11.260	0.477
MSCGM-5 x Day 3	11.640	0.477
MSCGM-5 x Day 6	11.167	0.477
MSCGM-5 x Day 9	10.140	0.477
MSCGM-1 x Day 3	12.435	0.441
MSCGM-1 x Day 6	12.361	0.477
MSCGM-1 x Day 9	12.693	0.477
MSCGM x Day 3	14.665	0.522
MSCGM x Day 6	12.898	0.477
MSCGM x Day 9	12.989	0.477
MSCGM-NC x Day 3	9.392	0.674
MSCGM-NC x Day 6	10.475	0.674
MSCGM-NC x Day 9	9.804	0.674
MSCGM-100-NC x Day 3	10.816	0.674
MSCGM-100-NC x Day 6	10.731	0.674
MSCGM-100-NC x Day 9	11.384	0.674

All Pairwise Multiple Comparison Procedures (Holm-Sidak method):
Overall significance level = 0.05

Comparisons for factor: **Col 1**

Comparison	**Diff of Means**	**t**	**P**	**P<0.050**
MSCGM vs. MSCGM-100	4.618	11.672	<0.001	Yes
MSCGM-1 vs. MSCGM-100	3.597	9.354	<0.001	Yes
MSCGM vs. MSCGM-NC	3.627	7.525	<0.001	Yes
MSCGM vs. MSCGM-5	2.535	6.406	<0.001	Yes
MSCGM vs. MSCGM-50	2.443	6.175	<0.001	Yes
MSCGM vs. MSCGM-10	2.337	5.907	<0.001	Yes
MSCGM-10 vs. MSCGM-100	2.281	5.860	<0.001	Yes
MSCGM-50 vs. MSCGM-100	2.175	5.588	<0.001	Yes
MSCGM-1 vs. MSCGM-NC	2.606	5.511	<0.001	Yes
MSCGM-5 vs. MSCGM-100	2.083	5.352	<0.001	Yes
MSCGM vs. MSCGM-100-NC	2.540	5.270	<0.001	Yes
MSCGM-100-NC vs. MSCGM-100	2.078	4.360	<0.001	Yes
MSCGM-1 vs. MSCGM-5	1.514	3.937	0.002	Yes
MSCGM-1 vs. MSCGM-50	1.422	3.699	0.005	Yes
MSCGM-1 vs. MSCGM-10	1.317	3.424	0.012	Yes
MSCGM-1 vs. MSCGM-100-NC	1.519	3.212	0.023	Yes
MSCGM-10 vs. MSCGM-NC	1.290	2.705	0.092	No
MSCGM vs. MSCGM-1	1.021	2.610	0.109	No
MSCGM-50 vs. MSCGM-NC	1.184	2.483	0.137	No
MSCGM-5 vs. MSCGM-NC	1.092	2.291	0.196	No
MSCGM-NC vs. MSCGM-100	0.991	2.079	0.279	No
MSCGM-100-NC vs. MSCGM-NC	1.087	1.975	0.307	No
MSCGM-10 vs. MSCGM-5	0.197	0.507	0.997	No

MSCGM-10 vs. MSCGM-100-NC	0.202	0.425	0.996	No
MSCGM-10 vs. MSCGM-50	0.106	0.272	0.998	No
MSCGM-50 vs. MSCGM-5	0.0916	0.235	0.994	No
MSCGM-50 vs. MSCGM-100-NC	0.0966	0.203	0.974	No
MSCGM-5 vs. MSCGM-100-NC	0.00502	0.0105	0.992	No

Comparisons for factor: **Col 2**

Comparison	**Diff of Means**	**t**	**P**	**P<0.050**
Day 3 vs. Day 9	0.218	0.818	0.800	No
Day 3 vs. Day 6	0.197	0.737	0.712	No
Day 6 vs. Day 9	0.0217	0.0813	0.935	No

Comparisons for factor: **Col 2 within MSCGM-100**

Comparison	**Diff of Means**	**t**	**P**	**P<0.05**
Day 9 vs. Day 3	0.371	0.550	0.928	No
Day 6 vs. Day 3	0.288	0.427	0.891	No
Day 9 vs. Day 6	0.0830	0.123	0.902	No

Comparisons for factor: **Col 2 within MSCGM-50**

Comparison	**Diff of Means**	**t**	**P**	**P<0.05**
Day 3 vs. Day 6	0.159	0.236	0.994	No
Day 3 vs. Day 9	0.106	0.157	0.984	No
Day 9 vs. Day 6	0.0529	0.0784	0.938	No

Comparisons for factor: **Col 2 within MSCGM-10**

Comparison	**Diff of Means**	**t**	**P**	**P<0.05**
Day 3 vs. Day 6	0.386	0.572	0.920	No
Day 9 vs. Day 6	0.313	0.465	0.873	No
Day 3 vs. Day 9	0.0727	0.108	0.914	No

Comparisons for factor: **Col 2 within MSCGM-5**

Comparison	**Diff of Means**	**t**	**P**	**P<0.05**
Day 3 vs. Day 9	1.500	2.225	0.082	No
Day 6 vs. Day 9	1.028	1.525	0.244	No
Day 3 vs. Day 6	0.472	0.701	0.485	No

Comparisons for factor: **Col 2 within MSCGM-1**

Comparison	**Diff of Means**	**t**	**P**	**P<0.05**
Day 9 vs. Day 6	0.332	0.493	0.946	No
Day 9 vs. Day 3	0.258	0.397	0.905	No
Day 3 vs. Day 6	0.0747	0.115	0.909	No

Comparisons for factor: **Col 2 within MSCGM**

Comparison	**Diff of Means**	**t**	**P**	**P<0.05**
Day 3 vs. Day 6	1.767	2.499	0.042	Yes
Day 3 vs. Day 9	1.676	2.370	0.039	Yes
Day 9 vs. Day 6	0.0912	0.135	0.893	No

Comparisons for factor: **Col 2 within MSCGM-NC**

Comparison	**Diff of Means**	**t**	**P**	**P<0.05**
Day 6 vs. Day 3	1.084	1.137	0.592	No
Day 6 vs. Day 9	0.671	0.704	0.733	No
Day 9 vs. Day 3	0.412	0.432	0.666	No

Comparisons for factor: **Col 2 within MSCGM-100-NC**

Comparison	**Diff of Means**	**t**	**P**	**P<0.05**
Day 9 vs. Day 6	0.653	0.685	0.871	No
Day 9 vs. Day 3	0.568	0.596	0.800	No
Day 3 vs. Day 6	0.0851	0.0893	0.929	No

Comparisons for factor: **Col 1 within Day 3**

Comparison	Diff of Means	t	P	P<0.05
MSCGM vs. MSCGM-100	5.985	8.465	<0.001	Yes
MSCGM vs. MSCGM-NC	5.273	6.184	<0.001	Yes
MSCGM-1 vs. MSCGM-100	3.756	5.782	<0.001	Yes
MSCGM vs. MSCGM-50	3.503	4.954	<0.001	Yes
MSCGM vs. MSCGM-10	3.332	4.713	<0.001	Yes
MSCGM vs. MSCGM-100-NC	3.848	4.513	<0.001	Yes
MSCGM-5 vs. MSCGM-100	2.960	4.391	<0.001	Yes
MSCGM vs. MSCGM-5	3.025	4.278	<0.001	Yes
MSCGM-10 vs. MSCGM-100	2.653	3.935	0.003	Yes
MSCGM-1 vs. MSCGM-NC	3.044	3.778	0.005	Yes
MSCGM-50 vs. MSCGM-100	2.483	3.683	0.007	Yes
MSCGM vs. MSCGM-1	2.229	3.261	0.025	Yes
MSCGM-5 vs. MSCGM-NC	2.248	2.723	0.115	No
MSCGM-100-NC vs. MSCGM-100	2.137	2.588	0.154	No
MSCGM-10 vs. MSCGM-NC	1.941	2.351	0.253	No
MSCGM-50 vs. MSCGM-NC	1.771	2.145	0.365	No
MSCGM-1 vs. MSCGM-100-NC	1.619	2.009	0.440	No
MSCGM-1 vs. MSCGM-50	1.273	1.960	0.449	No
MSCGM-1 vs. MSCGM-10	1.103	1.698	0.622	No
MSCGM-100-NC vs. MSCGM-NC	1.425	1.494	0.738	No
MSCGM-1 vs. MSCGM-5	0.795	1.225	0.868	No
MSCGM-5 vs. MSCGM-100-NC	0.824	0.997	0.933	No
MSCGM-NC vs. MSCGM-100	0.712	0.862	0.949	No
MSCGM-5 vs. MSCGM-50	0.478	0.709	0.962	No
MSCGM-10 vs. MSCGM-100-NC	0.516	0.625	0.952	No
MSCGM-5 vs. MSCGM-10	0.307	0.456	0.957	No
MSCGM-50 vs. MSCGM-100-NC	0.346	0.419	0.895	No
MSCGM-10 vs. MSCGM-50	0.170	0.253	0.801	No

Comparisons for factor: **Col 1 within Day 6**

Comparison	Diff of Means	t	P	P<0.05
MSCGM vs. MSCGM-100	3.930	5.830	<0.001	Yes
MSCGM-1 vs. MSCGM-100	3.393	5.034	<0.001	Yes
MSCGM-5 vs. MSCGM-100	2.200	3.264	0.038	Yes
MSCGM-50 vs. MSCGM-100	2.036	3.020	0.077	No
MSCGM-10 vs. MSCGM-100	1.979	2.936	0.094	No
MSCGM vs. MSCGM-NC	2.422	2.934	0.091	No
MSCGM vs. MSCGM-10	1.951	2.894	0.098	No
MSCGM vs. MSCGM-50	1.894	2.810	0.118	No

MSCGM vs. MSCGM-100-NC	2.166	2.624	0.183	No
MSCGM vs. MSCGM-5	1.730	2.566	0.201	No
MSCGM-1 vs. MSCGM-NC	1.886	2.284	0.360	No
MSCGM-100-NC vs. MSCGM-100	1.764	2.136	0.455	No
MSCGM-1 vs. MSCGM-10	1.414	2.097	0.466	No
MSCGM-1 vs. MSCGM-50	1.357	2.013	0.512	No
MSCGM-1 vs. MSCGM-100-NC	1.629	1.974	0.520	No
MSCGM-NC vs. MSCGM-100	1.508	1.826	0.615	No
MSCGM-1 vs. MSCGM-5	1.193	1.770	0.631	No
MSCGM-5 vs. MSCGM-NC	0.692	0.839	0.997	No
MSCGM vs. MSCGM-1	0.537	0.796	0.996	No
MSCGM-50 vs. MSCGM-NC	0.528	0.640	0.999	No
MSCGM-10 vs. MSCGM-NC	0.472	0.571	0.999	No
MSCGM-5 vs. MSCGM-100-NC	0.436	0.528	0.998	No
MSCGM-50 vs. MSCGM-100-NC	0.272	0.330	1.000	No
MSCGM-5 vs. MSCGM-10	0.221	0.328	0.999	No
MSCGM-100-NC vs. MSCGM-NC	0.256	0.269	0.998	No
MSCGM-10 vs. MSCGM-100-NC	0.216	0.261	0.991	No
MSCGM-5 vs. MSCGM-50	0.164	0.243	0.963	No
MSCGM-50 vs. MSCGM-10	0.0566	0.0840	0.933	No

Comparisons for factor: **Col 1 within Day 9**

Comparison	**Diff of Means**	**t**	**P**	**P<0.05**
MSCGM vs. MSCGM-100	3.938	5.842	<0.001	Yes
MSCGM-1 vs. MSCGM-100	3.643	5.403	<0.001	Yes
MSCGM vs. MSCGM-5	2.849	4.226	0.001	Yes
MSCGM vs. MSCGM-NC	3.185	3.858	0.005	Yes
MSCGM-1 vs. MSCGM-5	2.553	3.788	0.006	Yes
MSCGM-1 vs. MSCGM-NC	2.889	3.499	0.016	Yes
MSCGM-10 vs. MSCGM-100	2.210	3.278	0.031	Yes
MSCGM-50 vs. MSCGM-100	2.006	2.975	0.074	No
MSCGM vs. MSCGM-50	1.933	2.867	0.096	No
MSCGM-100-NC vs. MSCGM-100	2.334	2.827	0.102	No
MSCGM vs. MSCGM-10	1.729	2.564	0.192	No
MSCGM-1 vs. MSCGM-50	1.637	2.428	0.252	No
MSCGM-1 vs. MSCGM-10	1.433	2.126	0.443	No
MSCGM vs. MSCGM-100-NC	1.604	1.943	0.570	No
MSCGM-10 vs. MSCGM-NC	1.456	1.764	0.692	No
MSCGM-10 vs. MSCGM-5	1.120	1.662	0.744	No
MSCGM-100-NC vs. MSCGM-NC	1.581	1.658	0.719	No
MSCGM-5 vs. MSCGM-100	1.089	1.616	0.720	No
MSCGM-1 vs. MSCGM-100-NC	1.309	1.585	0.709	No
MSCGM-50 vs. MSCGM-NC	1.253	1.517	0.721	No
MSCGM-100-NC vs. MSCGM-5	1.245	1.508	0.686	No
MSCGM-50 vs. MSCGM-5	0.917	1.360	0.744	No
MSCGM-NC vs. MSCGM-100	0.753	0.912	0.934	No
MSCGM vs. MSCGM-1	0.296	0.439	0.996	No
MSCGM-5 vs. MSCGM-NC	0.336	0.407	0.990	No
MSCGM-100-NC vs. MSCGM-50	0.328	0.398	0.971	No
MSCGM-10 vs. MSCGM-50	0.204	0.302	0.944	No
MSCGM-100-NC vs. MSCGM-10	0.125	0.151	0.880	No

Appendix C: Fibrin Degradation Product Mass ANOVA:

Day3:

One Way Analysis of Variance Monday, April 27, 2015, 1:05:20 PM

Data source: Day 3 in Notebook1

Group Name	N	Missing	Mean	Std Dev	SEM
Aprotinin-100	6	0	8.680	1.062	0.434
Aprotinin-50	6	0	11.162	1.103	0.450
Aprotinin-10	6	0	11.333	1.785	0.729
Aprotinin-5	6	0	11.640	0.964	0.394
Aprotinin-1	6	0	12.602	0.780	0.318
Aprotinin-0	6	0	14.127	1.577	0.644

Source of Variation	DF	SS	MS	F	P
Between Groups	5	97.082	19.416	12.192	<0.001
Residual	30	47.777	1.593		
Total	35	144.859			

The differences in the mean values among the treatment groups are greater than would be expected by chance; there is a statistically significant difference (P = <0.001).

Power of performed test with alpha = 0.050: 1.000

All Pairwise Multiple Comparison Procedures (Holm-Sidak method):
Overall significance level = 0.05

Comparisons for factor:

Comparison	Diff of Means	t	P	P<0.050
Aprotinin-0 vs. Aprotinin-100	5.447	7.476	<0.001	Yes
Aprotinin-1vs. Aprotinin-100	3.922	5.383	<0.001	Yes
Aprotinin-0 vs. Aprotinin-50	2.965	4.069	0.004	Yes
Aprotinin-5 vs. Aprotinin-100	2.960	4.063	0.004	Yes
Aprotinin-0 vs. Aprotinin-10	2.794	3.835	0.007	Yes
Aprotinin-10 vs. Aprotinin-100	2.653	3.641	0.010	Yes
Aprotinin-0 vs. Aprotinin-5	2.487	3.413	0.017	Yes
Aprotinin-50 vs. Aprotinin-100	2.482	3.407	0.015	Yes
Aprotinin-0vs.Aprotinin-1	1.525	2.093	0.275	No
Aprotinin-1 vs. Aprotinin-50	1.440	1.976	0.298	No
Aprotinin-1 vs. Aprotinin-10	1.269	1.742	0.382	No
Aprotinin-1 vs. Aprotinin-5	0.962	1.320	0.584	No
Aprotinin-5 vs. Aprotinin-50	0.478	0.656	0.887	No
Aprotinin-5 vs. Aprotinin-10	0.307	0.421	0.895	No
Aprotinin-10 vs. Aprotinin-50	0.171	0.235	0.816	No

Day 6:

One Way Analysis of Variance Monday, April 27, 2015, 1:06:16 PM

Data source: Day 6 in Notebook1

Group Name	N	Missing	Mean	Std Dev	SEM
Aprotinin-100	6	0	17.647	1.796	0.733
Aprotinin-50	6	0	22.165	1.814	0.741
Aprotinin-10	6	0	22.280	3.441	1.405
Aprotinin-5	6	0	23.587	1.529	0.624
Aprotinin-1	6	0	24.963	1.363	0.556
Aprotinin-0	6	0	27.025	3.413	1.393

Source of Variation	DF	SS	MS	F	P
Between Groups	5	301.502	60.300	10.579	<0.001
Residual	30	171.004	5.700		
Total	35	472.506			

The differences in the mean values among the treatment groups are greater than would be expected by chance; there is a statistically significant difference (P = <0.001).

Power of performed test with alpha = 0.050: 1.000

All Pairwise Multiple Comparison Procedures (Holm-Sidak method):
Overall significance level = 0.05

Comparisons for factor:

Comparison	Diff of Means	t	P	P<0.050
Aprotinin-0 vs. Aprotinin-100	9.378	6.803	<0.001	Yes
Aprotinin-1 vs. Aprotinin-100	7.316	5.308	<0.001	Yes
Aprotinin-5 vs. Aprotinin-100	5.940	4.309	0.002	Yes
Aprotinin-0 vs. Aprotinin-50	4.860	3.526	0.016	Yes
Aprotinin-0 vs. Aprotinin-10	4.745	3.442	0.019	Yes
Aprotinin-10 vs. Aprotinin-100	4.633	3.361	0.021	Yes
Aprotinin-50 vs. Aprotinin-100	4.518	3.278	0.024	Yes
Aprotinin-0 vs. Aprotinin-5	3.438	2.494	0.138	No
Aprotinin-1 vs. Aprotinin-50	2.798	2.030	0.308	No
Aprotinin-1 vs. Aprotinin-10	2.683	1.946	0.315	No
Aprotinin-0 vs. Aprotinin-5	2.062	1.496	0.543	No
Aprotinin-5 vs. Aprotinin-50	1.422	1.032	0.774	No
Aprotinin-1 vs. Aprotinin-5	1.376	0.998	0.694	No
Aprotinin-5 vs. Aprotinin-10	1.307	0.948	0.578	No
Aprotinin-10 vs. Aprotinin-50	0.115	0.0834	0.934	No

Day 9:

One Way Analysis of Variance Monday, April 27, 2015, 1:01:34 PM

Data source: Day 9 in Notebook1

Group Name	N	Missing	Mean	Std Dev	SEM
Aprotinin-100	6	0	8.680	1.062	0.434
Aprotinin-50	6	0	11.162	1.103	0.450
Aprotinin-10	6	0	11.333	1.785	0.729
Aprotinin-5	6	0	11.640	0.964	0.394
Aprotinin-1	6	0	12.602	0.780	0.318
Aprotinin-0	6	0	14.127	1.577	0.644

Source of Variation	DF	SS	MS	F	P
Between Groups	5	97.082	19.416	12.192	<0.001
Residual	30	47.777	1.593		
Total	35	144.859			

The differences in the mean values among the treatment groups are greater than would be expected by chance; there is a statistically significant difference (P = <0.001).

Power of performed test with alpha = 0.050: 1.000

All Pairwise Multiple Comparison Procedures (Holm-Sidak method):
Overall significance level = 0.05

Comparisons for factor:

Comparison	Diff of Means	t	P	P<0.050
Aprotinin-0 vs. Aprotinin-100	5.447	7.476	<0.001	Yes
Aprotinin-1 vs. Aprotinin-100	3.922	5.383	<0.001	Yes
Aprotinin-0 vs. Aprotinin-50	2.965	4.069	0.004	Yes
Aprotinin-5 vs. Aprotinin-100	2.960	4.063	0.004	Yes
Aprotinin-0 vs. Aprotinin-10	2.794	3.835	0.007	Yes
Aprotinin-10 vs. Aprotinin-100	2.653	3.641	0.010	Yes
Aprotinin-0 vs. Aprotinin-5	2.487	3.413	0.017	Yes
Aprotinin-50 vs. Aprotinin-100	2.482	3.407	0.015	Yes
Aprotinin-0 vs. Aprotinin-1	1.525	2.093	0.275	No
Aprotinin-1 vs. Aprotinin-50	1.440	1.976	0.298	No
Aprotinin-1 vs. Aprotinin-10	1.269	1.742	0.382	No
Aprotinin-1 vs. Aprotinin-5	0.962	1.320	0.584	No
Aprotinin-5 vs. Aprotinin-50	0.478	0.656	0.887	No
Aprotinin-5 vs. Aprotinin-10	0.307	0.421	0.895	No
Aprotinin-10 vs. Aprotinin-50	0.171	0.235	0.816	No

Appendix D: Suture Diameter

Quantified using 3 images, a left (near the needle), center (approximately 2 cm from needle), and right (near the end of the suture)

Aprotinin (100 micrograms of aprotinin/ml media) - hMSC seeded:

Suture	Left Max	Left Min	Center Max	Center Min	Right Max	Right Min	Average
Aprotinin-1	1.452	0.945	1.276	1.187	1.557	1.416	1.306
Aprotinin-2	1.025	1.290	1.328	0.900	1.748	1.487	1.253
Aprotinin-3	1.367	1.169	1.336	1.203	1.288	0.968	1.222
Aprotinin-4	1.406	0.988	1.448	1.307	1.589	1.200	1.323
Aprotinin-5	1.557	1.087	1.662	1.249	1.723	1.534	1.469
Aprotinin-6	1.603	1.373	1.215	0.929	1.077	0.768	1.161
Average Diameter	1.289	**Stdev**	0.106				

MSCGM (media alone) - hMSC seeded:

Suture	Left Max	Left Min	Center Max	Center Min	Right Max	Right Min	Average
Control-4	1.190	0.947	1.166	0.957	1.250	1.036	1.091
Control-5	1.290	0.788	1.277	0.575	1.577	1.307	1.135
Control-7	1.025	0.935	0.689	0.613	1.391	0.898	0.925
Control-10	1.063	0.680	1.261	0.831	1.093	0.828	0.959
Control-12	1.111	0.740	1.275	1.202	1.021	0.462	0.969
Control-13	1.171	0.747	1.047	0.768	1.125	0.757	0.936
Average Diameter	1.003	**Stdev**	0.088				

Non-seeded Aprotinin (100 micrograms of aprotinin/ml media):

Suture	Left Max	Left Min	Center Max	Center Min	Right Max	Right Min	Average
NC-Aprotinin-1	1.570	1.253	1.754	1.503	1.817	1.314	1.535
NC-Aprotinin-2	1.753	1.508	1.663	1.358	1.640	1.272	1.532
NC-Aprotinin-3	1.754	1.348	1.330	1.148	1.731	1.213	1.421
Average Diameter	1.496	**Stdev**	0.065				

Non-seeded MSCGM (media alone):

Suture	Left Max	Left Min	Center Max	Center Min	Right Max	Right Min	Average
NC-MSCGM-1	1.990	1.781	1.923	1.499	1.827	1.435	1.742
NC-MSCGM-2	1.677	1.524	1.649	1.508	2.277	1.676	1.719
NC-MSCGM-3	1.676	1.412	1.689	1.539	1.830	1.732	1.647
Average Diameter	1.702	**Stdev**	0.050				

Diameter ANOVA:

One Way Analysis of Variance Wednesday, March 18, 2015, 10:50:50 AM

Data source: Data 2 in Diameter Data

Dependent Variable: Col 2

Normality Test (Shapiro-Wilk) Passed (P = 0.703)

Equal Variance Test: Passed (P = 0.981)

Group Name	N	Missing	Mean	Std Dev	SEM
MSCGM-100	6	0	1.289	0.106	0.0432
MSCGM	6	0	1.003	0.0884	0.0361
MSCGM-100 NC	3	0	1.496	0.0653	0.0377
MSCGM NC	3	0	1.702	0.0499	0.0288
PBS NC	4	0	1.289	0.0919	0.0459

Source of Variation	DF	SS	MS	F	P
Between Groups	4	1.133	0.283	35.958	<0.001
Residual	17	0.134	0.00788		
Total	21	1.267			

The differences in the mean values among the treatment groups are greater than would be expected by chance; there is a statistically significant difference (P = <0.001).

Power of performed test with alpha = 0.050: 1.000

All Pairwise Multiple Comparison Procedures (Holm-Sidak method):
Overall significance level = 0.05

Comparisons for factor: **Col 1**

Comparison	Diff of Means	t	P	P<0.050
MSCGM NC vs. MSCGM	0.700	11.154	<0.001	Yes
MSCGM-100 NC vs. MSCGM	0.493	7.862	<0.001	Yes
MSCGM NC vs. MSCGM-100	0.414	6.594	<0.001	Yes
MSCGM NC vs. PBS NC	0.413	6.100	<0.001	Yes
MSCGM-100 vs. MSCGM	0.286	5.585	<0.001	Yes
PBS NC vs. MSCGM	0.286	5.001	<0.001	Yes
MSCGM-100 NC vs. MSCGM-100	0.207	3.302	0.017	Yes
MSCGM-100 NC vs. PBS NC	0.207	3.052	0.021	Yes
MSCGM NC vs. MSCGM-100 NC	0.207	2.851	0.022	Yes
PBS NC vs. MSCGM-100	0.000323	0.00565	0.996	No

Appendix E: Suture Mechanics

UTS

UTS Data (Pa):

Sample	Aprotinin - Seeded	MSCGM - Seeded	Aprotinin - Unseeded	MSCGM - Unseeded	PBS - Unseeded
1	52095.9	16654.6	801732.1	472204.3	1111005.1
2	62925.0	2942.0	874853.8	660526.9	1459941.6
3	42561.3	8320.1	1247399.9	352514.6	809458.4
4	62805.5	41217.3	-	-	1013624.0
5	141816.7	55208.3	-	-	-
6	57040.0	37193.8	-	-	-
Average	69874.1	26922.7	974661.9	495081.9	1098507.3
Stdev	36057.6	20671.1	239010.9	155275.3	271750.7

UTS Data (MPa):

Sample	Aprotinin - Seeded	MSCGM - Seeded	Aprotinin - Unseeded	MSCGM - Unseeded	PBS - Unseeded
1	0.05210	0.01665	0.80173	0.47220	1.11101
2	0.06293	0.00294	0.87485	0.66053	1.45994
3	0.04256	0.00832	1.24740	0.35251	0.80946
4	0.06281	0.04122	-	-	1.01362
5	0.14182	0.05521	-	-	-
6	0.05704	0.03719	-	-	-
Average	0.06987	0.02692	0.97466	0.49508	1.12680
Stdev	0.03606	0.02067	0.23901	0.15528	0.32553

UTS ANOVA:

One Way Analysis of Variance Wednesday, March 18, 2015, 10:34:03 AM

Data source: UTS in Diameter and Mechanical Data

Dependent Variable: Col 2

Normality Test (Shapiro-Wilk) Failed (P < 0.050)

Test execution ended by user request, ANOVA on Ranks begun

Kruskal-Wallis One Way Analysis of Variance on Ranks Wednesday, March 18, 2015, 10:34:03 AM

Data source: UTS in Diameter and Mechanical Data

Group	N	Missing	Median	25%	75%
MSCGM-100	6	0	0.0599	0.0497	0.0826
MSCGM	6	0	0.0269	0.00697	0.0447

H = 6.564 with 1 degrees of freedom. P(est.)= 0.010 P(exact)= 0.009

The differences in the median values among the treatment groups are greater than would be expected by chance; there is a statistically significant difference (P = 0.009)

To isolate the group or groups that differ from the others use a multiple comparison procedure.

All Pairwise Multiple Comparison Procedures (Tukey Test):

Comparison	Diff of Ranks	q	P<0.05
MSCGM-100 vs MSCGM	32.000	3.623	Yes

Note: The multiple comparisons on ranks do not include an adjustment for ties.

One Way Analysis of Variance Wednesday, February 18, 2015, 4:21:03 PM

Data source: UTS in Notebook1

Dependent Variable: Col 2

Normality Test (Shapiro-Wilk) Failed (P < 0.050)

Equal Variance Test: Failed (P < 0.050)

Group Name	N	Missing	Mean	Std Dev	SEM
MSCGM-100	6	0	0.0698	0.0361	0.0147
MSCGM	6	0	0.0269	0.0207	0.00844
MSCGM-100 NC	3	0	0.975	0.239	0.138
MSCGM NC	3	0	0.495	0.155	0.0896
PBS NC	4	0	1.099	0.272	0.136

Source of Variation	DF	SS	MS	F	P
Between Groups	4	4.443	1.111	48.091	<0.001
Residual	17	0.393	0.0231		
Total	21	4.836			

The differences in the mean values among the treatment groups are greater than would be expected by chance; there is a statistically significant difference (P = <0.001).

Power of performed test with alpha = 0.050: 1.000

All Pairwise Multiple Comparison Procedures (Tukey Test):

Comparisons for factor: **Col 1**

Comparison	Diff of Means	p	q	P	P<0.050
PBS NC vs. MSCGM	1.072	5	15.448	<0.001	Yes
PBS NC vs. MSCGM-100	1.029	5	14.829	<0.001	Yes
PBS NC vs. MSCGM NC	0.603	5	7.352	<0.001	Yes
PBS NC vs. MSCGM-100 NC	0.124	5	1.509	0.821	No
MSCGM-100 NC vs. MSCGM	0.948	5	12.472	<0.001	Yes
MSCGM-100 NC vs. MSCGM-100	0.905	5	11.907	<0.001	Yes
MSCGM-100 NC vs. MSCGM NC	0.480	5	5.466	0.010	Yes
MSCGM NC vs. MSCGM	0.468	5	6.161	0.004	Yes
MSCGM NC vs. MSCGM-100	0.425	5	5.596	0.008	Yes
MSCGM-100 vs. MSCGM	0.0429	5	0.692	0.987	No

E

E Data:

E Data (Pa):

Sample	Aprotinin - Seeded	MSCGM - Seeded	Aprotinin - Unseeded	MSCGM - Unseeded	PBS - Unseeded
1	40875.3	10080.6	801732.1	472204.3	789784.3
2	44609.2	7244.5	874853.8	660526.9	1197654.9
3	47975.0	8175.1	1247399.9	352514.6	492859.4
4	44111.3	41245.8	-	-	962748.3
5	100339.7	29363.9	-	-	-
6	99178.7	29988.5	-	-	-
Average	62848.2	21016.4	974661.9	495081.9	860761.7
Stdev	28682.0	14377.5	239010.9	155275.3	296809.8

E Data (MPa):

Sample	Aprotinin - Seeded	MSCGM - Seeded	Aprotinin - Unseeded	MSCGM - Unseeded	PBS - Unseeded
1	0.04088	0.01008	0.80173	0.47220	0.78978
2	0.04461	0.00724	0.87485	0.66053	1.19765
3	0.04798	0.00818	1.24740	0.35251	0.49286
4	0.04411	0.04125	-	-	0.96275
5	0.10034	0.02936	-	-	-
6	0.09918	0.02999	-	-	-
Average	0.06285	0.02102	0.97466	0.49508	0.86076
Stdev	0.02868	0.01438	0.23901	0.15528	0.29681

E ANOVA:

One Way Analysis of Variance Wednesday, March 18, 2015, 10:41:44 AM

Data source: Suture STiffness in Diameter and Mechanical Data

Dependent Variable: Col 2

Normality Test (Shapiro-Wilk) Failed (P < 0.050)

Test execution ended by user request, ANOVA on Ranks begun

Kruskal-Wallis One Way Analysis of Variance on Ranks Wednesday, March 18, 2015, 10:41:44 AM

Data source: Suture STiffness in Diameter and Mechanical Data

Group	N	Missing	Median	25%	75%
MSCGM-100	6	0	0.0463	0.0433	0.0995
MSCGM	6	0	0.0197	0.00794	0.0328

H = 7.410 with 1 degrees of freedom. P(est.)= 0.006 P(exact)= 0.004

The differences in the median values among the treatment groups are greater than would be expected by chance; there is a statistically significant difference (P = 0.004)

To isolate the group or groups that differ from the others use a multiple comparison procedure.

All Pairwise Multiple Comparison Procedures (Tukey Test):

Comparison	Diff of Ranks	q	P<0.05
MSCGM-100 vs MSCGM	34.000	3.850	Yes

Note: The multiple comparisons on ranks do not include an adjustment for ties.

All Pairwise Multiple Comparison Procedures (Tukey Test):

Comparisons for factor: **Col 1**

Comparison	Diff of Means	p	q	P	P<0.050
MSCGM-100 NC vs. MSCGM	0.916	5	10.856	<0.001	Yes
MSCGM-100 NC vs. MSCGM-100	0.875	5	10.361	<0.001	Yes
MSCGM-100 NC vs. MSCGM NC	0.626	5	6.425	0.002	Yes
MSCGM-100 NC vs. PBS NC	0.0767	5	0.841	0.974	No
PBS NC vs. MSCGM	0.840	5	10.897	<0.001	Yes
PBS NC vs. MSCGM-100	0.798	5	10.354	<0.001	Yes
PBS NC vs. MSCGM NC	0.550	5	6.027	0.004	Yes
MSCGM NC vs. MSCGM	0.290	5	3.437	0.155	No
MSCGM NC vs. MSCGM-100	0.248	5	2.942	0.273	Do Not Test
MSCGM-100 vs. MSCGM	0.0418	5	0.607	0.992	Do Not Test

A result of "Do Not Test" occurs for a comparison when no significant difference is found between two means that enclose that comparison. For example, if you had four means sorted in order, and found no difference between means 4 vs. 2, then you would not test 4 vs. 3 and 3 vs. 2, but still test 4 vs. 1 and 3 vs. 1 (4 vs. 3 and 3 vs. 2 are enclosed by 4 vs. 2: 4 3 2 1). Note that not testing the enclosed means is a procedural rule, and a result of Do Not Test should be treated as if there is no significant difference between the means, even though one may appear to exist.

One Way Analysis of Variance Wednesday, February 18, 2015, 5:27:52 PM

Data source: Stiffness in Notebook1

Dependent Variable: Col 2

Normality Test (Shapiro-Wilk) Failed (P < 0.050)

Equal Variance Test: Failed (P < 0.050)

Group Name	N	Missing	Mean	Std Dev	SEM
MSCGM-100	6	0	0.0628	0.0287	0.0117
MSCGM	6	0	0.0210	0.0144	0.00587
MSCGM-100 NC	3	0	0.937	0.237	0.137
MSCGM NC	3	0	0.311	0.227	0.131
PBS NC	4	0	0.861	0.297	0.148

Source of Variation	DF	SS	MS	F	P
Between Groups	4	3.228	0.807	28.306	<0.001
Residual	17	0.485	0.0285		
Total	21	3.712			

The differences in the mean values among the treatment groups are greater than would be expected by chance; there is a statistically significant difference (P = <0.001).

Power of performed test with alpha = 0.050: 1.000

SAF

SAF Data:

SAF Data (Strain):

Sample	Aprotinin - Seeded	MSCGM - Seeded	Aprotinin - Unseeded	MSCGM - Unseeded	PBS - Unseeded
1	1.2745	1.4106	1.8637	2.2238	2.2025
2	1.4106	0.3990	1.5040	1.6711	2.1046
3	0.8872	1.0177	1.7376	2.3408	2.5056
4	1.4238	0.9993	-	-	1.5561
5	1.4134	1.8801	-	-	-
6	0.5751	1.2403	-	-	-
Average	1.1641	1.1578	1.7018	2.0786	2.0922
Stdev	0.3539	0.4925	0.1825	0.3577	0.3960

SAF ANOVA:

One Way Analysis of Variance Wednesday, February 18, 2015, 5:50:55 PM

Data source: SAF in Diameter and Mechanical Data

Dependent Variable: Col 2

Normality Test (Shapiro-Wilk) Passed (P = 0.407)

Equal Variance Test: Passed (P = 0.938)

Group Name	N	Missing	Mean	Std Dev	SEM
MSCGM-100	6	0	1.164	0.354	0.144
MSCGM	6	0	1.158	0.493	0.201
MSCGM-100 NC	3	0	1.702	0.183	0.105
MSCGM NC	3	0	2.079	0.358	0.207
PBS NC	4	0	2.092	0.396	0.198

Source of Variation	DF	SS	MS	F	P
Between Groups	4	3.890	0.972	6.281	0.003
Residual	17	2.632	0.155		
Total	21	6.522			

The differences in the mean values among the treatment groups are greater than would be expected by chance; there is a statistically significant difference (P = 0.003).

Power of performed test with alpha = 0.050: 0.917

All Pairwise Multiple Comparison Procedures (Holm-Sidak method):
Overall significance level = 0.05

Comparisons for factor: **Col 1**

Comparison	**Diff of Means**	**t**	**P**	**P<0.050**
PBS NC vs. MSCGM	0.934	3.679	0.018	Yes
PBS NC vs. MSCGM-100	0.928	3.654	0.018	Yes
MSCGM NC vs. MSCGM	0.921	3.309	0.033	Yes
MSCGM NC vs. MSCGM-100	0.914	3.287	0.030	Yes
MSCGM-100 NC vs. MSCGM	0.544	1.955	0.341	No
MSCGM-100 NC vs. MSCGM-100	0.538	1.932	0.305	No
PBS NC vs. MSCGM-100 NC	0.390	1.299	0.613	No
MSCGM NC vs. MSCGM-100 NC	0.377	1.173	0.590	No
PBS NC vs. MSCGM NC	0.0136	0.0453	0.999	No
MSCGM-100 vs. MSCGM	0.00625	0.0275	0.978	No

Appendix F: Cell Viability

6 coverslips were seeded with 35,000 cells (approximately 5,000 cells per cm) and cultured for 7 days. LIVE/DEAD assay was used to determine the quantities of live and dead cells

Aprotinin (100 micrograms of aprotinin/ml media):

	Live Cells/Green (#)	Dead Cells/Red (#)	Total Cells/Blue (#)
Coverslip 1	254	16	270
	253	5	258
Average (%)	96.75	3.25	
Coverslip 2	300	4	304
	245	4	249
Average (%)	96.54	1.46	
Coverslip 3	342	4	246
	375	7	382
Average (%)	98.51	1.49	
Coverslip 4	172	17	189
	253	7	260
Average (%)	94.16	5.84	
Coverslip 5	281	4	285
	290	0	290
Average (%)	99.30	0.70	
Coverslip 6	315	9	324
	332	19	351
Average (%)	95.91	4.09	
TOTALS			
Live Cells Avg (%)	**Live Cells Stdev(%)**	**Dead Cells Avg (%)**	**Dead Cells Stdev (%)**
97.08	2.00	2.92	2.00

MSCGM:

	Live Cells/Green (#)	Dead Cells/Red (#)	Total Cells/Blue (#)
Coverslip 1	106	2	108
	96	0	96
Average (%)	99.07	0.93	
Coverslip 2	41	1	43
	199	0	199
Average (%)	98.84	1.16	
Coverslip 3	104	3	107
	134	3	137
Average (%)	95.71	4.29	
Coverslip 4	85	5	90
	56	2	58
Average (%)	95.50	4.50	
Coverslip 5	64	0	64
	104	3	107
Average (%)	98.60	1.40	
Coverslip 6	117	3	120
	120	3	123
Average (%)	97.53	2.47	
TOTALS			
Live Cells Avg (%)	**Live Cells Stdev(%)**	**Dead Cells Avg (%)**	**Dead Cells Stdev (%)**
97.84	1.33	2.16	1.33

Appendix G: Cell Proliferation

6 coverslips were seeded with 35,000 cells (approximately 5,000 cells per cm) and cultured for 3 days.
LIVE/DEAD assay was used to determine the quantities of live and dead cells
Aprotinin (100 micrograms of aprotinin/ml media):

	Total Cells - Blue (#)	Ki-67+ Cells - Red (#)	Ki-67+ Cells (%)
Coverslip 1	118	20	16.95
	157	14	8.92
		Coverslip Average (%)	12.93
Coverslip 2	38	9	23.68
	64	16	25.00
		Coverslip Average (%)	
Coverslip 3	78	16	20.51
	82	5	6.10
		Coverslip Average (%)	13.31
Coverslip 4	28	4	14.29
	28	8	32.00
		Coverslip Average (%)	23.14
Coverslip 5	101	14	13.86
	56	22	39.29
		Coverslip Average (%)	
Coverslip 6	118	16	13.56
	83	18	21.69
		Coverslip Average (%)	17.63

TOTALS	
Ki-67+ Avg (%)	**Ki-67+ Stdev (%)**
19.65	5.86

MSCGM:

	Total Cells - Blue (#)	Ki-67+ Cells - Red (#)	Ki-67+ Cells (%)
Coverslip 1	220	18	8.18
	271	11	4.06
		Coverslip Average (%)	6.12
Coverslip 2	206	12	5.83
	228	25	10.96
		Coverslip Average (%)	8.40
Coverslip 3	12	9	75.00
	60	4	6.67
		Coverslip Average (%)	40.83
Coverslip 4	56	4	7.14
	51	13	25.49
		Coverslip Average (%)	16.32
Coverslip 5	153	18	11.76
	157	10	6.37
		Coverslip Average (%)	9.07
Coverslip 6	22	11	50.00
	76	14	18.42
		Coverslip Average (%)	34.21
TOTALS			
Ki-67+ Avg (%)		**Ki-67+ Stdev (%)**	
19.16		14.78	

Appendix H: Cell Adhesion

Day 0 Data:

Standard Curve				MSCGM				Aprotinin			
72917	82550	88314	92049	10580	8253	15890	8791	9731	10634	10127	12691
42793	39538	79890	64822					10694	11745	17362	15655
34242	24883	27770	29191	7814	12718	8675	8483	8951	9365	8887	9049
16731	13668	15480	20372	12505	13943	12804	11275	8708	10927	10427	11991
9680	10117	8529	7119					9243	12217	11085	9482
6318	5505	5588	5978								
4027	3726	3785	2596								
2427	2326	2375	2354								

OD	Cells
83958	30000
56761	15000
29022	7500
16563	3750
8861	1875
5847	937.5
3534	468.75
2371	234.375

1 Correlation Coeff

MSCGM	OD				Cells				Cells*5			
1	10580	8253	15890	8791	2195.316	1392.036	4028.328	1577.753	10976.58	6960.178	20141.64	7888.766
2	7814	12718	8675	8483	1240.493	2933.354	1537.71	1471.432	6202.464	14666.77	7688.55	7357.158
3	12505	13943	12804	11275	2859.826	3356.224	2963.041	2435.23	14299.13	16781.12	14815.2	12176.15

Aprotinin	OD				Cells				Cells*5			
1	9731	10634	10127	12691	1902.241	2213.957	2038.94	2924.033	9511.206	11069.78	10194.7	14620.17
2	10694	11745	17362	15655	2234.669	2597.474	4536.462	3947.206	11173.34	12987.37	22682.31	19736.03
3	8951	9365	8887	9049	1632.985	1775.898	1610.892	1666.815	8164.926	8879.49	8054.462	8334.074
4	8708	10927	10427	11991	1549.102	2315.1	2142.5	2682.393	7745.508	11575.5	10712.5	13411.97
5	9243	12217	11085	9482	1733.784	2760.408	2369.642	1816.286	8668.918	13802.04	11848.21	9081.432

Days 0, 1, & 2 Data:

94202	91648	95667	94476	21461	20746	22364	22018	25863	23569	27972	21856
54520	54791	54706	55387	28046	23822	31740	22109	17368	21991	20620	18011
35085	37470	34625	36295	16961	21825	18844	21429	18641	36702	31763	30698
26996	26288	25069	25008	24010	24689	27839	25087	18942	23873	19383	19676
21974	20442	21029	21305	25422	25710	25218	26197	22435	26472	21123	23922
20135	18119	19033	17341					23195	25354	23550	26173
18858	17492	17232	18531					27503	18146	19021	20161
15996	15988	15603	16388								

OD	Cells
93998	30000
54851	15000
35869	7500
25840	3750
21188	1875
18657	937.5
18028	468.75
15994	0

	Correl Coeff
0.999951	

	OD				Cells				Cells*5			
AD0	21461	20746	22364	22018	1993.723	1717.304	2342.822	2209.059	9968.613	8586.518	11714.11	11045.29
AD1	28046	23822	31740	22109	4539.484	2906.485	5967.584	2244.239	22697.42	14532.43	29837.92	11221.2
	16961	21825	18844	21429	254.0226	2134.445	981.9904	1981.351	1270.113	10672.23	4909.952	9906.757
	25422	25710	25218	26197	3525.045	3636.386	3446.179	3824.66	17625.23	18181.93	17230.89	19123.3
AD2	24010	24689	27839	25087	2979.166	3241.667	4459.457	3395.534	14895.83	16208.34	22297.29	16977.67
CD0	25863	23569	27972	21856	3695.536	2808.675	4510.875	2146.43	18477.68	14043.38	22554.38	10732.15
	17368	21991	20620	18011	411.3688	2198.621	1668.592	659.9526	2056.844	10993.1	8342.96	3299.763
	18641	36702	31763	30698	903.5106	7885.893	5976.476	5564.747	4517.553	39429.47	29882.38	27823.73
CD1	18942	23873	19383	19676	1019.877	2926.202	1190.368	1303.642	5099.386	14631.01	5951.839	6518.208
	22435	26472	21123	23922	2777.327	2777.527	2777.727	2777.927	13886.64	13887.64	13888.64	13889.64
CD2	23195	25354	23550	26173	2664.087	3498.756	2801.33	3815.382	13320.44	17493.78	14006.65	19076.91
	27503	18146	19021	20161	4329.56	712.1436	1050.419	1491.143	21647.8	3560.718	5252.093	7455.713

Day 1 Data:

134463	138592	135480	130474	34808	17964	17218	18240	17606	18686	18958	20782
66704	66373	69366	68003	26938	28152	24700	20682	5902	11460	6248	6536
40105	41099	38014	38864	15148	17236	17736	15950	7730	8072	8188	8766
20461	22211	20017	21583	10000	9152	11400	10544	15012	15918	16056	17418
11249	12324	11658	12016	6820	6140	6076	5814	8538	8199	9021	9684
7018	7318	7457	8262					14628	14409	13260	14811
7121	7026	6589	8266								
2423	2097	2113	2032								

OD	Cells
134752	30000
67612	15000
39521	7500
21068	3750
11812	1875
7514	937.5
7251	468.75
2166	0

	Correl Coeff
0.999411	

	OD				Cells				Cells*5		
Aprotinin D3	34808	17964	17218	18240	7061.436	3195.738	3024.531	3259.08	35307.18	15978.69	15122.66
Aprotinin D3	26938	28152	24700	20682	5255.271	5533.884	4741.65	3819.519	26276.36	27669.42	23708.25
Aprotinin D3	15148	17236	17736	15950	2549.466	3028.662	3143.412	2733.525	12747.33	15143.31	15717.06
MSCGM D3	10000	9152	11400	10544	1368	1173.384	1689.3	1492.848	6840	5866.92	8446.5
MSCGM D3	6820	6140	6076	5814	638.19	482.13	467.442	407.313	3190.95	2410.65	2337.21
MSCGM D3	8410	7646	8738	8179	1003.095	827.757	1078.371	950.0805	5015.475	4138.785	5391.855
Aprotinin D1	17606	18686	18958	20782	3113.577	3361.437	3423.861	3842.469	15567.89	16807.19	17119.31
Aprotinin D1	11754	15073	12603	13659	1770.543	2532.254	1965.389	2207.741	8852.715	12661.27	9826.943
Aprotinin D1	12668	13379	13573	14774	1980.306	2143.481	2188.004	2463.633	9901.53	10717.4	10940.02
MSCGM D1	15012	15918	16056	17418	2518.254	2726.181	2757.852	3070.431	12591.27	13630.91	13789.26
MSCGM D1	14820	15164	14658	16115	2474.19	2553.023	2437.011	2771.278	12370.95	12765.12	12185.06
MSCGM D1	14628	14409	13260	14811	2430.126	2379.866	2116.17	2472.125	12150.63	11899.33	10580.85

Day 1&2 Data:

98039	91404	102253	111739	22307	18475	17197	22957	15746	15936	15220	17054
56883	51563	53600	52089	26796	26248	25563	25267	13703	13499	13322	14055
32239	32041	31852	28214	29112	29635	30028	28179	14888	15453	16964	19287
19328	18834	16609	17460								
10983	11132	9687	11363								
7630	7822	7048	6645								
8576	8959	7214	7488								
3777	3417	4671	4497								

Optical Density	Cells
100859	30000
53534	15000
31087	7500
18058	3750
10791	1875
7286	937.5
8059	468.75
4091	0

	correl coeff
0.999467	

Day1	OD				Cell				x5			
Aprotinin	22307	18475	17197	22957	5281.576	4084.843	3685.567	5484.415	26407.88	20424.21	18427.83	27422.07
MSCGM	15746	15936	15220	17054	3232.576	3291.913	3068.306	3641.064	16162.88	16459.56	15341.53	18205.32

Day2												
Aprotinin	26796	26248	25563	25267	6683.604	6512.407	6298.34	6206.069	33418.02	32562.04	31491.7	31030.35
Aprotinin	29112	29635	30028	28179	7406.721	7569.969	7692.901	7115.43	37033.6	37849.84	38464.51	35577.15
MSCGM	13703	13499	13322	14055	2594.547	2530.838	2475.561	2704.477	12972.73	12654.19	12377.8	13522.38
MSCGM	14888	15453	16964	19287	2964.591	3140.916	3612.988	4338.43	14822.96	15704.58	18064.94	21692.15

Day 2 Data:

X	114486	108143	108981	22396.5	20665.5	22555.5	19738.5	15595	14063	15324	14812
X	52455	59464	56846	20089	19145	19723	16593	13290	14519	13535	12617
X	36522	35557	35058								
X	22044	21279	19318								
X	16280	15888	15849								
X	17726	18060	17608								
X	15889	15572	13764								
X	10866	10719	11632								

Error in standard curve column one, excluded from standard curve calculations

OD	Cells
110536.7	30000
56255	15000
35712.33	7500
20880.33	3750
16005.67	1875
17798	937.5
15075	468.75
11072.33	0

	Correl
0.9973	Coeff

OD				Cells				Cells/Suture			
Aprotinin											
22396.5	20665.5	22555.5	19738.5	4960.154	4318.421	5019.101	3974.754	24800.77	21592.1	25095.5	19873.77
20089	19145	19723	16593	4104.695	3754.726	3969.008	2808.623	20523.47	18773.63	19845.04	14043.11
MSCGM											
15595	14063	15324	14812	2438.634	1870.676	2338.167	2148.353	12193.17	9353.38	11690.83	10741.76
13290	14519	13535	12617	1584.102	2039.729	1674.931	1334.6	7920.509	10198.64	8374.653	6673.002

Day 3 Data:

99010	99327	96887	94801	25866	20605	18959	23455	24202	19899	20893	20113
56711	57271	53481	54885	10793	10016	9261	9594	28245	25827	26741	29692
29710	26971	27778	29518	10317	10290	10961	11033	13729	15119	15293	16710
16843	13533	16639	15019	12915	13888	11606	8370	12426	12382	13359	13131
11174	9724	9517	9645	10783	10239	9369	10056	25876	25445	25716	31544
7080	6669	6788	6252	18091	18981	10020	9102	29441	31629	28111	31025
5103	5136	4772	6347								
3772	3975	3752	4167								

OD	Cells
97506.25	30000
55587	15000
28494.25	7500
15508.5	3750
10015	1875
6697.25	937.5
5339.5	468.75
3916.5	0

	Correl Coeff
1	

		OD				Cells				Cells*5			
MSCGM	1	25866	20605	18959	23455	6806	5150	4632	6048	34032	25752	23160	30238
	2	10793	10016	9261	9594	2061	1817	1579	1684	10306	9083	7896	8420
	3	10317	10290	10961	11033	1912	1903	2114	2137	9558	9515	10572	10684
	4	12915	13888	11606	8370	2729	3036	2317	1299	13647	15179	11587	6493
	5	10783	10239	9369	10056	2058	1887	1613	1829	10291	9436	8066	9146
	6	18091	18981	10020	9102	4359	4639	1818	1529	21794	23195	9090	7646
Aprotinin	1	24202	19899	20893	20113	6283	4928	5241	4995	31413	24640	26205	24977
	2	28245	25827	26741	29692	7555	6794	7082	8011	37777	33971	35409	40054
	3	13729	15119	15293	16710	2986	3423	3478	3924	14928	17116	17390	19621
	4	12426	12382	13359	13131	2576	2562	2869	2797	12878	12808	14346	13987
	5	25876	25445	25716	31544	6810	6674	6759	8594	34048	33369	33796	42969
	6	29441	31629	28111	31025	7932	8621	7513	8430	39659	43103	37566	42152

Day 5 Data:

100766	100855	98178	98562	32060	28648	29051	29894	6036	24605	5540	5967
58876	53576	52705	62235	14460	16148	16266	14270	14007	13747	14236	14579
32183	30282	32083	29251	19870	21230	20465	19741	23019	24044	24376	26835
17759	17862	17742	16593	29176	28396	29249	31125	27678	28341	28267	29301
11292	11184	11322	9712	29424	26703	27522	26450	14224	14102	13903	15551
7184	6863	7807	6951	31560	30998	28772	28784	17885	17544	17763	17749
8334	6782	5852	7001								
2271	2269	2313	2136								

OD	Cells
99590	30000
56848	15000
30950	7500
17489	3750
10878	1875
7201	937.5
6992	468.75
2247	0

	Correl Coeff
0.998194	

		OD				Cells				Cellsx5			
Aprotinin	1	32060	28648	29051	29894	8379.14	7324.832	7449.359	7709.846	41895.7	36624.16	37246.8	38549.23
	2	14460	16148	16266	14270	2940.74	3462.178	3498.794	2881.876	14703.7	17310.89	17493.97	14409.38
	3	19870	21230	20465	19741	4612.43	5032.67	4796.285	4572.569	23062.15	25163.35	23981.43	22862.85
	4	29176	28396	29249	31125	7487.984	7246.964	7510.541	8090.225	37439.92	36234.82	37552.71	40451.13
	5	29424	26703	27522	26450	7564.616	6723.827	6976.898	6645.65	37823.08	33619.14	34884.49	33228.25
	6	31560	30998	28772	28784	8224.64	8050.982	7363.148	7366.856	41123.2	40254.91	36815.74	36834.28
MSCGM	1	6036	24605	5540	5967	337.724	6075.545	184.46	316.403	1688.62	30377.73	922.3	1582.015
	2	14007	13747	14236	14579	2800.763	2720.423	2871.524	2977.511	14003.82	13602.12	14357.62	14887.56
	3	23019	24044	24376	26835	5585.471	5902.196	6004.784	6764.615	27927.36	29510.98	30023.92	33823.08
	4	27678	28341	28267	29301	7025.102	7229.969	7207.103	7526.609	35125.51	36149.85	36035.52	37633.05
	5	14224	14102	13903	15551	2867.816	2830.118	2768.627	3277.859	14339.08	14150.59	13843.14	16389.3
	6	17885	17544	17763	17749	3999.065	3893.696	3961.367	3957.041	19995.33	19468.48	19806.84	19785.21

Appendix I: Cell Proliferation on Sutures

		Cells	Ki-67+	Ki-67+Cells			Cells	Ki-67+	Avg	Suture Avg
Day 0	MSCGM1	54	3	0.055556		Aprotinin1	229	8	0.034934	
		87	2	0.022989	0.039272		66	3	0.045455	0.040195
	MSCGM2	65	2	0.030769		Aprotinin2	90	6	0.066667	
		64	4	0.0625	0.046635		55	7	0.127273	0.09697
	MSCGM3	83	5	0.060241		Aprotinin3	89	8	0.089888	
		70	4	0.057143	0.058692		77	6	0.077922	0.083905
Day 1	MSCGM1	90	7	0.077778		Aprotinin1	84	11	0.130952	
		65	1	0.015385	0.046581		72	6	0.083333	0.107143
	MSCGM2	78	4	0.051282		Aprotinin2	120	9	0.075	
		109	10	0.091743	0.071513		81	7	0.08642	0.08071
	MSCGM3	92	4	0.043478		Aprotinin3	92	9	0.097826	
		77	7	0.090909	0.067194		79	8	0.101266	0.099546
Day 2	MSCGM1	120	35	0.291667		Aprotinin1	57	9	0.157895	
		96	23	0.239583	0.265625		90	40	0.444444	0.30117
	MSCGM2	121	47	0.38843		Aprotinin2	233	102	0.437768	
		87	18	0.206897	0.297663		191	81	0.424084	0.430926
	MSCGM3	109	35	0.321101		Aprotinin3	153	90	0.588235	
		101	31	0.306931	0.314016		202	95	0.470297	0.529266

AVG	Day 0	Day 1	Day 2	Stdev		
Aprotinin	7.368969	9.579956	42.04539	2.973411	1.36089	11.44083
MSCGM	4.819952	6.176249	29.24347	0.980406	1.332355	2.461545